



universität  
wien

# DIPLOMARBEIT

## Hunting for co-factors of endosomal toll-like receptors

Zur Erlangung des akademischen Grades  
**Magistra der Naturwissenschaften (Mag. rer.nat.)**  
an der Formal- und Naturwissenschaftlichen Fakultät  
der Universität Wien

Verfasserin:	Irene Maria Aspalter
Matrikel-Nummer:	0303898
Studienrichtung (lt. Studienblatt):	A 490 – Molekulare Biologie
Betreuer:	Prof. Dr. Thomas Decker / Prof. Dr. Giulio Superti-Furga

Wien, im

April 2009

*Wissen ohne ausgleichende Liebe  
ist tödlich.*

(Epikur)

## **Dedication**

I dedicate my thesis to my family, who always believed in me and who strongly supported me during my studies at the University of Vienna and my thesis at the Research Center for Molecular Medicine.

Ich möchte meine Diplomarbeit meiner Familie widmen.

Wie schon Epikur wusste, ist Wissen ohne ausgleichende Liebe nicht sonderlich bekömmlich.

Ich möchte meiner Familie dafür danken, dass sie, abgesehen von der Umsetzung meines Studiums, stets für soviel ausgleichende Liebe gesorgt hat.

## Acknowledgement

I would like to thank everybody, who supported me during my studies and my thesis.

Primarily I would like to thank my mom and my dad for giving me the opportunity to study whatever fascinated me, for the freedom to do this in my distinct way, and for their constant and strong support. Furthermore, I would like to thank my sisters Christa, Manuela and Katharina for motivating me ever since; in a way only they are able to. Thank-you, for being my hardest reviewers and best friends.

I would like to thank Prof. Dr. Giulio Superti-Furga (CeMM) for giving me the great opportunity to realize my thesis in his laboratory. I am really grateful for the supportive environment I got offered at the Research Center for Molecular Medicine.

Especially I would like to thank Dr. Christoph Baumann (CeMM) for his exceptional supervision and encouragement. I deeply enjoyed our science discussions, which have been a significant motivation and great delight. Our teamwork was a wonderful combination of science and joy and made the time at CeMM an extraordinary experience, scientifically as well as personally.

I would like to thank Prof. Dr. Thomas Decker (University of Vienna) for his supervision and for representing my thesis at the University of Vienna.

Moreover, I would like to thank the innate immunity team at CeMM for all the supportive discussions and advices. Especially I would like to thank Dr. Andreas Pichlmair for reviewing parts of my thesis and his encouragement.

Moreover, I would like to thank everybody at the Research Center for Molecular Medicine for their great support, a wonderful year, a lot of fun, and so many happy hours.

I also would like to thank Prof. Dr. Barbara Hamilton (University of Vienna) for her courtesy during my studies and my thesis. Her help was simply great.

Furthermore, I would like to thank Mag. Marianne Raith and Mag. Michael Orthofer for all the nights of science discussions, joined suffering and joy, and the intellectual support during my studies. It would have been a long and lonely way without them.

Last but not least I would like to thank my friends Annemarie Resch, Kathrin Hudl, Barbara Wippl, Marianne Eibensteiner, Sigrid Vogel, and Barbara Niklas for six wonderful years in Vienna and for keeping the right balance between studies and recreation.

# Table of contents

<b>ABSTRACT</b>	<b>7</b>
<b>ZUSAMMENFASSUNG</b>	<b>8</b>
<b>INTRODUCTION</b>	<b>9</b>
<b>1.1. THE ADAPTIVE IMMUNITY</b>	<b>9</b>
<b>1.2. THE INNATE IMMUNE SYSTEM</b>	<b>10</b>
1.2.1. PROPERTIES OF INNATE IMMUNITY	10
1.2.2. PATTERN RECOGNITION RECEPTORS	11
1.2.3. INTERACTION OF INNATE AND ADAPTIVE IMMUNITY	11
<b>1.3. TOLL-LIKE RECEPTORS</b>	<b>13</b>
1.3.1. THE TOLL-RECEPTOR	13
1.3.2. TOLL-LIKE RECEPTORS	15
1.3.3. STRUCTURE OF TOLL AND TOLL-LIKE RECEPTORS	16
1.3.4. SIGNAL INDUCTION BY TLRs	18
1.3.5. THE TLR "SIGNALOSOME"	19
1.3.6. CELLS INVOLVED IN TOLL-LIKE RECEPTOR SIGNALING	21
1.3.7. TOLL-LIKE RECEPTOR 4	22
<b>1.4. TANDEM AFFINITY PURIFICATION</b>	<b>28</b>
1.4.1. THE GS-TAP TAG	28
1.4.2. PROCEDURE OF TANDEM-AFFINITY-PURIFICATION	28
<b>1.5. STRUCTURE OF THE PROJECT</b>	<b>30</b>
<b>MATERIAL AND METHODS</b>	<b>32</b>
<b>2.1. CELL CULTURE</b>	<b>32</b>
2.1.1. RAW264.7 MACROPHAGES (ATCC)	32
2.1.2. HTLR3-HEK293 (INVIVOGEN)	32
2.1.3. HEK293T (CANCER RESEARCH UK)	32
2.1.4. HELA (ATCC)	32
2.1.5. HEK293-GP (ATCC)	32
2.1.6. FREEZING CELLS	32
2.1.7. THAWING CELLS	33
<b>2.2. TRANSIENT TRANSFECTION OF HEK-CELLS AND LYSIS</b>	<b>33</b>
2.2.1. TRANSIENT TRANSFECTION OF HEK-CELLS	33
2.2.2. LYSIS OF HEK CELLS	33
<b>2.3. GENERATING STABLE CELL LINES</b>	<b>34</b>
2.3.1. CLONING OF ENTRY-POINTS AND INTERACTION-CANDIDATES USING GATEWAY® CLONING KIT (INVITROGEN)	34
2.3.2. RETROVIRAL TRANSFECTION SYSTEM TO GENERATE STABLE RAW264.7 CELLS	38

<b>2.4. LIGANDS OF ENDOSOMAL TOLL-LIKE RECEPTORS</b>	<b>40</b>
2.4.1. TLR3 LIGAND	40
2.4.2. TLR7/8 LIGAND	40
2.4.3. TLR9 LIGAND	40
2.4.4. LIPID COMPOUNDS	40
<b>2.5. DE-GLYCOSYLATION ASSAY</b>	<b>40</b>
<b>2.6. TANDEM-AFFINITY-PURIFICATION</b>	<b>41</b>
2.6.1. EXPAND STABLE RAW264.7 CELLS	41
2.6.2. PREPARATION OF CELL-LYSATE	41
2.6.3. TANDEM-AFFINITY-PURIFICATION	41
<b>2.7. MASS-SPECTROMETRY</b>	<b>43</b>
2.7.1. ONE-DIMENSIONAL SDS-PAGE AND SILVER STAINING	43
2.7.2. <i>IN SITU</i> TRYPTIC DIGESTION METHOD	43
2.7.3. LIQUID CHROMATOGRAPHY AND MASS SPECTROMETRY	43
2.7.4. DATA ANALYSIS	44
<b>2.8. CO-IMMUNO-PRECIPITATION</b>	<b>44</b>
2.8.1. TRANSIENT TRANSFECTION IN HEK293T CELLS	44
2.8.2. LYSIS	45
2.8.3. IMMUNOPRECIPITATION	45
<b>2.9. WESTERN-BLOT</b>	<b>46</b>
2.9.1. SDS POLY-ACRYLAMID GEL	46
2.9.2. IMMUNE-BLOT SEMI-DRY	47
<b>2.10. IMMUNE-FLUORESCENCE</b>	<b>48</b>
<b>2.11. REPORTER GENE ASSAY</b>	<b>49</b>
<b>2.12. QUANTITATIVE REAL TIME PCR</b>	<b>49</b>
2.12.1. RNA PREPARATION	49
2.12.2. REVERSE TRANSCRIPTION	49
2.12.3. QRT-PC REACTION	50
2.12.4. USED PRIMERS	50
<b>RESULTS</b>	<b>52</b>
<b>3.1. THE IDEAL CELL-LINE FOR TANDEM AFFINITY PURIFICATION OF TLRs</b>	<b>52</b>
3.1.1. VERIFICATION OF BAIT EXPRESSION BY FLOW CYTOMETRY AND WESTERN-BLOT	52
3.1.2. MTLR-TAP CONSTRUCTS ARE HIGHLY GLYCOSYLATED	55
<b>3.2. PULLDOWN OF ENDOSOMAL TOLL-LIKE-RECEPTORS</b>	<b>57</b>
3.2.1. TANDEM AFFINITY PURIFICATION	57
3.2.2. SILVER-GEL OF TAP ELUATES	57
3.2.3. MASS SPECTROMETRY AND STATISTICAL ANALYSIS	58

<b>3.3. THE INTERACTOR CANDIDATES</b>	<b>64</b>
3.3.1. SERINE/THREONINE-PROTEIN KINASE TAO1 (TAOK1)	64
3.3.2. POLYMERASE DELTA-INTERACTING PROTEIN 3 (POLDIP3)	65
3.3.3. RAS P21 PROTEIN ACTIVATOR 3 (RASA3)	66
3.3.4. RAFTLIN LIPID RAFT LINKER 1 (RFTN1)	67
3.3.5. YAMAGUCHI SARCOMA VIRAL (V-YES-1) ONCOGENE HOMOLOG (LYN)	68
3.3.6. MONOCYTE DIFFERENTIATIONANTIGEN CD14 (CD14)	69
3.3.7. ACID SPHINGOMYELINASE-LIKE PHOSPHODIESTERASE 3B PRECURSOR (SMPDL3B)	70
<b>3.4. VALIDATION OF THE CANDIDATES</b>	<b>71</b>
3.4.1. VALIDATION OF TAOK1	72
3.4.2. VALIDATION OF POLDIP3	73
3.4.3. VALIDATION OF RASA3	75
3.4.4. VALIDATION OF RFTN1	77
3.4.5. VALIDATION OF LYN	78
3.4.6. VALIDATION OF CD14	80
3.4.7. VALIDATION OF SMPDL3B	84
<b>3.5. CD14 AND SMPDL3B INFLUENCE ENDOSOMAL TLR SIGNALING</b>	<b>88</b>
<b><u>DISCUSSION</u></b>	<b><u>92</u></b>
<b>4.1. TANDEM AFFINITY PURIFICATION</b>	<b>93</b>
<b>4.2. VALIDATION OF IDENTIFIED CANDIDATES</b>	<b>94</b>
<b>4.3. TAO KINASE 1 (TAOK1)</b>	<b>94</b>
<b>4.4. POLYMERASE DELTA-INTERACTING PROTEIN 3 (POLDIP3)</b>	<b>95</b>
<b>4.5. RAS P21 PROTEIN ACTIVATOR 3 (RASA3)</b>	<b>96</b>
<b>4.6. RAFTLIN LIPID RAFT LINKER 1 (RFTN1)</b>	<b>97</b>
<b>4.7. YAMAGUCHI SARCOMA VIRAL (V-YES-1) ONCOGENE HOMOLOG (LYN)</b>	<b>97</b>
<b>4.8. MONOCYTE DIFFERENTIATIONANTIGEN CD14 (CD14)</b>	<b>98</b>
<b>4.9. ACID SPHINGOMYELINASE-LIKE PHOSPHODIESTERASE 3B PRECURSOR (SMPDL3B)</b>	<b>99</b>
<b><u>REFERENCES</u></b>	<b><u>101</u></b>

## Abstract

Toll-like receptors (TLRs) are trans-membrane proteins that mediate the recognition of pathogen associated molecular patterns (PAMPs) in innate immunity. Ten structurally highly related TLRs have been identified in mammals, which are either located at the plasma membrane (TLR2, -4, -5, -6 and -11 in mouse) or in the membrane of the endosome (TLR3, -7, -8 and -9). Upon ligand binding, TLRs induce an intracellular signaling cascade to activate transcription factors which initiate the expression of cytokines, interferons and host defense proteins. Notably, a variety of very dissimilar ligands (PAMPs) has been assigned to the structurally highly related TLRs. The complexity of the interface between PAMP and TLR is best understood for the recognition of lipopolysaccharide (LPS) by TLR4. So far, three TLR co-factors have been identified, which are required for the recognition of LPS by TLR4.

The central hypothesis of my thesis postulates that TLRs generally function in protein complexes to mediate ligand binding. To identify receptor associated co-receptors and co-factors that are required for the innate immune response to viral infection we started to systematically search for endosomal Toll-like receptor complexes. To achieve this goal, we employed an interdisciplinary strategy combining biochemistry, cell biology, bioinformatics and proteomics.

The full length murine, endosomal TLRs (3, 7, 8, 9) have been C-terminally tagged with the GS- tandem affinity purification (TAP) cassette. Signaling competent RAW264.7 macrophages have been virally transduced to generate stable TLR expressing cell-lines. To assess the proper processing of the TLR-TAP fusion-proteins we analyzed the glycosylation state of the TLR constructs.

Tandem affinity purifications of RAW264.7 cell lysates containing the different TLR-fusion proteins were performed using special conditions for endosomal transmembrane proteins. Following the identification of co-purified proteins by mass-spectrometry, a bioinformatics approach, based on the CeMM pull down database, as well as in depth analysis of the literature, seven candidates have been selected.

To validate the interactions of the seven selected candidates with endosomal TLRs, co-immunoprecipitation of the human orthologs were performed using transiently transfected HEK293T cells. This allowed the verification of two candidate-TLR interactions. Functional assays, using cell biological, biochemical and immunological methods, were performed to gain insight into the function of those two candidates in innate immunity signaling.

This project helps to broaden our understanding of toll-like receptor mediated recognition of viral pathogens by the innate immune system.

## Zusammenfassung

Toll-like-Rezeptoren (TLRs) sind transmembran Proteine, welche für die Erkennung von Pathogen assoziierten molekularer Strukturen (PAMPs) in der angeborenen Immunität wichtig sind. Zehn strukturell sehr ähnliche TLRs wurden bis jetzt entdeckt, welche entweder in der Plasmamembran (TLR2, -4, -5, -6 und -11) oder in der Membran von Endosomen (TLR3, -7, -8 und -9) lokalisiert sind.

Durch Ligandenbindung können TLRs eine intrazelluläre Signalkaskade induzieren, wodurch die Expression von Zytokine, Interferone und Proteine zur Verteidigung der Zelle und des Organismus angeschaltet wird.

Obwohl die zehn TLRs strukturell stark konserviert sind, kann ein breites Spektrum an strukturell sehr unterschiedlichen Liganden gebunden werden. Die Komplexität der Bindung zwischen TLRs und PAMPs ist am besten bekannt für die Bindung von Lipopolysaccharid (LPS) durch TLR4, welche drei Cofaktoren benötigt.

Die zentrale Hypothese meiner Diplomarbeit geht davon aus, dass TLRs nicht alleine an ihre Liganden binden, sondern verschiedene Co-Faktoren benötigen und in Komplexe eingebunden sind, wie es für TLR4 der Fall ist. Um Rezeptor assoziierte Co-Faktoren zu identifizieren wurde systematisch nach endosomalen TLR Komplexen, die für eine angeborene Immunantwort nach viraler Infektion notwendig sind, gesucht. Eine interdisziplinäre Strategie welche Biochemie, Zellbiologie, Bioinformatik und Proteomik umfasst, wurde angewendet.

Die murinen, endosomalen TLRs (3, 7, 8 und 9) wurden am C-Terminus mit einer GS-Tandem Affinity-Purification (TAP) Kasette versehen. Diese Konstrukte wurden verwendet, um stabile RAW264.7 Makrophagen Zelllinien, mittels retroviralem Gen-Transfers, zu erzeugen. Um die richtige Prozessierung und Lokalisierung der rekombinanten Proteine zu überprüfen, wurde ein Glycosylierungszustand der vier Rezeptoren überprüft. Die Lysate der stabilen RAW264.7 Zell-Linien wurden für Tandem-Affinity-Purification verwendet, wobei spezielle Bedingungen für endosomale Transmembranproteine angewendet wurden.

Anschließend wurden die aufgereinigten Eluate im Massenspektrometer analysiert. Nach bioinformatischer Analyse, basierend auf der CeMM-pulldown Datenbank und Peptidanreicherung, wurde eine Liste von sieben Kandidaten erstellt.

Um zu überprüfen, ob diese sieben Kandidaten tatsächlich mit den endosomalen TLRs interagieren wurde Co-Immunpräzipitation angewendet, wobei die Interaktion von zwei Kandidaten mit TLRs gezeigt werden konnte. Des Weiteren wurden funktionelle Analysen für diese beiden Kandidaten durchgeführt, um Aufschluss über deren Funktion in der angeborenen Immunität zu erhalten.

Diese Arbeit soll dazu dienen das Verständnis von Toll-like Rezeptor vermittelter Pathogen Erkennung und der darauffolgenden Immunantwort zu erhöhen.



## Introduction

All multicellular organisms have evolved mechanisms to defend the host against pathogens. The components which are mediating host defense and immunity are denominated as immune system. The responding reaction of an organism to foreign substances is called immune response (information taken from Abbas, A. and Lichtman, A. 2000).

The immune system of higher vertebrates consists of innate and adaptive components that differ mainly in terms of pathogen recognition and the mechanisms and receptors used for immune recognition. The innate immune system has evolved before the adaptive immune system, and is, with different specificity, present in all multicellular organisms, whereas adaptive immunity is only found in vertebrates, with different specificity (information taken from Abbas, A. and Lichtman, A. 2000).

### 1.1. The Adaptive Immunity

Adaptive immunity is able to distinguish between closely related molecules, in contrast to innate immunity, whereby it is also termed as specific immunity. The name “adaptive immunity” is due to the ability to adapt to the infection. It can increase in magnitude and defensive capabilities with each successive exposure to a particular microbe (information taken from Abbas, A. and Lichtman, A. 2000). Moreover, the adaptive immune system is able to remember and respond more intensified to repeated exposures to the same pathogen.

Immunity is mediated by highly specific antigens that are generated by gene-rearrangement processes during the ontogeny of each individual organism. Such antigen receptors are generated by random processes and are potentially specific for any antigen, since they are not predetermined to recognize any particular structure (Janeway, 1989). Adaptive immunity is mediated by lymphocytes, which comprises two classes of specialized cells, T cells and B cells, and their products. Each lymphocyte displays a single kind of structurally unique receptor, called B-cell receptor and T-cell receptor. The repertoire of antigen receptors in the entire population of lymphocytes is very large and extremely diverse. The size and the diversity of this repertoire is very important to cover as many pathogens and antigens as possible. The generated receptor repertoire is not passed to the next generation, since the diversity of receptors is not germ-line encoded. Antigen receptors for common environmental pathogens have to be reinvented by every generation. The diverse repertoire of receptors is generated randomly, and lymphocytes bearing useful receptors are subsequently selected for clonal expansion after encountering the antigens for which they are specific. This process, which is termed as clonal selection, accounts for most of the basic properties of the adaptive immune system. The main reason for clonal selection is simply “the lack of space” on the genome.

Clonal expansion of one specific cell upon activation needs time, wherefore- compared to the innate immunity- the adaptive immune system takes longer to act and

respond upon pathogen entry. It takes three to five days for sufficient numbers of B-cell clones to be produced by clonal expansion, which further differentiate into effector cells. These few days, in which the adaptive immunity needs to evolve is enough time for most pathogens to damage the host. Thus innate immunity is very important to repress pathogen spreading in the first days of infection (Medzhitov and Janeway, 2000).

## **1.2. The Innate Immune System**

### **1.2.1. Properties of Innate Immunity**

The effector mechanisms of innate immunity, which include antimicrobial peptides, phagocytes, and the alternative complement pathway, are activated immediately upon infection and rapidly interfere with the replication of the infecting pathogen. These mechanisms react only to pathogens and the response is executed always in the same way to repeated infection (Medzhitov and Janeway, 1998).

The very first line of host defense is mediated by physical and chemical barriers, such as epithelia, and antimicrobial substances produced at the epithelial surface. Circulating blood proteins, including members of the complement system, display an important part of the innate immune system. Specialized immune cells with phagocytic properties, such as neutrophils and macrophages, dendritic cells and natural killer cells, are regarded as part of the innate immune system. A very characteristic part of innate immunity is displayed by proteins called cytokines that regulate and coordinate many of the activities of the cells of innate immunity (information taken from Abbas, A. and Lichtman, A. 2000).

Innate immune recognition is mediated by germ-line-encoded receptors, whereby the specificity of each receptor is genetically predetermined. Those receptors have evolved by natural selection to specific moieties of infectious microorganisms, so called pathogen associated molecular patterns (PAMPs).

Innate immunity is not recognizing distinct and specific structures of pathogens, but focuses on a few, highly conserved structures shared by many different microorganisms (Janeway, 1989). These structures are termed as pathogen-associated molecular patterns (PAMPs) and the corresponding receptor of the innate immune system are called pattern-recognition receptors (PRR), which are present on the cells mediating innate immunity. Prevalent and well-known examples for PAMPs are bacterial lipopolysaccharide, peptidoglycan, lipoteichoic acids, mannans, bacterial DNA, nucleic acids and glucans. The main characteristic of PAMPs is the specific existence on microorganism and absence on their host. The structures recognized by the innate immune system are usually an essential part of microorganisms and are therefore indispensable for the pathogen's life cycle. In addition, those PAMPs are usually unvarying structures shared by entire classes of pathogens and can therefore be viewed as molecular signatures of microbial invaders (Medzhitov and Janeway, 2000). Recognition of pathogens by pattern-recognition receptors

activates various types of innate immune responses and often results in direct induction of effector functions.

### **1.2.2. Pattern Recognition Receptors**

The receptors of the innate immune system are expressed on many cells, of capital importance on macrophages and dendritic cells, which are termed professional antigen-presenting cells (APC). Those cells can act immediately after infection, without proliferating first, which accounts for the rapid kinetics of innate immune responses.

PRR belong, according to their structure, to several families of proteins. Domains that are often involved in pattern recognition are Leucine-rich repeat domains, calcium-dependent lectin domains, and scavenger-receptor protein domains.

Functionally, PRR can be divided into three classes: secreted-, endocytic-, and signaling-PRRs. Secreted pattern-recognition molecules are emitted into the blood stream and tissue fluids and are binding to microbial cell walls, where they serve as opsonins by flagging the pathogens for the recognition by the complement system. The mannan-binding lectine is the best-characterized receptor of this class. Signaling receptors recognize PAMPs and activate signal-transduction pathways which induce the expression of a variety of immune-response genes, including inflammatory cytokines. Toll-like receptors (TLRs) are a prominent subgroup of this family and have a major role in the induction of immune and inflammatory responses. Endocytic PRRs are located on the surface of effector cells. Upon PAMP binding these receptors mediate the uptake and delivery of the pathogen into lysosomes, where it is destroyed. The pathogen-derived proteins can be processed, and the resulting peptide can be presented by majorhistocompatibility-complex (MHC) molecules on the surface of macrophages. An example for this type of receptors is the macrophage scavenger receptor which binds to bacterial cell walls. The presentation of pathogen-derived proteins by MHC molecules is furthermore important for communication with the adaptive immune system (Medzhitov and Janeway, 2000).

### **1.2.3. Interaction of Innate and Adaptive Immunity**

One function of innate immunity is to cushion pathogens in the first days of infection, until the adaptive immune system generates an adequate, specific response. However, it has become clear that the innate immune system has a much more important and fundamental role in host defense. The adaptive immune system has the capacity to recognize almost any antigenic structure, since antigen receptors are generated randomly. Thus, mechanisms are needed to distinguish between foreign and host structures, because adaptive immune receptors are not entirely capable to distinguish between bacterial, environmental or self. In contrast, the PRRs of the innate immune system are exclusively binding to microbial pathogen associated structures. Therefore the innate immune system is very important to

prevent binding of self antigens by the adaptive immune system, by controlling the activation of the specific immune response. The adaptive immune system would only shape specific response against a pathogen, whereas the pathogen itself has been recognized by the innate immune system (Medzhitov and Janeway, 2000).

Innate and adaptive immune responses are part of an integrated system of host defense in which different cells and molecules function cooperatively. Both, innate and adaptive immunity, are aligned by two important links. First, the innate immune response upon PAMP binding stimulates the adaptive immune system and influences the nature of the response. Secondly, the adaptive immune system uses many of the effector mechanisms of the innate immunity to eliminate pathogens and it is enhancing the efficiency of innate immunity (information taken from Abbas, A. and Lichtman, A. 2000).

PRRs on innate immune effector cells are in general the first structures to get in contact with pathogens. The activated receptors forward the signal of the present infection to the adaptive immune response (Medzhitov, 2001). Dendritic cells (DCs) have a key role in coupling innate and adaptive immune-recognition systems, due to their function as antigen presenting cells (APCs). Immature DCs are located in peripheral tissues, including the potential pathogen-entry sites, where they can detect and capture microbial invaders (Banchereau and Steinman, 1998).

Immature bone marrow dendritic cells (BMDCs) express a full set of PRR, which induce DC maturation upon activation. Mature DCs express high levels of MHC and co-stimulatory molecules (CD80 and CD86) and migrate to draining lymph nodes where they present pathogen-derived antigens to naïve T cells (Banchereau and Steinman, 1998). Furthermore, the activation of TLRs induces expression of various cytokines, including IL-12 in DCs, which are necessary for the differentiation of naïve T-cells into effector T-cells (Fig. 1.2.1.) (Akira et al., 2001).

Thus PRRs play a very important role in the crosstalk of innate and adaptive immunity. Toll-like receptors display a very important subclass of PRRs, that is mainly responsible for cytokine and interferon production upon infection.

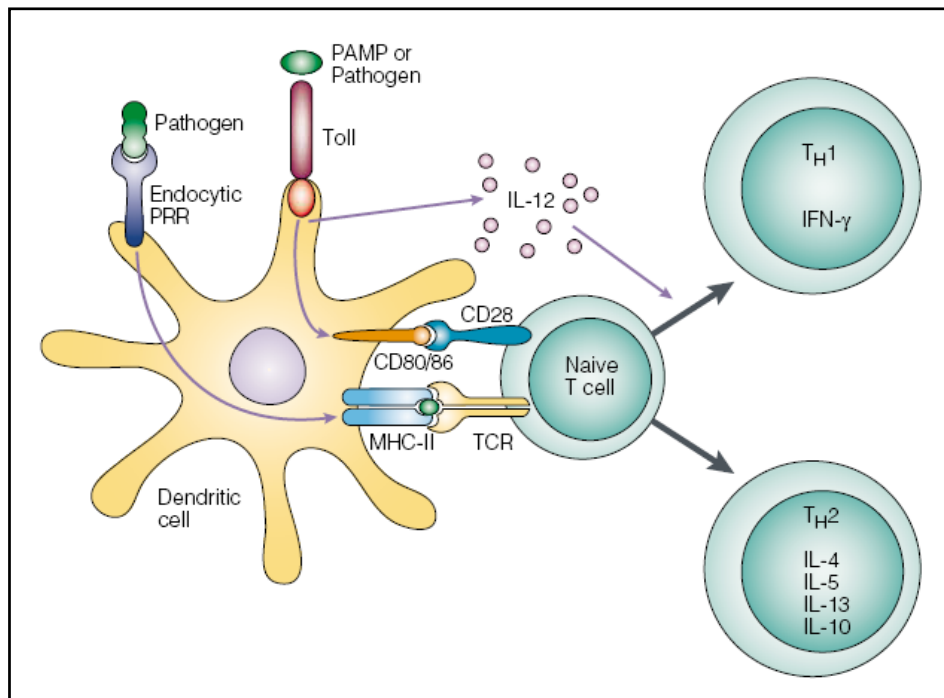


**Figure 1.2.1.: Role of TLRs in control of adaptive immunity.** TLRs sense the presence of pathogens through recognition of PAMPs. Recognition of PAMPs by TLRs expressed on antigen-presenting cells (APC), such as DCs, induces cell-surface expression of co-stimulatory (CD80 and CD86) molecules and major histocompatibility complex class II (MHC II) molecules. TLR activation also leads to expression of cytokines, such as interleukin-12 (IL)-12, and chemokines and their receptors, and trigger many other events associated with DC maturation. Induction of CD80/86 on APCs by TLRs leads to the activation of T cells specific for pathogens that trigger TLR signaling. IL-12 induced by TLRs also contributes to the differentiation of activated T cells into into effector T-cells like T helper (TH)1 effector cells. Illustration and information taken from (Medzhitov, 2001).

### 1.3. Toll-like Receptors

#### 1.3.1. The Toll-receptor

Toll-like receptors are part of the endocytic PRR family and have a unique and essential function in immunity. TLRs are type I transmembrane receptors, characterized by an intracellular toll/IL-1 receptor (TIR) domain and extracellular leucine-rich repeat (LRR) domains. LRR domains are found in a diverse set of proteins where they are involved in ligand recognition and signal transduction (Hashimoto et al., 1988).

The TIR domain is conserved in a number of transmembrane and cytoplasmic proteins in animal and plants as well (Aravind et al., 2001).

Toll and Toll-related proteins are widely expressed in insects, plants, and animals. The toll-receptor in *Drosophila* (dToll) was the first identified member of the Toll family. It was initially discovered as a gene that controls dorsoventral axis formation in the fruit fly embryo (Hashimoto et al., 1988). Moreover, dToll was not only shown to be involved in embryo axis formation but has been shown to be involved in defense against fungi (Lemaitre et al., 1996). Flies that lack the dToll protein are highly susceptible for fungal infections (Lemaitre et al., 1996).

So far nine members of the toll-family have been identified in *Drosophila*, a few examples are: dToll, 18-wheeler (18W), MstProx, SDSDm2245, Tollo, and Tehao (Means et al., 1999). At least dToll, Tehao and 18W are involved in immune responses against fungal and bacterial pathogens (Luna et al., 2002).

Further members of the dToll pathway encode the Toll ligand Spätzle, the dToll adaptor protein Tube, the protein kinase Pelle, the transcription factor Dorsal and the Dorsal inhibitor Cactus (Fig. 1.3.1.). Dorsal is a member of the nuclear factor- $\kappa$ B (NF- $\kappa$ B) family and Cactus is homologue to the mammalian inhibitor of  $\kappa$ B (I $\kappa$ B). Spätzle serves as a ligand for dToll, and is secreted as a precursor protein that has to be cleaved by the serine proteases Easter (DeLotto and DeLotto, 1998) prior to dToll activation (Belvin and Anderson, 1996).

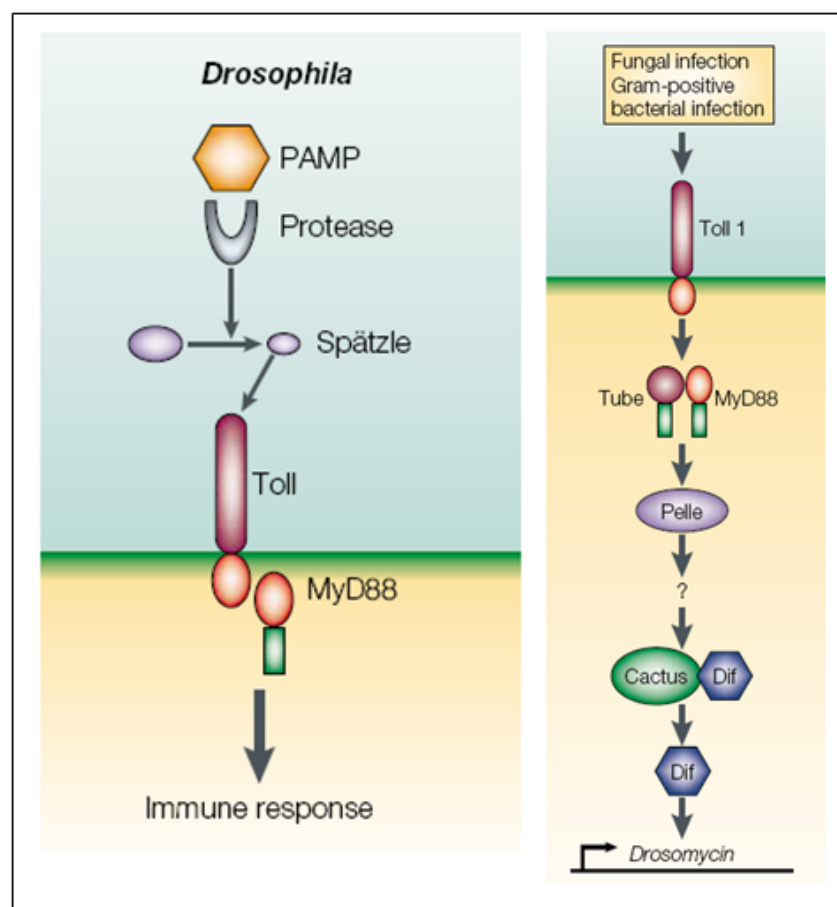


**Figure 1.3.1.:** Pattern recognition of drosophilas dToll by Spätzle and downstream signaling transduction after activation of dToll in drosophila. Illustration and information taken from (Medzhitov, 2001).

Besides its function in developmental patterning, the similarity between the mammalian IL-1R pathway and the drosophila dToll pathway, suggested the involvement in fruit-fly immunity. This suggestion was further confirmed by a dToll knock out fruit-fly, which rapidly succumbed to fungal infection. Drosomycin is a target gene of the drosophila dToll pathway and has antifungal properties. If one of the pathway components is missing, such as Spätzle, Tube or Pelle, the flies show higher susceptibility for fungal infections as well (Lemaitre et

al., 1996). The dToll innate immune pathway and the drosophila developmental patterning pathway only differ in the NF- $\kappa$ B like member Dorsal that is rather involved in the development, whereas drosophila immunity factor (DIF) is present in the innate immune pathway (Shin et al., 2005).

The dToll receptor in drosophila does not directly bind to pathogens, but it recognizes the cleaved form of Spätzle (Fig.1.3.1.). Instead, the processing of Spätzle upon infection into a biologically active form activates the dToll pathway (Levashina et al., 1999). The dToll pathway in drosophila can also be activated by gram-positive infection, indicating that several pattern-recognition molecules might act upstream of the protease cascade that controls cleavage of Spätzle (Khush et al., 2001). Thus, the pattern recognition event in drosophila seems to occur upstream of dToll and further triggers a protease cascade, comparable to the complement activation by the lectin pathway in mammals (Lemaitre et al., 1996). Different target genes are activated upon different ligands. A fungal infection triggers the expression of Drosomycin, whereas Dipterincine is made in response to gram negative bacteria (Lemaitre et al., 1997).

In mammals homologues proteins to dToll have been identified, which are termed as Toll-like receptors.

### 1.3.2. Toll-like Receptors

Toll like receptors are evolutionary highly conserved pattern recognition receptors that bind a variety of pathogen associated molecular patterns (PAMPs) (Tab.1.3.2.). The discovery of mammalian TLRs followed the discovery of Toll in *Drosophila melanogaster*.

In 1997 Medzhitov and Janeway identified a gene in mammals with high sequence homology to dToll. The gene encoded a transmembrane protein containing an extra cellular domain, harboring leucine-rich repeats (LRRs) and an intracellular signaling domain with high homology to the interleukin-1 (IL-1) receptor (Medzhitov et al., 1997). Upon constitutive activation this protein showed increased production of the pro-inflammatory cytokines IL-1, IL-6 and IL-8 (Medzhitov and Janeway, 1997). Because of this properties and the relation to dToll, Medzhitov proposed human Toll (hToll, later called TLR4) the first described PRR, linking the innate- and adaptive immune system in mammals (Medzhitov et al., 1997).

During the following decade ten further TLRs have been identified in humans (Tab. 1.3.2.) (Akira et al., 2006). All these TLRs are type-I integral membrane glycoproteins characterized by extracellular domains harboring varying numbers of LRRs and a cytoplasmic signaling domain that is homologous to the IL1R intracellular domain, also called Toll/IL1R (TIR) domain (O'Neill and Bowie, 2007).

TLRs have been reported to be highly glycosylated on their extracellular domains (Choe et al., 2005; Zhu et al., 2009). Thus, TLRs need to be processed through the Golgi in order to be glycosylated (Latz et al., 2004).

The majority of TLRs localize to the plasma membrane, facing the extracellular space (Tab. 1.3.2.) (Takeda et al., 2003). However a subset of TLRs, namely TLR3, -7, -8, and -9, is located in the endosomes of specialized immune cells. These TLRs screen in-coming material for pathogens and seem to be particularly important for the recognition of viruses and bacteria, since they share the ability to sense nucleic acid (Bowie and Haga, 2005).

	localization	agonist	adaptor
<b>TLR1</b>	cell surface	<b>bacteria:</b> triacyl lipoproteins	MyD88/MAL
<b>TLR2</b>	cell surface	<b>bacteria:</b> lipoproteins, peptidoglycan, lipoteichoic acids; <b>fungi:</b> zymosan, mannans; <b>viruses:</b> glycoprotein of Measles virus, HSV-1	MyD88/MAL
<b>TLR3</b>	endosome	<b>viruses:</b> dsRNA in virally infected cells, poly-I:C, poly-I	TRIF
<b>TLR4</b>	cell surface	<b>bacteria:</b> lipopolysaccharide; <b>fungi:</b> mannans; <b>viruses:</b> glycoproteins of MMTV and RSV	MyD88/MAL TRIF/TRAM
<b>TLR5</b>	cell surface	<b>bacteria:</b> flagellin	MyD88
<b>TLR6</b>	cell surface	<b>bacteria:</b> diacyl lipoproteins	MyD88/MAL
<b>TLR7</b>	endosome	<b>viruses:</b> nucleotide analogs, ssRNA	MyD88
<b>TLR8</b>	endosome	<b>viruses:</b> nucleotide analogs, ssRNA	MyD88
<b>TLR9</b>	endosome	<b>bacteria:</b> unmethylated DNA motifs; <b>viruses:</b> DNA	MyD88
<b>TLR10</b>	cell surface	Unknown	Unknown
<b>TLR11</b>	cell surface	<b>parasite:</b> profilin-like molecule	MyD88

**Table 1.3.2.: Murine Toll-like receptors, their localization, agonists and signaling molecules.**

In the past few years, dozens of TLR ligands have been identified (Akira et al., 2001). Many more ligands are yet to be introduced; both for those with no known ligands and for those TLRs that already have assigned ligands (Tab. 1.3.2.).

TLR agonists are quite diverse in structure and origin; however, they share common themes due to their native function. In general many if not all TLRs are able to recognize several, structurally diverse ligands. Some of the toll-like receptors require accessory proteins to recognize their ligands. Mammalian TLRs and the *Drosophila* dToll differ in binding their ligands, since dToll is not binding to the initial ligand, but is downstream of a caspase cascade, whereas mammalian TLRs are reported to bind directly to their ligands (Medzhitov, 2001).

### 1.3.3. Structure of Toll and Toll-like Receptors

Toll and Toll-related proteins share a conserved modular structure (Rock et al., 1998). The extracellular domains (ectodomains) of these receptors contain blocks of repeats of a 24-



amino-acid motif, called a leucine rich repeat (LRR), usually with cysteine-rich capping structures at the amino and carboxyl termini of each block (Fig. 1.3.3.). TLRs only harbor a single block of LRRs, but dToll from *Drosophila* contains two discrete blocks of LRRs and associated capping structures (Gay and Gangloff, 2008).

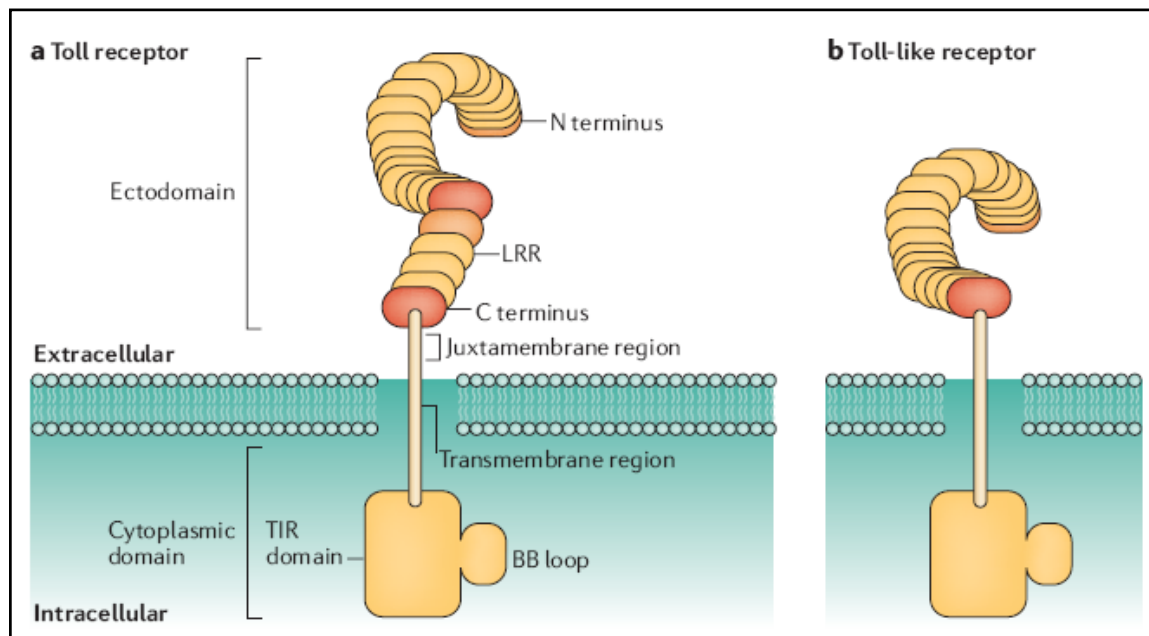


**Figure 1.3.3.: Structure of dToll and TLRs.** Schematic diagram of Toll receptor (a) and Toll-like receptor (b), showing the extracellular, transmembrane, juxtamembrane region and cytoplasmic domains of the receptors. dToll has two independent blocks of LRRs in the ectodomain. Illustration and information taken from (Gay and Gangloff, 2008).

These LRRs are found in a very large and diverse group of proteins, where their function ranges from RNA processing and transcriptional regulation to cell adhesion, bacterial pathogenesis and signal transduction (Buchanan and Gay, 1996).

The C-terminal capping structure of dToll and TLRs is connected to the single transmembrane  $\alpha$ -helix and the cytoplasmic domain, known as the Toll/ interleukin-1 receptor (TIR) domain, which couples downstream signal transduction to receptor engagement. Due to the hydrophobic core of each LRR, these domains fold into a curved structure, which is termed as horse-shoe like structure, due to its shape. The specificity of the molecular recognition of TLRs is mediated by the side chains of variable residues that protrude from the short parallel  $\beta$ -strand of each LRR. The arrangement of these side chains can be viewed as a combinatorial code that is able to bind specific ligands, whereby LRRs can generate a wide range of binding specificities for proteins and other biological molecules. Thus different members of the Toll-family are able to respond to stimuli with very different properties (Tab. 1.3.2.), although they share a similar structure. These stimuli range from the binding of dToll to the cytokine Spätzle, to binding of TLRs to hexacylated lipids, or to small molecules such as the imidazoquinolines (Fig. 1.3.4.) (Gay and Gangloff, 2008).

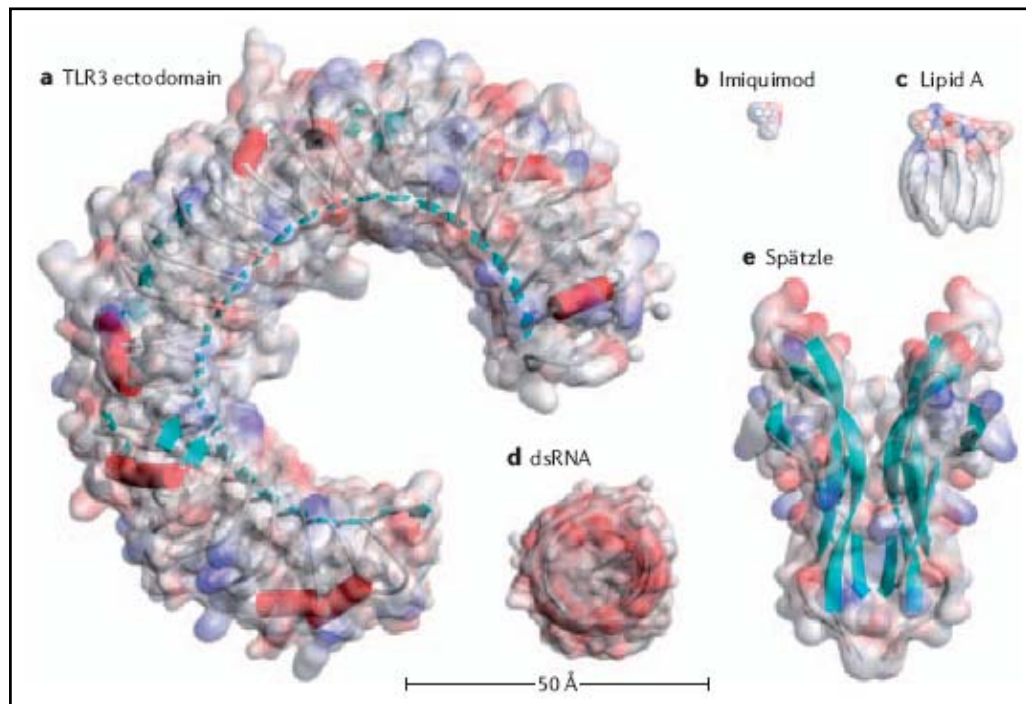


**Figure 1.3.4.: Structure of the TLR3 ectodomain and possible ligands. All molecules are illustrated to scale. Illustration and information taken from (Gay and Gangloff, 2008).**

The diversity of ligands recognized by single TLRs questions whether TLRs bind their ligands directly or whether the targeting is mediated indirectly (Gay and Gangloff, 2008). Co-receptors for several TLRs have been identified to mediate ligand binding. For example, the recognition of lipopolysaccharide (LPS) by TLR4 requires the co-receptors MD2, therefore LPS indirectly activates TLR4. Further co-factors, lipopolysaccharide binding protein (LPS) and Cd14, have been identified to mediate the binding of LPS by TLR4. Tight ligand binding induces a conformational change and activate the downstream signaling cascade of TLRs (Nagai et al., 2002).

#### 1.3.4. Signal Induction by TLRs

The basic mechanism of signaling by dToll and TLRs seems to involve ligand-induced dimerization or oligomerization. Both *in vivo* and *in vitro* experiments in *Drosophila* have shown that the binding of Spätzle crosslinks two dToll ectodomains in a symmetric complex. This crosslinking is necessary and sufficient for signal transduction (Fig. 1.3.5.).

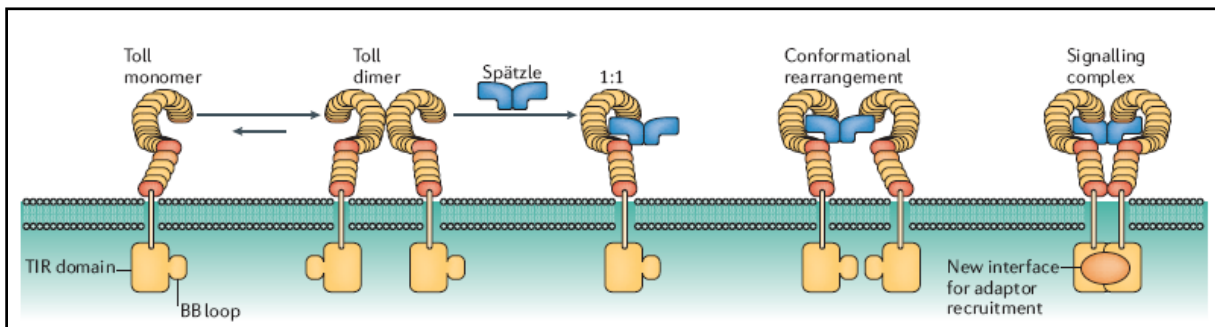


**Figure 1.3.5.: Model for dToll activation by Spätzle.** In the absence of ligand, dToll ectodomains are found in equilibrium between monomers and dimers. The first block of LRRs might mediate this interaction and further block tight binding by steric constraint. The ligand Spätzle dissociates the dToll dimers and binds only to one receptor but is recruiting a second receptor molecule. This results in a conformational rearrangement, whereby the BB loop of the signaling TIR domain is likely to be involved in receptor-receptor contacts. This complex generates a new interface for adaptor recruitment. Illustration and information taken from (Gay and Gangloff, 2008).

Similar mechanisms are likely to apply also for vertebrate TLRs (Latz et al., 2007). Furthermore, the process of ligand binding is likely to induce a series of conformational changes, even though receptor cross-linking is a crucial event in signal transduction (Weber et al., 2005).

Recent evidence indicates that the juxtamembrane region of the ectodomain of dToll is mediating receptor-receptor interaction. A steric constrain that is imposed by the N-terminal region, prevents self-association of the receptors, whereas binding of Spätzle relieves this constrain. Therefore the N-terminal region of the dToll ectodomain has auto-inhibitory function and prevents unregulated dimerization (Hu et al., 2004). For vertebrate TLRs several observations argue for a similar mechanism for receptor engagement, since many TLR-specific antibodies can crosslink two TLR molecules but do not induce signaling (Shimazu et al., 1999).

Receptor activation is a sequential process, whereby ligand binding induces a conformational change in the C-terminal region of the ectodomain that makes stable receptor–receptor interactions possible. This conformational change arranges the transmembrane helices of the receptor dimer in a manner that allows downstream signaling to occur (Gay and Gangloff, 2008).

### 1.3.5. The TLR “Signalosome”

Activation of signal transduction pathways by TLRs leads to the induction of various genes that function in host defense, including inflammatory cytokines, chemokines, major histocompatibility complex (MHC) and co-stimulatory molecules. Mammalian TLRs also induce multiple effector molecules such as inducible nitric oxide synthase and antimicrobial peptides, which can directly destroy microbial pathogens (Medzhitov, 2001).

TLRs activate the same signaling molecules that are used for IL1R signaling through a conserved Toll/IL1 Receptor (TIR) domain (Kawai and Akira, 2005). Five adaptor molecules are known to signal downstream of TLRs (Bowie, 2007). These are Myeloid differentiation factor 88 (MyD88), TIR-domain containing adaptor molecule inducing IFN- $\beta$  (TRIF), MyD88 adaptor-like (MAL) protein (also called TIR adaptor like protein (TIRAP)), TRIF-adaptor related adaptor molecule (TRAM) and sterile  $\alpha$ - and armadillo-motif-containing protein (SARM). Usage of different combinations of adaptor proteins partly explains differences in cytokine production after TLR triggering (O'Neill and Bowie, 2007).

Upon ligand binding to TLRs, downstream signaling partners, are interacting with the cytoplasmic portion of the respective TLRs. With the exception of TLR3, MyD88 interacts with the cytoplasmic part of all TLRs upon stimulation. TLR3 and TLR4 use a MyD88 independent TRIF- or TRAM-mediated pathway whereas for TLR7, -8 and -9 MyD88 is required (O'Neill and Bowie, 2007). TLR4 and TLR2 require the bridging molecule TRAM (Fitzgerald et al., 2003), whereas TLR3 directly recruits TRIF to its TIR domain (Hoebe et al., 2003).

The recruitment of MyD88, or other signaling partners, results in formation of a complex with IL1R associated kinase-1 (IRAK-1) and IRAK-4 (Suzuki et al., 2002), as well as IRAK-2 (Keating et al., 2007). This complex further engages tumor necrosis factor receptor (TNFR) associated factor 6 (TRAF6) (Kawai and Akira, 2006) that activates the NF- $\kappa$ B and Janus kinase (JNK) signaling cascade, as well as Interferon regulatory factor (IRF) 7 and/or IRF5 (Honda et al., 2005; Takaoka et al., 2005). These signaling cascades result in binding of activated transcription factors to the corresponding NF- $\kappa$ B, ATF-2/cJun (AP1) and IRF-binding sites and lead to the expression of IFN- $\alpha/\beta$  and pro-inflammatory cytokines such as IL12p40 and IL6 (Honda et al., 2005) (Fig. 1.3.6.).

Moreover, TRIF can recruit TRAF-family-member-associated NF- $\kappa$ B activator (TANK) binding kinase 1 (TBK1) via TRAF3 (Oganesyan et al., 2006). This recruitment results in the phosphorylation of IRF3 and -7, which form hetero- or homodimers and translocate into the nucleus to bind and activate the IFN-promoter (Honda et al., 2006).

The extracellular signal-regulated kinase (ERK) can be activated in a Sky-dependent way upon TLR activation, and regulates IL-2 and IL-10 production in DCs (Slack et al., 2007).

TLR7 and -9 mediated IFN- $\alpha$  production is restricted to plasmacytoid dendritic cells (pDC) (Uematsu and Akira, 2007). This subset of dendritic cells (DCs) has also been described as interferon producing cells (IPC) due to the vast amounts of IFN- $\alpha/\beta$  produced after virus infection (Liu, 2005). Furthermore, pDC and conventional dendritic cells (cDC) use a MyD88 dependent signaling pathway, which, in pDC, suggests either a branching of signaling events downstream of this molecule or engagement of additional molecules beside MyD88 (Schmitz et al., 2007). In case of pDC, TLR7/9 triggering leads to formation of a complex consisting of MyD88, IRAK-1, IRAK-4, TRAF-3 and -6, TBK1 and IRF7 (Uematsu and Akira, 2007).



On human macrophages high amounts of TLR2 and TLR4 are expressed, whereas only spars TLR7 and TLR9. In humans, TLR9 is exclusively expressed on pDCs and B-cells (Iwasaki and Medzhitov, 2004).

TLR ligands can induce differential cytokine responses, depending on which cell type they are expressed. For incidence the activation of TLR9 on pDCs mainly leads to the production of IFN- $\alpha$ , whereas the activation of TLR9 on cDCs results in the secretion of IFN- $\beta$ , IL6 and other pro-inflammatory cytokines. The reason for the diverse expression pattern upon stimulation is due to partialities in downstream signaling components. The signaling pathways of cDCs are strongly depending on IRF1 but not on IRF7. Contrary to pDCs, that need IRF7 but do not require IRF1 (Schmitz et al., 2007). This finding suggests that activation of PRR is coupled differently to downstream signaling molecules in a cell-type specific manner.

The cells of the innate immune system are clearly specialized, resulting in optimal defense against a diverse range of pathogens, without harming the host.

### **1.3.7. Toll-like Receptor 4**

Beside the endosomal TLRs, which are the key-players of my thesis, I would like to describe TLR4 in more detail, since this plasma membrane associated PRR is the first characterized and best studied mammalian TLR. Its properties are representative for other TLRs (Medzhitov et al., 1997). It is expressed in a variety of cell types, most predominantly in the cells of the immune system, including macrophages and DCs (Medzhitov et al., 1997).

TLR4 functions as the signal-transducing receptor for LPS (Poltorak et al., 1998). TLR4 is recognizing LPS as a complex, comprising several accessory molecules. LPS is first bound to the secreted protein LBP (LPS-binding protein). LBP assigns LPS to Cd14, which is a high-affinity LPS receptor that can either be secreted into the serum, or can be found as a glycoposphoinositol (GPI)-linked protein on the surface of macrophages (Wright et al., 1990). MD-2 is a further component of the LPS receptor complex (Shimazu et al., 1999) that lacks a transmembrane region and is expressed on the cell surface in association with the ectodomain of TLR4 (Shimazu et al., 1999). The molecular mechanism of TLR-mediated recognition is one of the most challenging issues in Toll biology. Several lines of evidence indicate that TLR4 might interact with LPS directly (Poltorak et al., 2000). However, it is clear that CD14 and MD-2 have an assistant function in the binding of LPS by TLR4 (Poltorak et al., 2000) (Fig. 1.3.7.).

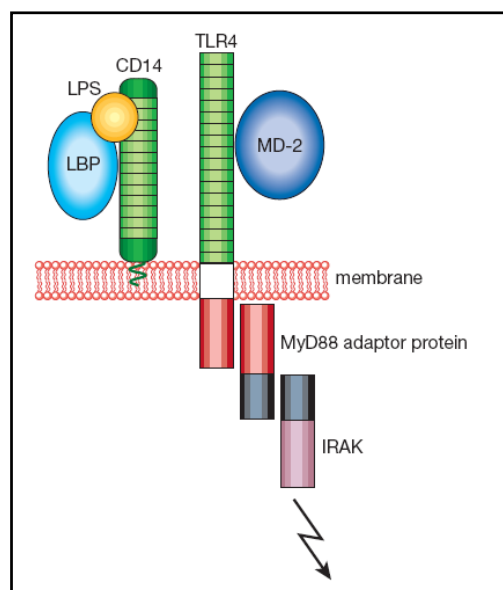


**Figure 1.3.7.:** Recognition of LPS on the surface of phagocytes. LPS is captured by LBP, and the complex is recognized by CD14, on the macrophage surface. CD14 associates with the cell surface. MD-2 is a secreted protein that binds to the extracellular domain of TLR4 and is important in its signaling. Illustration and information taken from (Aderem and Ulevitch, 2000).

TLR4 is implicated in the recognition of taxol, a diterpene purified from the bark of the western yew (*Taxus brevifolia*) (Byrd-Leifer et al., 2001). In addition, TLR4 has been shown to be involved in the recognition of endogenous ligands, such as heat shock proteins (HSP60 and HSP70), the extra domain A of fibronectins, oligosaccharides of hyaluronic acid, heparan sulfate and fibrinogen. However, all of these endogenous ligands require very high concentrations to activate TLR4 (Takeda and Akira, 2005).

### 1.3.8. Endosomal Toll-like Receptors

Endosomal TLRs represent the subset of TLRs that recognizes mainly viral components and induce antiviral responses. Four different TLRs are associated with the endosome, TLR3, -7, -8 and -9, that recognize pathogen nucleic acids on the endosomal membrane. After pattern recognition, these receptors activate an intrinsic signaling pathway to induce pro-inflammatory cytokines and host defense.

Endosomal TLRs show different expression patterns on different cell types. TLR3 is present on cDCs, whereas TLR7, -8 and -9 are expressed on pDCs. All endosomal toll-like receptors are able to sense nucleic acid that gains access into endosomes. The activation of endosomal TLRs leads to the production of IFN- $\alpha/\beta$  upon virus infection (Uematsu and Akira, 2007).

Until now only little is known about endosomal TLRs and possible co-factors. One accessory protein, of endosomal TLRs is Unc93b1 that has been shown to be required for TLR3, -7 and -9 signaling. A single point mutation in the endoplasmic reticulum (ER) resting membrane protein Unc93b1 abolishes signaling via TLR3, -7 and -9 (Brinkmann et al., 2007).



Furthermore, the Ploegh lab has shown that the function of the polytopic membrane protein UNC93b1 is to deliver the nucleotide-sensing receptors TLR7 and TLR9 from the ER to endolysosomes (Kim et al., 2008).

### Toll-like Receptor 3

TLR3 was the first identified antiviral TLR and is recognizing double-stranded RNA (dsRNA), which is solely produced in pathogens (Schroder and Bowie, 2005). Most viruses produce dsRNA at some point of their infection cycle, whereby TLR3 plays an important role in host response to viruses (Medzhitov, 2001). The synthetic dsRNA analogue polyinosinic-polycytidylic acid (polyI:C) induces IFN- $\alpha/\beta$ . This finding supported the conception that long dsRNA serves as determinant for virus infection (Field et al., 1967).

TLR3 is expressed on many cell types, although predominantly on cDC (Iwasaki and Medzhitov, 2004; Reis e Sousa, 2004). TLR3 is activating the NF- $\kappa$ B pathway upon stimulation with dsRNA and polyI:C *in vitro* (Alexopoulou et al., 2001). TLR3 on CD8 positive cDC (CD8<sup>+</sup> DC) can recognize dsRNA in virus-infected cells (Schulz et al., 2005). Cells loaded with polyI:C can be phagocytosed by CD8<sup>+</sup> DCs and further activate the production of IFN- $\beta$  and other pro-inflammatory cytokines, such as IL6. The cytokine production results in increased ability of the DC to activate T-cells (Schulz et al., 2005). Furthermore, it was proposed that mRNA and poly-inosinic acid (poly-I) are sufficient to activate TLR3, suggesting that special forms of ssRNA might have stimulatory activity on TLR3 (Marshall-Clarke et al., 2007). Macrophages lacking a functional TLR3 signaling cascade were compromised in their ability to suppress vaccinia virus replication *in vitro*. Infection of TLR3 deficient mice with murine cytomegalovirus (MCMV) resulted in increased viral titers in the spleen, slightly increased mortality, decreased serum levels of IFN- $\alpha/\beta$  and other cytokines and decreased activation of natural killer (NK) cells (Edelmann et al., 2004). Nevertheless several *in vivo* studies demonstrated that TLR3 is dispensable for the outcome of a virus infection. TLR3-deficient animals show almost unchanged susceptibility to viruses such as vesicular stomatitis virus (VSV) lymphochoriomeningitis virus (LCMV) and reovirus (ReoV) when experimentally infected (Edelmann et al., 2004).

Upon ligand binding TLR3 uses a MyD88 independent TRIF- or TRAM-mediated pathway (O'Neill and Bowie, 2007). Structurally TLR3 has interesting features that distinguish it from other mammalian TLRs. TLR3 does not contain the conserved proline residue in the position equivalent to proline-712 of mouse TLR4 (Medzhitov, 2001). So far the N-terminus of TLR3 is the only endosomal TLR ectodomain that has been successfully crystallized (Fig. 1.3.8.) (Choe et al., 2005). The LRRs form a horseshoe-like structure that was initially thought to provide a binding-pocket for the ligand (Choe et al., 2005). Surprisingly, extensive mutagenesis analysis suggest, that dsRNA binds on the lateral side of the TLR3 ectodomain (Bell et al., 2006).



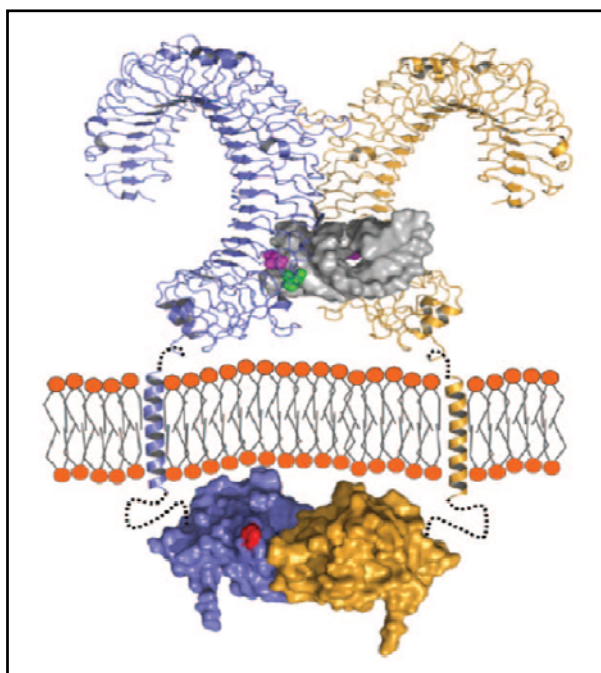


**Figure 1.3.8.:** A proposed signaling complex of full-length TLR3 binding a 19-bp dsRNA molecule. The model includes the 22-residue transmembrane helices and the TIR domains. Single receptors are shown in blue or orange. Linker regions between the LRR-CT and the transmembrane domain as well as the transmembrane domain and the TIR domain are denoted by black dotted lines. Illustration and information taken from (Bell et al., 2006).

Cd14 is, so far, the only co-factor of TLR3 that has been identified to assist binding of polyI:C. Cd14 is physically interacting with polyI:C, where it enables polyI:C internalization by TLR3 (Lee et al., 2006).

In the experimental procedures of this thesis polyinosine-polycytidylic acid (polyI:C) was used as ligand for TLR3 stimulation. PolyI:C is a synthetic analog of double-stranded RNA (dsRNA). dsRNA is known to induce interferons (IFN) and other cytokines production. IFN induction is mediated by two different pathways. The first pathway leading to NF- $\kappa$ B activation depends on the dsRNA-responsive protein kinase (PKR) (Chu et al., 1999), whereas the second pathway is PKR-independent and involves TLR3 (Alexopoulou et al., 2001).

### **Toll-like Receptor-7 and -8**

TLR7 and TLR8 show a high degree of similarity to TLR9 and both are located on the X-chromosome. Both receptors are mainly localized at the endoplasmic reticulum (ER) and at endosomes (Jurk et al., 2002).

TLR7 and TLR8 are structurally highly conserved proteins, and have been initially found to recognize imidazoquinolins (e.g. R848, Imiquimod, etc) (Hemmi et al., 2002). Furthermore, human TLR7 and human TLR8 have been shown to recognize guanosine or uridine-rich single-stranded RNA (ssRNA) from viruses such as human immunodeficiency virus, vesicular stomatitis virus and influenza virus (Heil et al., 2004). Although ssRNA is abundant in the host, usually the host-derived ssRNA is not detected by TLR7 or TLR8. This

might be due to the fact that TLR7 and TLR8 are expressed in the endosome, and host-derived ssRNA is not delivered to the endosome (Akira et al., 2001). TLR7 recognizes RNA that is delivered into endosomes but the molecular details leading to TLR7 activation are only poorly understood. Various studies have proposed the existence of sequence-dependent “immunostimulatory motifs” leading to TLR7 activation (Heil et al., 2004). More recently it was demonstrated that three or more uridine molecules on a ribose backbone are necessary and sufficient for TLR7 stimulation (Diebold et al., 2006). Activation of TLR7 can lead to differential cytokine responses depending on the used stimulus. In murine pDC, a RNA homopolymer consisting of uridine nucleotides (poly-U) induces high amounts of IFN- $\alpha$  but little IL6, whereas R848 and Loxoribine elicit much less IFN- $\alpha/\beta$  but potent IL6 responses (Diebold et al., 2006).

Upon ligand binding TLR7 and TLR8 are signaling via the adaptor molecule MyD88 (O'Neill and Bowie, 2007). The lab of Barton has shown that TLR7 is cleaved after shuttling to the endolysosome, resulting in absence of full-length protein in the endosomes, where the ligand is recognized (Ewald et al., 2008).

In our project we are using the small synthetic compound imiquimod (Fig. 1.3.9.) to stimulate TLR7 and TLR8. Imiquimod (R837), an imidazoquinoline amine analogue to guanosine, is an immune response modifier with potent indirect antiviral activity. The antiviral activity of imiquimod was first shown in guinea pigs infected with herpes simplex virus (Miller et al., 1999). This low molecular synthetic molecule induces the production of cytokines such as IFN- $\alpha$ . This activation is MyD88-dependent and leads to the induction of the transcription factor NF- $\kappa$ B (Hemmi et al., 2002).

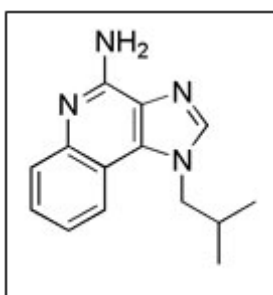


Figure 1.3.9.: Chemical structure of imiquimod (picture taken from [www.invivogen.com](http://www.invivogen.com))

### Toll-like Receptor 9

TLR9 can be activated by unmethylated 2′deoxyribo(cytidine-phosphate-guanosine) (CpG) DNA motifs that are present in bacterial and viral DNA. In mammalian genomes such motifs are mainly methylated (Hemmi et al., 2002). Although TLR9 was initially described as a receptor activated in bacterial infection, it became clear that TLR9 is further important for recognition of DNA viruses such as herpes simplex virus 2 (HSV-2), HSV-1 and MCMV (Krug et al., 2004a; Krug et al., 2004b; Lund et al., 2003). pDC are the main cell type producing IFN- $\alpha$

after stimulation with CpG DNA and viruses but other cell types can produce pro-inflammatory cytokines like IL6 (Akira et al., 2006).

The endosomal localization of TLR9 can be seen as a mechanism to minimize responses to self-DNA that can be released from cells during necrotic cell death. The endosomal localization guarantees for the specificity of TLR9, since extracellular DNA is quickly degraded and does not allow activation of TLR9 (Barton et al., 2006). The endosomal localization of TLR9 not only prevents recognition of self DNA, but also increases the effectiveness in recognizing pathogenic DNA (Barton et al., 2006).

Upon DNA binding TLR9 undergoes a conformational change that initiates downstream signaling *in vitro* (Latz et al., 2007). However, it is still not entirely clear how this works *in vivo* and whether cell type specific TLR9-dependent cytokine expression patterns can solely be explained by conformational change of the receptor (Latz et al., 2007). Ploegh and his group recently showed that TLR9 is proteolytically cleaved after stimulation. The inhibition of lysosomal proteolysis results in TLR9 inactivity (Park et al., 2008).

Synthetically generated CpG is used in experimental approaches to activate TLR9. Basically two types of CpG oligonucleotides are generally used, that differ in their sequence: CpG-A (also called D-type CpG) with a 3' poly-C sequence and CpG-B (also called K-type CpG) can both stimulate TLR9, but lead to different cytokine production in pDC (Klinman, 2004; Krieg, 2002). CpG-A elicits IFN- $\alpha$  from pDC, whereas CpG-B promotes lower levels of IFN- $\alpha$  but initiates large amounts of IL6 and TNF- $\alpha$ . Interestingly, pDC retain CpG-A in early endosomes for a longer time than CpG-B, which is transported into lysosomal compartments quickly after uptake (Honda et al., 2005). Similarly to CpG-B in pDC, CpG-A is transported into lysosomal compartments in cDC and can elicit a TLR9 dependent IFN- $\alpha$  response (Honda et al., 2005). Interestingly, signaling by CpG DNA requires its internalization into late endosomal or lysosomal compartments (Hacker et al., 1998). The shuttling from the endoplasmic reticulum (ER), where resting TLR9 is located, might be mediated by the polytopic membrane protein UNC93b1 that serves as essential accessory protein of TLR9 (Kim et al., 2008).

## 1.4. Tandem Affinity Purification

Proteins never function alone, but are integrated in complexes and are further constantly interacting among each other, which is one of the most important characteristics of molecular life. Not only the identification of new proteins, but also the characterization of the interaction between different components is a very important part of science and it reflects the processes which occur within a cell and an organism.

Many different methods evolved to characterize interacting partners of distinct proteins. A new and very popular method is called tandem affinity purification (TAP), where a distinct peptide is used as bait to fish for cooperating factors. TAP is a two-step affinity purification peptide pulldown that allows the isolation of protein complexes under close-to-physiological conditions, preparatory for mass spectrometry analysis. This method not only increases the overall yield, which is necessary for subsequent analysis by mass-spectrometry, it further ensures improved purity of the resulting samples. In general this method is prevalent for proteomics and for the detection of binding partners of distinct bait-proteins (Burckstummer et al., 2006).

### 1.4.1. The GS-TAP Tag

To conduct the identification of binding partners for a distinct protein, the bait-peptide has to be linked to a certain tag, which is further used to extract the lure-protein together with bound peptides. A commonly used tag is the GS-TAP-tag, which consists of a protein-G, a cleavage site for the tobacco etch virus (TEV) protease and a streptavidin-binding peptide (Fig. 1.4.1.).

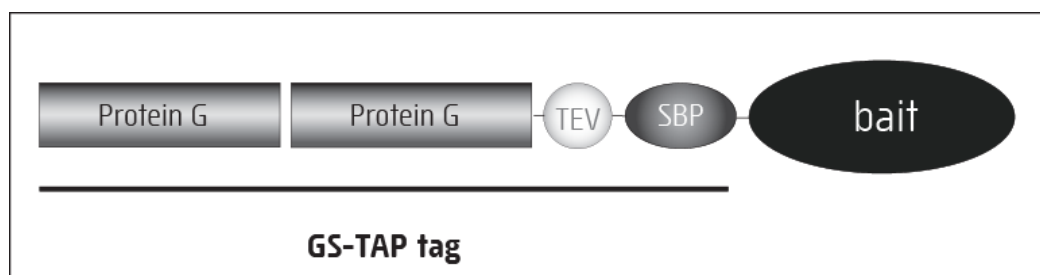


**Figure 1.4.1.:** Composition of the GS-TAP-tag. Two protein-G sites are followed by a cleavage site for the tobacco etch virus (TEV). Furthermore, a streptavidin binding protein (SBP) is integrated in the GS-TAP-tag. Illustration taken from (Burckstummer et al., 2006).

The fusion protein and associated components are recovered from cell extracts by two sequential purification steps.

### 1.4.2. Procedure of Tandem-Affinity-Purification

The method requires large initial quantities of cells, depending on the bait protein, the number of cells needed range from  $5 \times 10^7$  to  $1 \times 10^9$ . Therefore usually stable cell lines are

taken to ease the expansion of fusion-protein expressing cells. Usually retroviral gene transfer is performed to generate stable cell lines (Fig. 1.4.2.).

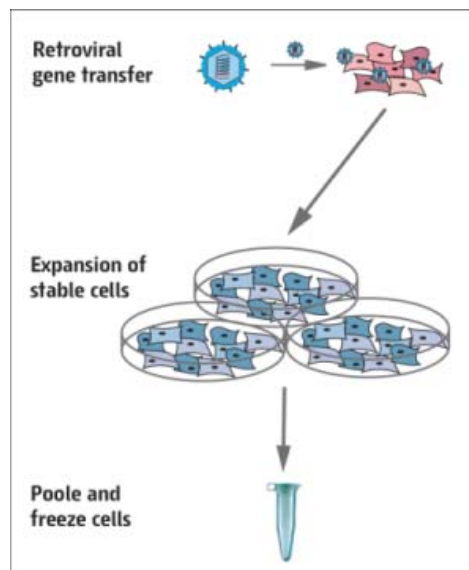


**Figure 1.4.2.: Scheme for generating and expanding stable cell lines. Illustration adapted from (Burckstummer et al., 2006).**

The lysate of stable transfected cell lines is further used for TAP. In the first step the tagged bait protein is bound to protein G sepharose via its protein G. After a first washing step the complex bound to the beads is eluted by TEV cleavage. The eluate is further bound to streptavidin beads via the streptavidin binding protein. After a second washing step the protein complex is eluted with biotin (Fig. 1.4.3.).

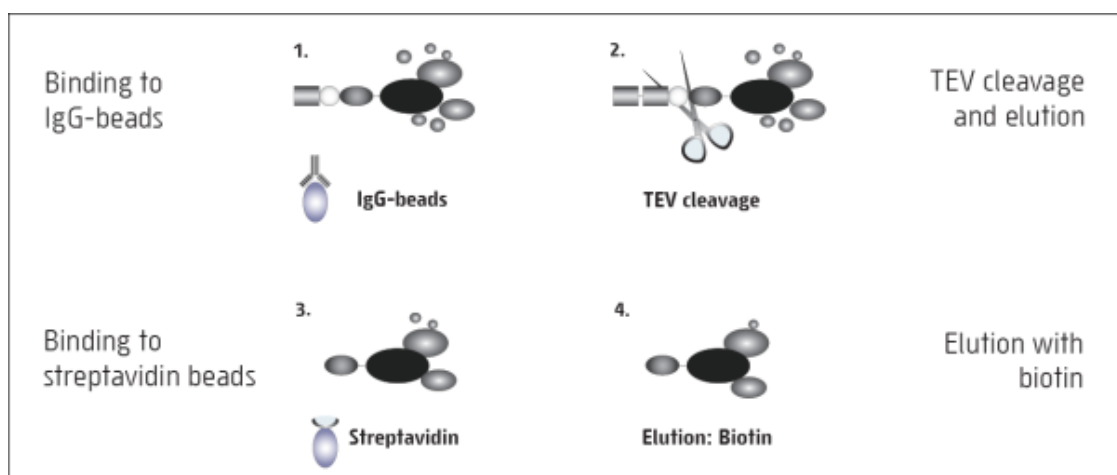


**Figure 1.4.3.: Scheme for the four different steps of tandem-affinity purification. In the first step the bait protein is bound to IgG beads via the protein-G (1). After a first washing step the bound proteins are eluted by TEV cleavage (2) and further bound on streptavidin beads via the streptavidin binding protein (3). After a second washing step the protein-complex is eluted with biotin (4). Illustration adapted from (Burckstummer et al., 2006).**

Finally the eluate can be analyzed by western-blot or can be sent to mass-spectrometry analysis.

## **1.5. Structure of the Project**

The following scheme shows an overview of the project (Fig. 1.5.1).

In the first point the murine toll-like receptors are C-terminally fused to a GS-TAP tag and are further retrovirally transduced into RAW264.7 macrophages to generate stable cell-lines. Secondly stable transduced RAW264.7 cells are expanded and collected for tandem affinity purification in large scale. In the third step, TAP is performed for each endosomal toll-like receptor in duplicates. Afterwards the eluted samples are sent to mass-spectrometry, where the captured proteins are analyzed. Furthermore, the resulting data is evaluated and interpreted using a bioinformatics approach. The resulting data and the selected candidates are further validated by immune-precipitation, to show if the predicted interaction is real.

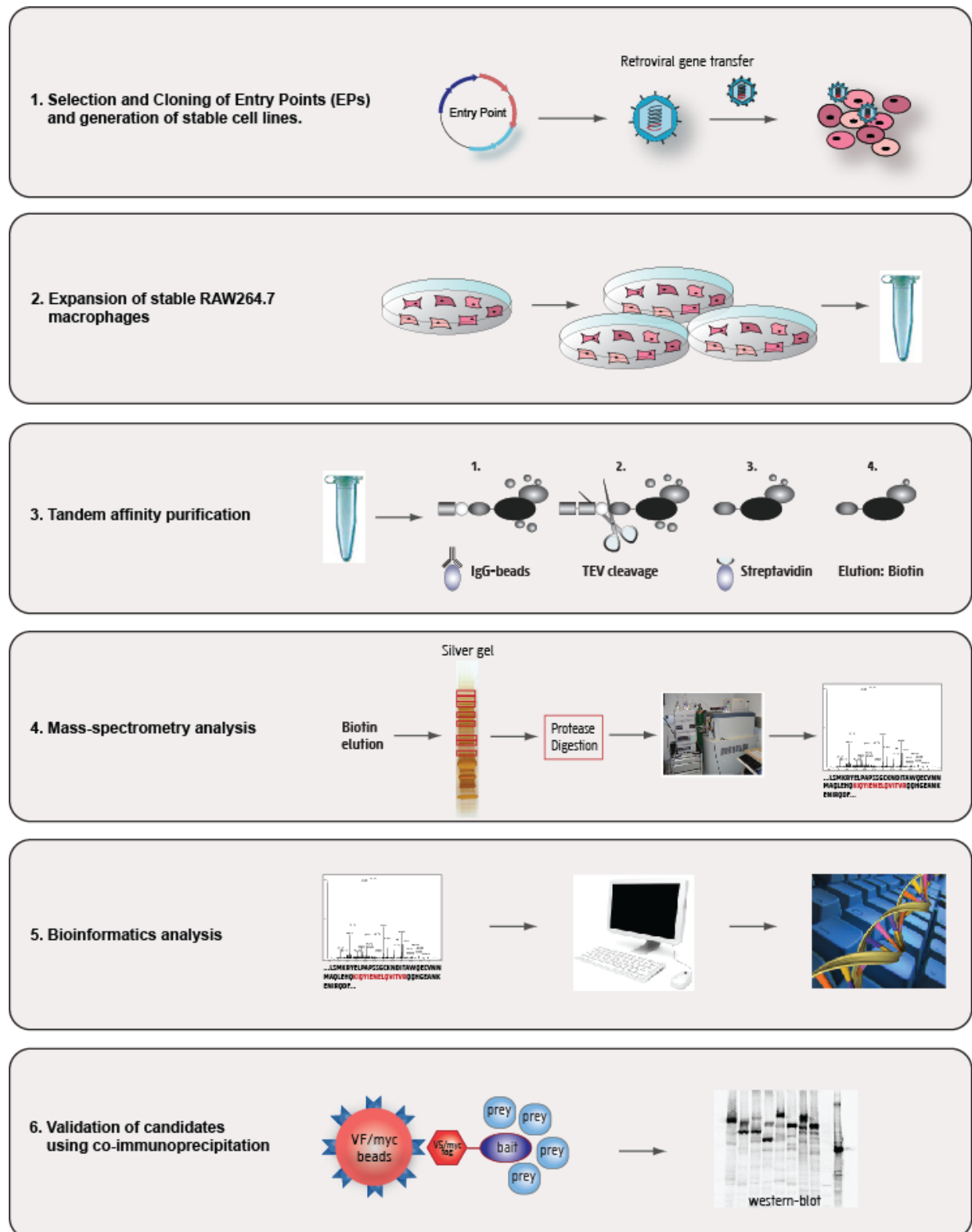


Figure 1.5.1.: Schematic structure of the project. Illustration adapted from (Burckstummer et al., 2006).

## **Material and Methods**

### **2.1. Cell Culture**

#### **2.1.1. RAW264.7 Macrophages (ATCC)**

For tandem affinity purification and selected functional assays RAW264.7 macrophages were used. The cells were cultured in DMEM (PAA) medium containing 10% FCS (Gibco) at 37° C with 5% CO<sub>2</sub>. To detach the cells from the culture plate RAW-dissociation-buffer was used.

#### **2.1.2. hTLR3-HEK293 (InvivoGen)**

For selected functional assays HEKnull cells from InvivoGen were used, which are stably expressing the human TLR3 constructs harboring an HA-tag at the C-term. The cells were cultured in DMEM (PAA) medium containing 10% FCS (Gibco) at 37° C with 5% CO<sub>2</sub>. To detach the cells from the culture plate 0,05% Trypsin-EDTA (PAA) was used.

#### **2.1.3. HEK293T (Cancer Research UK)**

For co-immunoprecipitation HEK293T cells were used, which have been a kind gift from Cancer Research UK. The cells were cultured in DMEM (PAA) medium containing 10% FCS (Gibco) at 37° C with 5% CO<sub>2</sub>. To detach the cells from the culture plate 0,05% Trypsin-EDTA (PAA) was used.

#### **2.1.4. HeLa (ATCC)**

For immune-fluorescence slides 3 x 10<sup>5</sup> cells were seeded per well on a six well plate, including 1-3 coverslips (13mm) per well. The cells were cultured in DMEM (PAA) medium containing 10% FCS (Gibco) at 37° C with 5% CO<sub>2</sub>. To detach the cells from the culture plate 0,05% Trypsin-EDTA (PAA) was used.

#### **2.1.5. HEK293-GP (ATCC)**

For generating stable cell lines using retroviral gene transfer HEK293-GP cells were used for virus production. The cells were stably expressing gag and pol gens from retrovirus. The cells were cultured in DMEM (PAA) medium containing 10% FCS (Gibco) at 37° C with 5% CO<sub>2</sub>. To detach the cells from the culture plate 0,05% Trypsin-EDTA (PAA) was used.

#### **2.1.6. Freezing Cells**

Usually half of a dense 15cm plate was frozen as one aliquot of cells. Therefore the cells were taken off the cell-culture-plate, either with RAW dissociation buffer or with trypsin, depending on the cell-line. Further the cells were centrifuged at 300g and room temperature



for 5min. The pellet was resuspended in DMEM (20% FCS). The cell suspension was mixed in a one to one ration with DMEM containing 20% FCS and 20% DMSO (Merck). The cells were put on ice immediately and were further put on -80° C in a cryo-box. After one day the cells were transferred to a liquid nitrogen tank.

### 2.1.7. Thawing Cells

Usually half of a dense 15cm plate was frozen as one aliquot of cells. The cryo-tube was taken out of the liquid nitrogen tank and heated in a 37° C water bath as fast as possible. The cells were transferred into 10ml of the culture medium and the suspension was centrifuged at 300° C and room temperature for 5min. The pellet was resuspended in 25ml culture medium and the cells were seeded on a 15cm cell-culture-plate.

### Reagent

- RAW-dissociation buffer: 135mM KCl, 15mM sodium citrate

## 2.2. Transient Transfection of HEK-cells and Lysis

### 2.2.1. Transient Transfection of HEK-cells

The cells were plated one day before transfection according to table 2.2.1. In general lipid based transfection using Polyfect (QIAGEN) was performed. The DNA was diluted in serum free DMEM and Polyfect was added according to table 2.2.1. The mixture was incubated for 10min on room temperature and was further put on the cells

Plate format	Cells per well	DMEM (w/o FCS)	Polyfect	DNA
24 well plate	1,5 x 10 <sup>5</sup>	20µl	4µl	1µg
6 well plate	6 x 10 <sup>5</sup>	100µl	20µl	2µg
10cm plate	6 x 10 <sup>6</sup>	1ml	64µl	10µg

**Table 2.2.1.: Transient transfection schedule for HEK293 cells.**

The cells were incubated at least for 24h after transfection, without changing the medium.

### 2.2.2. Lysis of HEK Cells

All steps were performed on ice or at 4° C. One six well of cells was used for western-blot. The medium was removed and the cells were scraped of the plate using a rubber scraper and 1ml PBS (PAA). Further the cells were centrifuged at 300g and 4° C for 5min. After the PBS was removed, the cells were resuspended in 100µl IP-buffer and lysed for 15min on ice. The lysate was centrifuged at 16200g at 4° C for 10 minutes. Further the protein concentration of the lysate was measured using Bradford reagent (BioRad).

**Reagent**

- IP-buffer:  
50mM Tris (Sigma)/HCl (Merck) (pH 7,5), 150mM NaCl (Merck), 5mM EDTA (Fulka), 5mM EGTA (Fulka), 1% NP-40 (Calbiochem), before use 1mM Na<sub>3</sub>VO<sub>4</sub> (Sigma) and a cocktail inhibitor tablet (Roche) was added.

**2.3. Generating Stable Cell Lines****2.3.1. Cloning of Entry-points and Interaction-candidates using Gateway® Cloning Kit (InvitroGen)****cDNA of Entrypoints**

The murine and human toll-like-receptor cDNA-constructs, as well as the human cDNA-constructs for our chosen interactors were ordered from Invitrogen based on the accession numbers in Table 2.3.1.

	murine accession NR.	human accession Nr.
TLR-3	NM_126166	NM_003265
TLR-7	NM_133211	NM_016562
TLR-8	NM_133212	NM_138636
TLR-9	NM_031178	NM_017442
TaoK1	NM_144825	NM_020791
Poldip3	NM_178627	NM_032311
Cd14	NM_009841	NM_000591
Lyn	NM_010747	NM_002350
Smpd13b	NM_133888	NM_014474
Rasa3	NM_009025	NM_007368
Rftn1	NM_181397	NM_015150

**Table 2.3.1.: Accession numbers of used sequences.**

**PCR of cDNA using a KOD Polymerase Kit (Novagen)**

PCR was performed with gateway-cassette flanked primers (ordered from InvitroGen) (Tab. 2.3.2/Tab. 2.3.3). Each PCR reaction contained 32,6µl H<sub>2</sub>O, 5µl 10x PCR buffer, 2µl MgCl<sub>2</sub>, 2µl (10µM) of both primers, 5µl of dNTP solution, 1µl template and 0,4µl of KOD polymerase. The amplification was performed using the following conditions:

Primary denaturation:	98° C	01 min	
Denaturation:	98° C	15 sec	} 30 cycles
Annealing:	52° C	15 sec	
Extension:	72° C	1,2 min	
Final Extension:	52° C	04 min	

The PCR product was loaded on a 1% Agarose (InvitroGen) and the bands with the right size were cut out and purified using a QIAquick gel extraction kit (QIAGEN).

**Sense *attB1* primer :** 5' - Gggg aca agt ttg tac aaa aaa gca ggc tcc (NNN)<sub>5-10</sub> -3'  
**Antisense *attB1* primer:** 5' – gggg ac cac ttt gta caa gaa agc tgg gt STOP (NNN)<sub>5-10</sub> -3'

**Table 2.3.2.: Gateway-primer for N-terminal fusion.**

**Sense *attB1* primer:** 5' - Gggg aca agt ttg tac aaa aaa gca ggc tag act gcc atg (NNN)<sub>5-10</sub> -3'  
**Antisense *attB1* primer:** 5' – gggg ac cac ttt gta caa gaa agc tgg gtt NOSTOP (NNN)<sub>10-15</sub> -3'

**Table 2.3.3.: Gateway-primer for C-terminal fusion.**

### BP Reaction

To clone the PCR product into a pDONR201-vector (InvitroGen) (Fig. 2.3.4.), containing a kanamycin resistance cassette, a BP reaction under the following conditions was performed.

template	4µl
pDONR	1µl (150ng/µl)
BP clonase	2µl
H <sub>2</sub> O	3µl
<b>total</b>	<b>10µl</b>

The reaction was performed at room temperature for 1h.

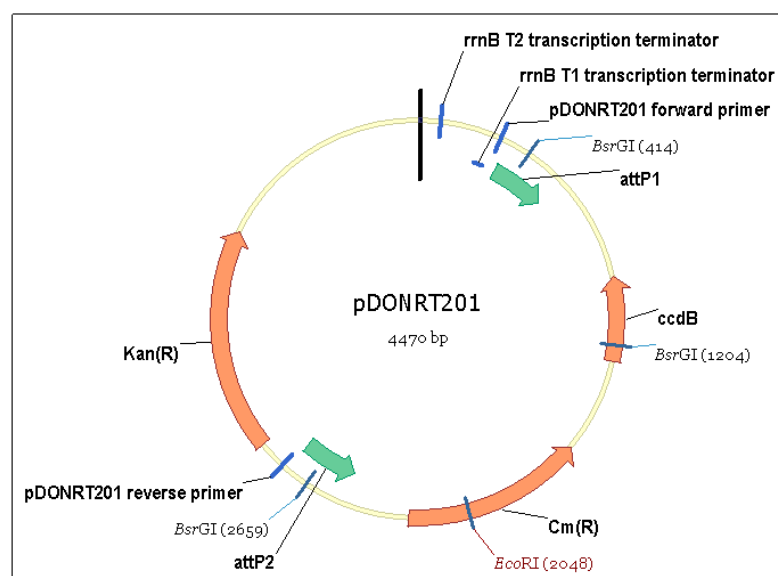


Figure 2.3.4.: Vector map of pDONRT201.

### Transformation into MAX Efficiency DH5 $\alpha$ Bacteria

2 $\mu$ l of BP reaction were transformed into MAX Efficiency DH5 $\alpha$  bacteria (InvitroGen) following the provided protocol. Afterwards the transformed bacteria were plated on an LB-agar plate containing kanamycin as selection media.

Three clones were picked from each plate and inoculated in 7ml LB-medium containing kanamycin and incubated over night at 37° C shaking.

On the next day 2ml of each culture were used to isolate the plasmid using a QIAprep spin miniprep kit (QIAGEN).

### Verify BP Reaction with BsrG1 Digestion

To verify if the TLR cassette was cloned into the pDONR201 vector a BsrG1 (New England Biolabs) digestion was performed in the following way:

NEB2	2 $\mu$ l
10x BSA	2 $\mu$ l
<b>BsrG1</b>	1 $\mu$ l
H <sub>2</sub> O	10 $\mu$ l
DNA	5 $\mu$ l
<b>Total: 20<math>\mu</math>l</b>	

The digestion was performed for 1h at 37° C. Afterwards the samples were loaded on a 1% agarose gel (InvitroGen), including a control digestion of the non fused pDONR201 vector. The miniprep of the clone that was showing the right digestion pattern was further used for LR-reaction.

### Maxiprep of pDONR-constructs

The remaining 5ml of the miniprep-culture were used to inoculate 250ml LB media, containing kanamycin for maxiprep. The culture was incubated over night at 37° C shaking. On the next day maxiprep was performed using a HiSpeed Plasmid Maxi Kit (QIAGEN).

### LR Reaction

The plasmid preparation of the pDONR-construct was further used to shuttle the gene of interest in any compatible gateway vector (Tab. 2.3.5.). For my thesis I have used three different vectors to tag the genes of interests with three different tags at the c-terminus. All three vectors carry an ampicillin resistance.

name	backbone	tag	resistance	company
pTRACER-CV5-gw	pTRACER-vector	V5-tag	ampicillin	InvitroGen
pcDNA-C6myc-gw	pcDNA-vector	6x myc-tag	ampicillin	selfmade
pRV-CTAP(S6)-gw	Moloney murine leukemia virus-based vector	TAP-tag	ampicillin	selfmade

**Table 2.3.5.: Vectors used for LR reactions.**

The LR reaction was performed under the following conditions:

pDONR	1µl (150ng/µl)
Vector	1µl (150ng/µl)
LR clonase	2µl
H <sub>2</sub> O	6µl
<b>Total:</b>	<b>10µl</b>

The reaction was performed at room temperature for 1h

### Transformation into Subcloning Efficiency DH5α Bacteria (InvitroGen)

2µl of LR reaction were transformed into Subcloning Efficiency DH5α bacteria (InvitroGen) following the provided protocol. Afterwards the transformed bacteria were plated on an LB-agar plate containing ampicillin as selection media. Three clones were picked from each plate and inoculated in 7ml LB-medium containing ampicillin and incubated over night at 37° C shaking. On the next day 2ml of each culture were used to isolate the plasmid using a QIAprep spin miniprep kit (QIAGEN).

### Verify LR Reaction with BsrG1 Digestion

To verify if the pDONR201-TLR-vector was fused successfully with the aim-vector a BsrG1 (New England Biolabs) digestion was performed in the following way:

NEB2	2µl
10x BSA	2µl
<b>BsrG1</b>	1µl
H <sub>2</sub> O	10µl
DNA	5µl
<b>Total:</b>	<b>20µl</b>

The digestion was performed for 1h at 37° C. Afterwards the samples were loaded on a 1% agarose gel (InvitroGen), including a control digestion of the non fused aim-vector. The miniprep of the clone that is showing the right digestion pattern was further used for maxiprep.

### Maxiprep of Final Vector Constructs

The remaining 5ml of the miniprep-culture were used to inoculate 250ml LB media, containing ampicillin for maxiprep. The culture was incubated over night at 37° C shaking. On the next day maxiprep was performed using a HiSpeed Plasmid Maxi Kit (QIAGEN).

### 2.3.2. Retroviral Transfection System to Generate Stable RAW264.7 Cells

#### Virus Production in HEK293 Cells

In the morning of the first day  $1 \times 10^7$  HEK293-GP cells, stably expressing gag and pol gens, were plated on a 10cm dish (Falcon) using DMEM (PAA) containing 10% FCS (Gibco). In the afternoon the plate should have been 70-80% confluent and was ready for transient transfection. 8µg of the vector containing the mTLR-cTAP constructs, as well as 2µg of the VSV-G plasmid, containing the retroviral envelope gene were diluted in 300µl serum-free-DMEM medium (PAA). 100µl of Polyfect (QIAGEN) were added and the solution is incubated for ten minutes at room temperature. During the incubation time the old medium of the HEK293-GP cells was removed and replaced by fresh DMEM (PAA) medium containing 10% FCS (Gibco). The transfection-mix was added to the cells and the plate was incubated over night at 37° C, 5% CO<sub>2</sub> in an S2 safety lab.

In the morning of the following day the medium was exchanged by 6ml fresh DMEM containing 10% FCS, cells were incubated for 24 hours in an S2 safety lab. Furthermore,  $5 \times 10^5$  target cells (RAW264.7) were seeded on a 6well plate (Falcon) using DMEM containing 10% FCS.

### **Stable Transfection of RAW264.7 Cells**

In the morning of the third day the medium of the target cells was replaced by 1ml DMEM (10% FCS). In the afternoon the first infection round was performed. The supernatant of the HEK293-GP virus producing cells was collected and 6ml fresh DMEM (10% FCS) was added on the cells that are incubated for further 24h. The supernatant was spun for 5 minutes at 1200rpm and further filtered through a 0,45µm cellulose-acetate filter. On the target RAW264.7 cells 5µg polybrene (Sigma) was added before the filtered virus supernatant was put on the cells. Virus producing cells, as well as target cells were incubated for 24 hours.

On the fourth day the second round of transfection was performed in the same way than the day before. Since RAW264.7 cells were growing very fast, the cells were transferred to a 10cm dish (Falcon) before the virus supernatant was added. Virus producing HEK293 cells were discarded.

The target cells had to be kept in an S2 safety lab for two passages before they could have been transferred to an S1 safety lab. The cells were expanded during the two passages to generate enough cells for flow-cytometry and cell sorting.

### **Flow-cytometry**

The pRV-CTAP(S6)-gw vector which was used to create mTLR-cTAP constructs harbors an IRES-GFP construct, which was used to check the viral-transfection-efficiency of the RAW264.7 cells via flow-cytometry.

Therefore the cells from a 10cm dish (Falcon) were detached from the plate and centrifuged for 5 minutes at 300g and room temperature. Afterwards the cells were washed once with 1x PBS (PAA) and centrifuged again for 5 minutes at 300g and room temperature. Afterwards the cells were taken up in 300µl 1x PBS and put on ice. The amount of GFP containing cells was detected using a FACScalibur machine. If the amount of GFP positive cells was greater than 3% the stably transfected cells were sorted out with fluorescence activated cell sorting (FACS).

### **Fluorescence Activated Cell Sorting (FACS)**

Cell sorting was performed by Dieter Prinz at the St. Anna Kinderspital.

The preparation for the cells was performed in the following way:

Two 15cm plates of generated stable RAW264.7 cells were washed one time with PBS (PAA) and the cells were detached from the plate using 3ml RAW dissociation buffer. The cells were taken off both plates with 10ml FACS buffer (PBS (PAA) with 3% FCS (Gibco)). Afterwards the cells were centrifuged at 300g and room temperature for 5 minutes. The supernatant was discarded and the cells were resuspended in 500µl FACS buffer. The cell-suspension was filtered through a cell strainer cap (Falcon) and was transferred to a polystyrene tube (Falcon). The cells were stored on ice until they were sorted. Depending on

how many cells were sorted out, they were either placed into 96 well plate ( $> 1 \times 10^4$ ) or a 24well plate ( $> 1 \times 10^5$ ). Further the cells were expanded and frozen.

## **2.4. Ligands of Endosomal Toll-like Receptors**

### **2.4.1. TLR3 Ligand**

Polyinosine-polycytidylic acid (polyI:C, InvivoGen)

### **2.4.2. TLR7/8 Ligand**

Imiquimod, R837 (InvivoGen)

### **2.4.3. TLR9 Ligand**

hCpG, ODN2006 (InvivoGen)

5'- tcc atg acg ttc ctg acg tt -3' (20 mer), human TLR9 ligand.

mCpG, ODN1826 (InvivoGen)

5'- tcc atg acg ttc ctg acg tt -3' (20 mer), murine TLR9 ligand.

### **2.4.4. Lipid Compounds**

Ceramide from bovine brain (Sigma)

Sphingomyelin from bovine brain (Sigma)

## **2.5. De-glycosylation Assay**

For the deglycosylation assay transiently transfected HEK293 cells as well as stably transfected RAW264.7 macrophages were used, which were transfected with TLR3, TLR7, TLR8 and TLR9. A 6well of the cells was lysed with 100µl IP-buffer and incubated for 20min on ice. Afterwards the lysate was spun at 16200g at 4° C for 10min. To the supernatant 12µl denaturing buffer (NewEngland Biolabs) was added and the lysates were incubated at 100° C for 10min. From each lysate two 30µl aliquots were taken. To each aliquot 4µl G5 buffer (NewEngland Biolabs) were added. To one of the two aliquots 6µl EndoH (NewEngland Biolabs) were added. Deglycosylation was performed at 37° C for 1h. Both aliquots were always treated in the same way, no matter if EndoH has been added or not. After the deglycosylation 10µl of each lysate was mixed with 5µl 4x sample-buffer and was loaded on a 7% polyacrylamid-gel.



**Reagent**

- IP-buffer:  
50mM Tris (Sigma)/HCl (Merck) (pH 7,5), 150mM NaCl (Merck), 5mM EDTA (Fulka), 5mM EGTA (Fulka), 1% NP-40 (Calbiochem), before use 1mM Na<sub>3</sub>VO<sub>4</sub> (Sigma) and a cocktail inhibitor tablet (Roche) was added.
- Sample-buffer (4x):  
200mM Tris (Sigma)/HCl (Merck) (pH 6,8), 40% glycerol (Serva), 8% sodiumdodecylsulfate (Serva), 0,004% of bromphenol blue (Sigma), before use 10%  $\beta$ -mercaptoethanol (Sigma) was added.

**2.6. Tandem-Affinity-Purification****2.6.1. Expand Stable RAW264.7 Cells**

For each endosomal TLR two TAP-pulldowns were performed using the stable RAW264.7 macrophage cell-lines. Per TAP pulldown roughly  $1,5 \times 10^9$  (40x 15cm dishes) stable RAW264.7 macrophages were used. Therefore 80 15cm dishes of the different cell-lines were generated. The cells were scraped off the plate using a plastic scraper and pooled in four fractions. Further they were spinned at 300g and 4° C for 10 minutes. The supernatant was discarded and the cells were resuspended in 10ml the four fractions were combined and centrifuged again at 300g and 4° C for 10 minutes. The supernatant was discarded and the cell-pellet was snap frozen in liquid nitrogen and stored at -80° C for further use.

**2.6.2. Preparation of Cell-lysate**

The stored cells were defrosted and the pellets were resuspended in 15ml ML-buffer and incubated on ice for 25 minutes. Further the cell-suspension was centrifuged at 1200g and 4° C for 10 minutes. The supernatant was taken off and centrifuged again at 15000g and 2° C for one hour. Afterwards the supernatant was divided in two equal fractions which were further used as duplicates for tandem-affinity-purification. A 30 $\mu$ l aliquot of the lysate was stored at -20° C for western-blot analysis.

**2.6.3. Tandem-Affinity-Purification**

All steps have been carried out on ice or at 4° C.

Per one lysate aliquot 200 $\mu$ l IgG beads-suspension (Sigma) was used. The beads-suspension was spinned at 150g for approximately 10 seconds. The supernatant was discarded and the beads were resuspended in 500 $\mu$ l ML-buffer. This step was repeated two times and finally the beads were resuspended in 100 $\mu$ l ML-buffer.

The lysate was combined with the washed beads-suspension and incubated at 2h and 4° C rotating on a wheel.

After the incubation the beads were collected by centrifuging the suspension at 150g and 4° C for one minute. The supernatant was removed (30µl aliquot for western-blot was kept) and the beads were transferred into a MoBiCol column (MoBiCol). The beads were washed with 10ml ML-buffer by gravity flow. A second washing step was performed with 5ml TEV-buffer. It was important that the beads did not dry during the two washing steps. 400µl TEV-buffer including 40µl TEV protease were added to the beads that were incubated for 1h at 16° C shaking at 300rpm.

In the meantime the 150µl streptavidin beads-suspension (Pierce) was washed three times with TEV-buffer, just in the same way than the IgG beads.

The TEV-eluate was eluted by gravity flow into a new tube (Eppendorf). 400µl TEV-buffer were added on the beads again and the column was emptied in the same tube as before by applying pressure. A 5µl aliquot was kept for western-blot analysis. The streptavidin beads were added to the TEV eluate and the suspension was incubated for one hour at 4° C rotating on a wheel.

Afterwards the suspension was spinned at 150g and a 15µl aliquot of the supernatant was taken for western-blot analysis. The beads were transferred to a new MoBiCol column where they were washed with 10ml TEV-buffer by gravity flow. The remaining buffer was removed by applying pressure. Afterwards the beads were resuspended with 60µl 2x sample-buffer, diluted in water, and the suspension was boiled for 5 minutes. The column was finally put into a new 1,5ml tube and the liquid was eluted by centrifuging at 300g for one minute.

The final eluate was stored at -20° C until it is send to mass-spectrometry.

### **Reagent**

- Membrane lysis buffer (MLB):  
50mM Tris (Sigma)/HCl (Merck) (pH 6), 150mM NaCl (Merck), 1mM EDTA (Fulka), 7,5% glycerol (Merck), 25mM NaF (Fisher Scientific), 0,2% NP-40 Calbiochem), adjust to pH 6 using HCl (Merck). The buffer is stored at 4° C, before use 1mM DTT (Sigma) and 1mM Na<sub>3</sub>VO<sub>4</sub> (Sigma) was added.
- TEV-buffer:  
10mM Tris (Sigma)/HCL (Merck) (pH 6), 100mM NaCl (Merck), 0,5 mM EDTA (Fulka), before use 1mM DTT (Sigma) was added.
- Sample-buffer (4x):  
200mM Tris (Sigma)/HCl (Merck) (pH 6,8), 40% glycerol (Merck), 8% sodiumdodecylsulfate (Serva), 0,004% of bromphenol blue (Sigma), before use 10% β-mercaptoethanol (Sigma) was added.

## 2.7. Mass-Spectrometry

The TAP samples were further handed over to the CeMM mass-spectrometry department, (head: Dr Keiryn Bennett) where all steps of MS analysis and protein identification were carried out.

### 2.7.1. One-dimensional SDS-PAGE and Silver Staining

The eluted samples were separated by 1D SDS-PAGE on a 4 – 12% bis-Tris gel (NuPAGE, Invitrogen, CA). After visualisation of the proteins by silver staining, entire lanes were sliced into 20 pieces.

### 2.7.2. *In situ* Tryptic Digestion Method

The 20 gel pieces were washed to remove residual SDS, proteins were reduced with dithiothreitol, alkylated by incubation with iodoacetamide and digested *in situ* with modified porcine trypsin (Promega Corp., Madison, WI) (Shevshenko). The resultant peptide mixture was extracted from the gel slices and desalted with customised reversed-phase stage tips (mann). The volume of the eluted sample was reduced to approximately 2  $\mu$ L in a vacuum centrifuge and reconstituted to 10  $\mu$ L with 5% formic acid. Depending on the intensity of the protein band staining, additional multiples of 8  $\mu$ L 5% formic acid were added to specific samples prior to analysis by LCMS.

### 2.7.3. Liquid Chromatography and Mass Spectrometry

Mass spectrometry was performed on a hybrid LTQ-Orbitrap mass spectrometer (ThermoFisher Scientific, Massachusetts, USA) using the Xcalibur version 2.0.6 coupled to an Agilent 1200 HPLC nanoflow system (binary pump system with one precolumn and one analytical column) via a nanoelectrospray ion source using liquid junction (Proxeon, Odense, DK). Solvents for LCMS were used in two phases: Phase A (A) consisted of 0.4% acetic acid, 0.005% HFBA in water and phase B (B) consisted of 0.4% acetic acid, 0.005% HFBA in 90% acetonitrile. Using a thermostatted micro-autosampler, 8  $\mu$ L of the tryptic peptide mixture was automatically loaded onto a trapping pre-column (Zorbax 300SB-C18 5 $\mu$ m, 5 $\times$ 0.3 mm, Agilent) with a binary pump at a flow rate of 40  $\mu$ L/min. 100% phase A was used for loading and washing the pre-column. After washing, the peptides were eluted by back flushing onto a 16 cm fused silica analytical column with an inner diameter of 50  $\mu$ m, packed with C18 reversed phase material (ReproSil-Pur 120 C18-AQ, 3 $\mu$ m, Dr. Maisch GmbH). The peptides were eluted from the analytical column running a gradient from 3 to 13% B within 4 min, 13 to 35% B within 35 min, 35 to 50% B within 11 min and finally increased to 100% B within 6 min and hold for 15 min at a constant flow rate of 100 nL/min. For internal calibration of the mass spectrometer, the signals of the following background ions were used as lock masses:

$[\text{Si}(\text{CH}_3)_2\text{O}]_5\text{H}^+$ ,  $[\text{Si}(\text{CH}_3)_2\text{O}]_6\text{H}^+$ ,  $[\text{Si}(\text{CH}_3)_2\text{O}]_6\text{H}^+ + \text{NH}_3$ ,  $[\text{Si}(\text{CH}_3)_2\text{O}]_7\text{H}^+ + \text{NH}_3$ , and  $[\text{Si}(\text{CH}_3)_2\text{O}]_8\text{H}^+ + \text{NH}_3$  at  $m/z$  371.101233,  $m/z$  445.120025,  $m/z$  462.146573,  $m/z$  536.165365 and  $m/z$  610.184156, respectively. The analyses were performed in a data-dependent acquisition mode using a top 10 collision-induced dissociation (CID) method (up to 10 CID spectra were acquired following each MS scan) and a dynamic exclusion for selected ions of 60 seconds. Maximal ion accumulation time allowed on the LTQ Orbitrap in CID mode was 150 ms for  $\text{MS}^n$  in the LTQ and 1000 ms in the C-trap. Automatic gain control was used to prevent overfilling of the ion traps and was set to 5000 ions in  $\text{MS}^n$  mode for the LTQ and 1 million ions for a full FTMS scan. Injection waveforms were activated for both LTQ and Orbitrap. Intact peptides were detected in the Orbitrap at 60,000 resolution. For statistical purposes, samples were analysed by LCMSMS as biological replicates and technical triplicates.

#### 2.7.4. Data Analysis

The acquired data were processed with Bioworks V3.3.1 SP1 (ThermoFisher, Manchester, UK), data files merged with an internally-developed program, and searched against the murine IPI database version v3.41 with the search engine MASCOT. Submission to MASCOT was via a Perl script that performs an initial search with relatively broad mass tolerances on both the precursor and fragment ions ( $\pm 10$  ppm and  $\pm 0.6$  Da, respectively). High-confidence peptide identifications are used to recalibrate all precursor and fragment ion masses prior to a second search with narrower mass tolerances ( $\pm 4$  ppm and  $\pm 0.3$  Da, respectively). One missed tryptic cleavage site was allowed. Carbamidomethyl cysteine was set as a fixed modification, and oxidised methionine was set as a variable modification. For unambiguous protein identification at least two unique peptides with a MASCOT peptide ion score greater than, or equal to, 20 were required. A false-positive detection rate of less than 1 percent was estimated by searching the data set against a reversed database.

## 2.8. Co-Immuno-Precipitation

### 2.8.1. Transient Transfection in HEK293T Cells

For the co-immunoprecipitation HEK293T cells were used. On the first day  $6 \times 10^6$  cells were plated on a 10cm dish. On the second day the cells were transiently transfected in the following way:

bait protein	10 $\mu$ g
prey protein	10 $\mu$ g
serum free DMEM (PAA)	1ml
Polyfect (QIAGEN)	64 $\mu$ l

The mixture was incubated for 10 minutes and directly added to the cells.

After 48h the cells were washed with 1x PBS (PAA) for one time and scratched off the plate. Further the suspension was centrifuged at 300g and 4° C for 5 minutes and the supernatant was removed. The cells were snap frozen in liquid nitrogen and stored at -80° C.

### **2.8.2. Lysis**

All steps were performed on ice or at 4° C. The cells were resuspended in 300µl IP-buffer and lysed for 15min on ice. The lysate was centrifuged at 16200g at 4° C for 10 minutes. The supernatant was separated in three aliquots à 100µl and the remaining lysate was kept for western-blot analysis.

Further the protein concentration of the lysate was measured using Bradford reagent (BioRad).

### **2.8.3. Immunoprecipitation**

A myc-IP and a V5-IP were performed to target the bait protein and the prey protein. For the myc-IP pre-coupled beads (Sigma) were used. For the V5- IP protein G-sepharose (GE Healthcare) and a V5 antibody (Invitrogen) were used.

50µl beads-suspension per IP were used. The beads-suspension was spinned at 150g for approximately 10 seconds. The supernatant was discarded and the beads were resuspended in 100µl IP-buffer. This step was repeated two times and finally the beads were resuspended in 25µl IP-buffer.

For the myc-IP 50µl beads-suspension were directly added to one 100µl aliquot of the lysate, which was further incubated for 2 hours rotating on a wheel at 4° C. For the V5-IP 1,5µl of the V5 antibody (InvivoGen) were added per 100µl aliquot of the lysate and the sample was incubated for one hour rotating on a wheel at 4° C. Afterwards 50µl protein G-sepharose-suspension were added and the sample was further incubated for one hour rotating on a wheel at 4° C.

The remaining 100µl aliquot of the sample was used as control with unspecific protein G-sepharose beads. 50µl beads-suspension was added to the aliquot, which was further incubated for 2 hours rotating on a wheel at 4° C.

After the incubation period three samples were washed in the same way. The suspensions were centrifuged for 20 seconds at 150g and the supernatant was discarded. The beads were resuspended in 150µl MLB-buffer. This step was repeated five times in total.

After the removal of the last supernatant the beads were resuspended in 60µl 2x sample-buffer and were snap frozen in liquid nitrogen and stored at -80° C.

**Reagent**

- IP-buffer:  
50mM Tris (Sigma)/HCl (Merck) (pH 7,5), 150mM NaCl (Merck), 5mM EDTA (Fulka), 5mM EGTA (Fulka), 1% NP-40 (Calbiochem), before use 1mM Na<sub>3</sub>VO<sub>4</sub> (Sigma) and a cocktail inhibitor tablet (Roche) was added.
- Membrane lysis buffer (MLB):  
50mM Tris (Sigma)/HCl (Merck) (pH 6), 150mM NaCl (Merck), 1mM EDTA (Fulka), 7,5% glycerol (Merck), 25mM NaF (Fisher Scientific), 0,2% NP-40 (Calbiochem), adjust to pH 6 using HCl (Merck). The buffer is stored at 4° C, before use 1mM DTT (Sigma) and 1mM Na<sub>3</sub>VO<sub>4</sub> (Sigma) was added.
- Sample-buffer (4x):  
200mM Tris (Sigma)/HCl (Merck) (pH 6,8), 40% glycerol (Serva), 8% sodiumdodecylsulfate (Serva), 0,004% of bromphenol blue (Sigma), before use 10% β-mercaptoethanol (Sigma) was added.

**2.9. Western-Blot****2.9.1. SDS Poly-acrylamid Gel**

For gel-electrophoresis the Mini-protean 3system (Bio-Rad) was used to make SDS-Polyacrylamid gels. Either 10% or 7% SDS-PAGE (Tab. 2.9.1.) were prepared according to the following formula, where amounts were declared for one minigel:

	<b>7% SDS-PAGE</b>	<b>10%PAGE</b>
30% Acrylamide/Bis (Bio-rad)	1,17ml	1,67ml
Running gel buffer	1,25ml	1,25ml
10% APS	50µl	50µl
Tetramethylethyldiamine (Merck)	5µl	5µl
Water	2,58ml	2,08ml
<b>Total volume:</b>	<b>5ml</b>	<b>5ml</b>

**Table 2.9.1.: Preparation schedule for separation-gel.**

The stacking gel (Tab. 2.9.2.) was filled up to a height of 7cm and was covered with 1ml isopropanol. After 15 minutes at room temperature the gel was polymerized and the isopropanol was removed. Following the stacking gel was layered on top of the separating gel. The stacking gel was performed according to the following table and has the same concentration independently of the PAA concentration of the separating gel:

Stacking gel buffer	0,5ml
Water	1,166ml
30% Acrylamide/Bis (Bio-rad)	0,334ml
10% APS	20µl
Tetramethylethylenediamine (Merck)	3µl
<b>Total volume:</b>	<b>2ml</b>

**Table 2.9.2.: Preparation schedule for stacking gel.**

The stacking gel was filled up until the edge of the glass plate and a comb was immediately inserted into the liquid gel. After 15 minutes at room temperature the gel was polymerized and the comb was removed. Slots were rinsed with water to avoid clotting of the chambers.

Afterwards the gel was inserted into a running-chamber, which was filled with 1x SDS running buffer. Usually 3µl of page ruler pre-stained protein ladder (Fermentas) was used as marker and 50µg of protein diluted in 4x sample buffer were loaded per slot. The electrophoresis was performed at 120V for approximately one hour until the bromophenol blue line has reached the bottom of the gel.

### **2.9.2. Immune-blot Semi-dry**

After SDS-PAGE, the proteins were transferred from the polyacrylamide gel to a nitrocellulose membrane (Whatman) using 1x immune-blot-transfer-buffer. Blotting was performed for 1h 15min at the amount of mm<sup>2</sup> of the membrane in milli ampere using a semi-dry blotting apparatus. The immune-blotting sandwich was made up of two pre-wetted filter papers, cut to the size of the gel. Next the preequilibrated membrane was placed on the filter papers and covered with the gel. At last another two pre-wetted filter papers were placed on top which faced the cathode. The sandwich was oriented in a way that the gel was at the cathode and the membrane at the anode.

After the transfer the membrane was blocked with 5% Milk (BioRad) in PBS-Tween (PAA/Sigma) for 1h. The primary antibody was diluted in 5% Milk/PBS-Tween and incubated for 1h at room temperature. After the first antibody three washing steps using 1x PBS-Tween for 5min were performed. The secondary antibody was incubated for 1h at room temperature and three washing steps using 1x PBS-Tween were performed.

The membrane was analyzed using an Odyssey Li-Cor machine, for which fluorescently labeled secondary antibodies or directly fluorescent labeled primary antibodies were used.

#### **Reagent**

- Gel buffer (4x):  
1.5M Tris-HCl pH8.8 (Sigma), 10% SDS (Serva) in deionized water

- Stacking gel buffer (4x):  
0.5M Tris-HCl pH 6.8 (Sigma), 10% SDS (Serva) in deionized water
- APS:  
10% ammonium persulphate (Merck) in deionised water
- Sample buffer (4x):  
0.2M Tris-HCl pH 6.8 (Sigma), 40% glycerol (Serva), 8% SDS (Serva), bromophenol blue (Sigma) in deionized water
- SDS running buffer (5x):  
250mM Tris (Sigma), 1.9M Glycine (Serva), 35mM SDS (Serva) in deionized water
- Immunoblot transfer buffer (1x):  
2mM TRIS-HCL (Sigma) pH 8.3, 96mM glycine (Serva), 20% methanol (Fluka)
- 1x PBS-Tween:  
500ml 10x PBS (PAA) are diluted in 4,5l deionised water, add 5ml TWEEN 20 (Sigma)
- V5-Antibody (InvivoGen), mAB, diluted 1:5000 in 5% Milk (BioRad) in PBS-Tween.
- pERK (Sigma), mAB, diluted 1:1000 in 5% Milk (BioRad) in PBS-Tween.
- ERK (Sigma), pAB, diluted 1:1000 in 5% Milk (BioRad) in PBS-Tween.
- Myc-800 (Rockland), directly labeled antibody, diluted 1:7000 in 5% Milk (BioRad) in PBS-Tween.
- Goat-anti-mouse-800 (InvitroGen), diluted 1:7000 in 5% Milk (BioRad) in PBS-Tween.

## 2.10. Immune-fluorescence

For immune fluorescence slides  $3 \times 10^5$  cells were seeded per well on a six well plate including one coverslip (13mm). The cells were seeded on the first day, on the second day the cells were transfected, following the transfection schedule for a six well plate (chapter 5.2.). On the third day the cells were fixed and stained with the according antibodies. After washing the cells one time with 1x PBS (PAA) the cells were fixed using 4% formaldehyde in a PTEMF solution for ten minutes. Afterwards the cells were washed again three times, before they were blocked in a 3% BSA (Sigma) PBS (PAA) solution for 30min. Afterwards the first antibody was incubated for one hour. After three washing steps with 1x PBS (PAA) the secondary antibody was incubated for one hour, including DAPI (Roth). After three further washing steps the coverslips were put on an object slide with the sunny side down using mowiol (Calbiochem). Afterwards the slides were stored at 4° C in the dark to avoid bleaching of the fluorophor.

### **Reagent**

- PTEMF-buffer:  
0,2% triton X 100 (Sigma), 20mM pipes-buffer pH6.8 (Sigma), 1mM MgCl<sub>2</sub> (Merck), 10mM EGTA (Fulka), 4% formaldehyde (Merck).



- V5-antibody:  
Mouse mAB, Invitrogen, 1:3000 dilution
- Myc-antibody:  
Rabbit pAB, Sigma, 1:1000 dilution
- Anti-mouse Alexa-Fluor 594:  
Goat anti-mouse Alexa Fluor 594, Molecular Probes, 1:3000 dilution
- Anti-rabbit Alexa-Fluor488:  
Goat anti-rabbit Alexa Fluor 488, Molecular Probes, 1:3000 dilution

### **2.11. Reporter Gene Assay**

On the first day the HEK cells were seeded on a 24well plate according to table 2.2.1. The cells should have been at least 70-80% confluent for transfection on the next day. On the second day the cells were transiently transfected with 100ng NF- $\kappa$ B-luciferase-reporter or the IFN- $\beta$ - luciferase-reporter and the 10ng renilla-reporter as well as 1 $\mu$ g of plasmid. After 24h the cells were stimulated with different ligands. Stimulation was performed for at least 8h, in order that the reporter constructs were transcribed.

Afterwards removing the medium the cells were washed one time with 1x PBS (PAA) and were snap frozen in liquid nitrogen and stored at -80° C.

The reporter gene assay was performed according to the provided protocol of the used kit, the dual-luciferase reporter assay system (Promega).

### **2.12. Quantitative Real Time PCR**

#### **2.12.1. RNA Preparation**

RNA was prepared from one 6well of cells using an RNeasy kit (QIAGEN) with on column DNA digestion (QIAGEN). RNA was prepared following the schedule provided in the kit. Afterwards the RNA concentration was measured and the quality is reviewed on a 1% agarose (InvitroGen) gel.

#### **2.12.2. Reverse Transcription**

1 $\mu$ g of RNA was diluted in 10 $\mu$ l of water and 1 $\mu$ l oligo(dt) primer (Fermentas) was add. The solution was heated at 65° C for 5min and the following reverse transcription mix was added after heating:

RT-buffer (Fermentas)	4µl
10mM dNTP mix (Fermentas)	2µl
RNAse inhibitors (Promega)	0,5µl
H <sub>2</sub> O	1,5µl
RevertAid M-MuLV reverse transcriptase (Fermentas)	1µl
<b>total:</b>	<b>9µl</b>

Reverse transcription was performed at 42° C for 1h, afterwards the enzyme was inhibited at 65° C for 5min.

### 2.12.3. qRT-PCR Reaction

Quantitative real time PCR was performed using the Corbett system. Therefore the RNA was diluted 1:20 in water and 2,5µl were used per reaction. The primers were diluted in the following way:

SensiMixPlus SYBR (Quantace)	5µl
H <sub>2</sub> O	2,25µl
Primer (10mM)	0,25µl
<b>Total:</b>	<b>7,5µl</b>

In total 10µl of cDNA-primer-mix were used for qRT-PCR, which was performed with the following settings:

Primary denaturation:	95° C	10 min	
Denaturation:	95° C	30 sec	} 40 cycles
Annealing:	60° C	15 sec	
Extension:	72° C	30 min	

### 2.12.4. Used Primers

Smpdl3b Primer 1:

Forward primer: 5' CAC AGA GCA ACC GCA TCT AT 3'

Reverse primer: 5' GCA CGT GGC CAA TAA CAT AC 3'

Smpdl3b Primer 2:

Forward primer: 5' AAG TCT ATG CTG CTC TGG GAA 3'

Reverse primer: 5' TGC CAC CTG GTT ATA GAT GC 3'

ASMase Primer 1:

Forward primer: 5' AAC CCT GGC TAC CGA GTT TA 3'

Reverse primer: 5' GCC TGG GTC AGA TTC AAG AT 3'

ASMase Primer2:

Forward primer: 5' GGA AGC TCT CAT GTG GTC CT 3'

Reverse primer: 5' AGG TTT CTC GAG CCC TGT AG 3'

For normalization cyclin B was taken as representative house-keeping gene.

CyclinB:

Forward Primer: 5' CAG CAA GTT CCA TCG TGT CAT CAA GT 3'

Reverse Primer: 5' GGA AGC GCT CAC CAT AGA TGC TC 3'

## Results

### 3.1. The Ideal Cell-Line for Tandem Affinity Purification of TLRs

To perform TAP with endosomal TLRs we were in need of a cell line that is capable of TLR signaling. Stimulation of RAW cells with the TLR ligands LPS (TLR4), Poly(I:C) (TLR3), Imiquimod (TLR7) and CpG (TLR9) readily resulted in the phosphorylation and, hence, activation of Erk kinase (Fig. 3.1.1.). After 15 minutes of LPS and imiquimod treatment a strong pERK signal appeared, which slowly decreased over time. For CpG stimulation ERK became phosphorylated after 30 minutes. The appearance of pERK upon poly(I:C) treatment happens quite late after approximately 100 minutes. This reflects the responsiveness of these cells to the respective ligands and suggests that all factors necessary for successful TLR pathway signaling are present. Therefore, we selected RAW264.7 macrophages as the cell line of choice for the identification of new interacting partners of endosomal toll-like receptors.

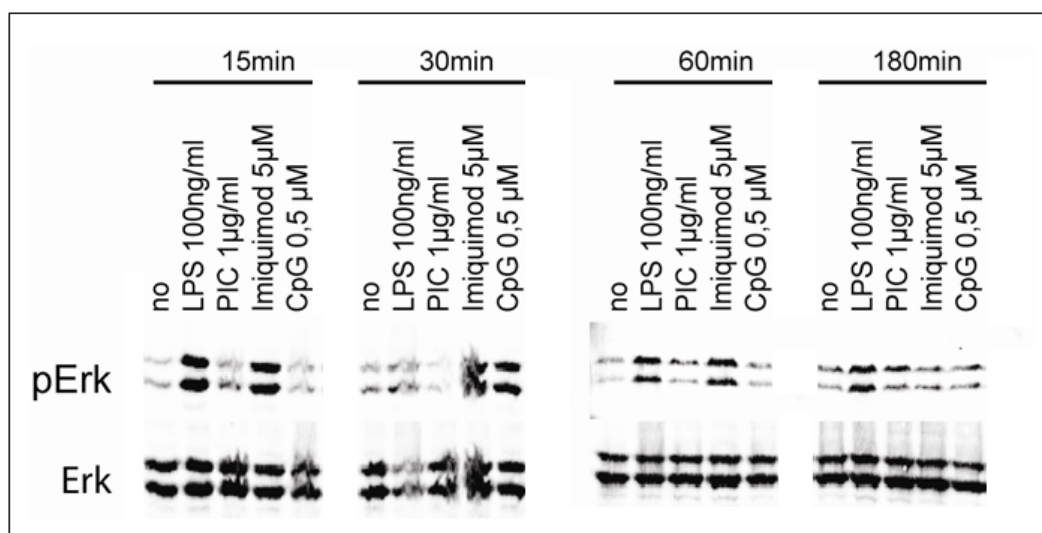
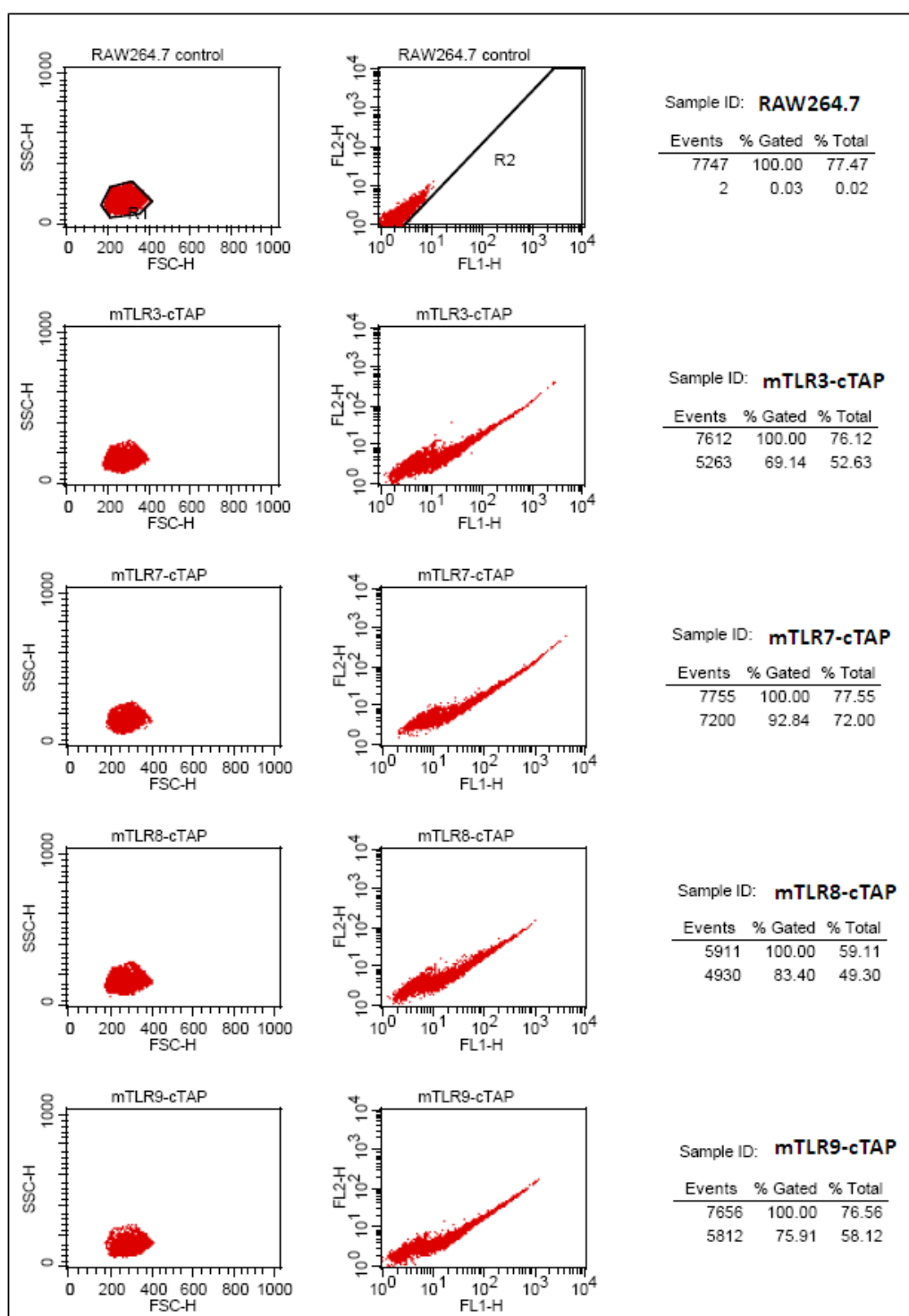


Figure 3.1.1.: pERK and ERK western-blot for stimulated RAW264.7 macrophages. Stimulated with 100ng/ml lipopolysaccharid (LPS), 1µg/ml poly(I:C) (PIC), 5µM imiquimod and 0,5µM CpG in a time dependent manner. Data kindly provided by Christoph Baumann.

#### 3.1.1. Verification of Bait Expression by Flow Cytometry and Western-Blot

After the generation of stable RAW264.7 macrophages, expressing murine TLR-TAP constructs, the transduction efficiency was measured via flow cytometry. The mTLR-cTAP constructs harbor an IRES-GFP reporter which was used to enrich transfected cells via fluorescence activated cell sorting. After the sorting and expansion of the cells the transfection efficiency was again analyzed via flow cytometry targeting the expressed IRES-GFP (Fig. 3.1.2.). As control parental RAW264.7 without over-expressed IRES-GFP have been used as reference cell-line.



**Figure 3.1.2.: Flow cytometry blot of stable transfected RAW264.7 macrophages, expressing either mTLR3, mTLR7, mTLR8, mTLR9 fused to a TAP-tag cassette.**

The transduction efficiency varied between 70% and 95% of not gated cells (Fig. 3.1.2.) which reflects enough fusion-protein for tandem affinity purification.

Since the verification of expressed IRES-GFP only indirectly indicates the actual expression of bait protein, a western-blot was performed to verify the expression of the TLR constructs in addition (Fig. 3.1.3.).

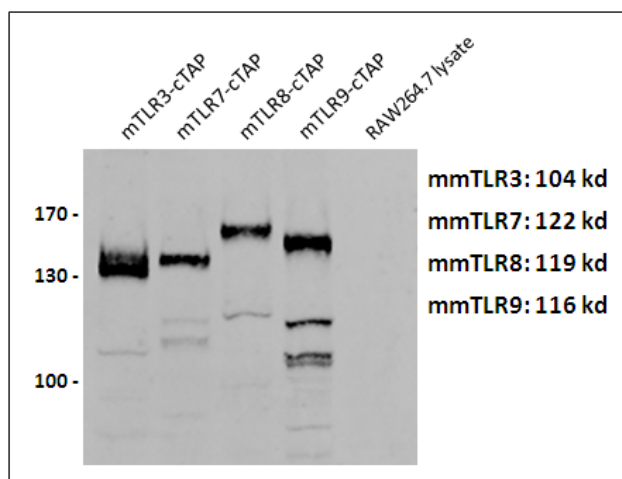


**Figure 3.1.3.: Western-blot of stable transfected RAW264.7 macrophages, expressing murine endosomal toll-like-receptors, fused to the GS-TAP tag. Western-blot incubated with  $\alpha$ -myc mAb.**

The TAP tag of the fusion-proteins harbors a myc-tag, which was visualized using an antibody against myc. Hence, the TLR-fusion proteins of the four stably integrated endosomal TLRs in RAW264.7 macrophages could be monitored by their myc-tag.

To calculate the expected molecular weight and to estimate the migration behavior of the TLRs on SDS-page, the reference sequence from the NCBI database, according to the accession number, was translated into the amino-acid sequence using the ExPasy database. The resulting properties are listed in Table 3.1.4.

	<b>Mus musculus</b>	<b>Homo sapiens</b>
TLR-3	2718 base pairs 905 amino acids 103 671 daltons	2715 base pairs 904 amino acids 103 829 daltons
TLR-7	3153 base pairs 1050 amino acids 121 837 daltons	3150 base pairs 1049 amino acids 120 922 daltons
TLR-8	3099 base pairs 1032 amino acids 119 339 daltons	3126 base pairs 1041 amino acids 119 828 daltons
TLR-9	3099 base pairs 1032 amino acids 116 348 daltons	3099 base pairs 1032 amino acids 115 860 daltons

**Table 3.1.4.: Properties of murine and human endosomal TLR constructs.**

The TLR-fusion-proteins were running at a higher size than predicted from the database. Two reasons might explain the size shift: first the fusion-proteins carry a TAP-tag which has a size of 22kd. Secondly toll-like-receptors are predicted to be highly glycosylated proteins which results in a shift towards a higher mass (Fig. 3.1.3. and Fig. 3.1.5.).

To investigate if the TAP-tagged TLR fusion proteins behaved similar in a human cell-line, not related to innate immunity, we performed stable transfection of the constructs into HEK293 cells and monitored the migration on an SDS-gel. Western-blot analysis, using an anti-myc-antibody, was performed (Fig. 3.1.5.). Interestingly, a large fraction of TLR7-cTAP constructs was migrating faster on SDS-page (marked by an asterisk), indicating a smaller size than predicted by the sequence. However, as shown in the literature, TLR7 is cleaved in order to be activated, which might serve as an explanation for the smaller size of mTLR7-cTAP (Park et al., 2008). Moreover, it is possible, that TLR7 is not glycosylated in HEK293 cells, in order of wrong procession. In general the sizes of the TLR-fusion proteins in HEK293 (Fig. 3.1.5.) differ from the ones in RAW264.7 cells (Fig. 3.1.3.). This result suggests that the same TLR-cTAP fusion proteins are differently processed in HEK293 cells and RAW264.7 macrophages.

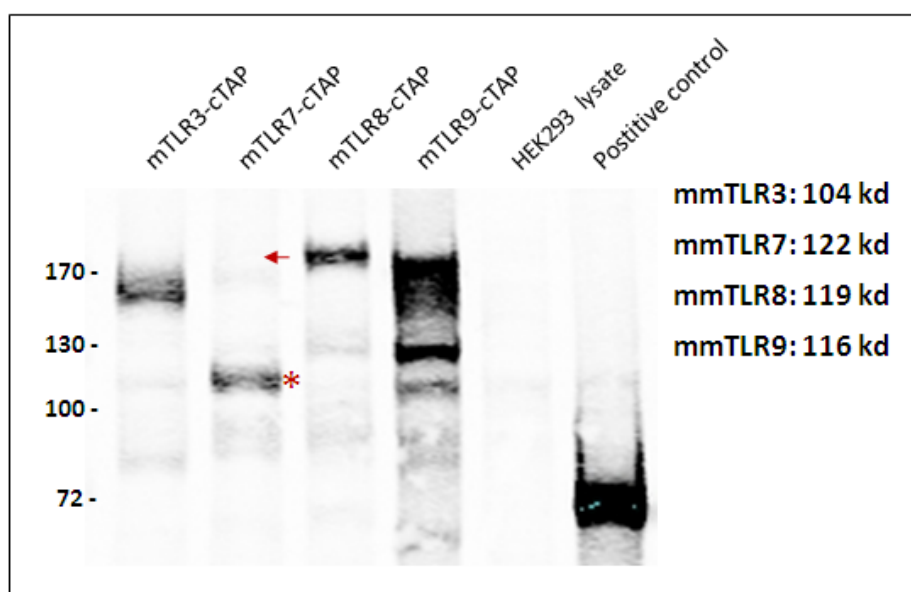


**Figure 3.1.5.:** Western-blot of transiently transfected HEK293 cells, expressing murine endosomal toll-like-receptors. Arrow indicates predicted size of TLR7, asterisk shows the effective running site of TLR7. Western-blot incubated with  $\alpha$ -myc mAb.

These data show that the murine TLR-TAP-constructs were highly expressed in stable RAW264.7 cells and transiently in HEK293 cells. However the same TLR-cTAP fusion proteins are differently processed in HEK293 cells and RAW264.7 macrophages. Nevertheless the monitored size of the fusion-proteins indicates that the TLR constructs are glycosylated in both cell-lines.

### 3.1.2. mTLR-TAP Constructs are Highly Glycosylated

Even though we showed above that our TLR constructs were expressed in the macrophage cell lines, the expression of the fusion-protein gives no indication on the procession or posttranslational modification of the constructs. Thus, a deglycosylation assay was performed to verify the predicted posttranslational glycosylation.

This assay is generally performed as validation of native processing of fusion proteins. The glycosylation status of TLRs would indicate that they are processed through the Golgi, where they are glycosylated, and finally shuttled to the end compartments, in the case of endosomal toll-like-receptors to the endoplasmic reticulum (Brinkmann et al., 2007).

To investigate whether the mTLR-cTAP constructs are shuttled to the right compartments we transiently transfected the murine TLR-cTAP constructs into HEK293 cells. The reason for taking HEK293 cells instead of RAW264.7 macrophages was to minimize cell specific effects. HEK293 cells are less TLR signaling competent than RAW264.7 macrophages, further a murine sequence was used for human cells. Our focus in this experiment was to see if the receptors are natively folded, which is necessary for glycosylation, and if the large TAP-tag interferes with the signal peptide and proper folding. The western-blot in Fig. 3.1.6. shows that all four endosomal toll-like receptors are glycosylated and are running at the predicted site, including the 22kd TAP-tag, when the sugar residues are removed. For mTLR7-cTAP two bands are visible. The smaller band is more prominent, which indicates, that this receptor is not only natively processed but also cleaved, which is necessary for activation (Park et al., 2008).

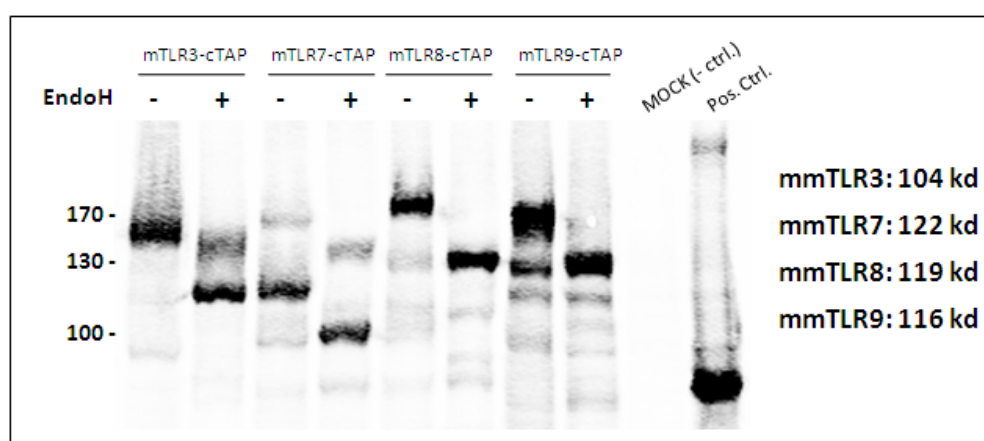


**Figure 3.1.6.: Deglycosylation assay of HEK293 cells transiently transfected mTLR-cTAP constructs. Western-blot incubated with  $\alpha$ -myc mAb.**

In summary, we established four stable RAW264.7 macrophages cell-lines, which are expressing endosomal TLR-cTAP constructs that have been shown to be delivered in the predicted compartments by successfully deglycosylation. These results suggest that the generated fusion proteins are signaling competent and are therefore suggested to bind possible co-factors.



## 3.2. Pulldown of Endosomal Toll-like-Receptors

### 3.2.1. Tandem Affinity Purification

Having established the mTLR-cTAP expressing stable cell lines we next started out to perform two-step tandem affinity purifications (TAP) of the four TLRs. Therefore we had to establish a special protocol for endosomal transmembrane proteins, to increase the purification yield.

Due to statistical significance, duplicates of the TAP-pulldowns, for the four endosomal toll-like-receptors, were performed. Tandem affinity purification is quite inefficient concerning the amounts of cell lysate necessary, but very efficient concerning purity. During the two pulldown steps a lot of bait protein was lost; therefore very high amounts of cells were necessary. To monitor the different steps of tandem-affinity-purification a western-blot was performed with aliquots of every TAP-pulldown step (Fig. 3.2.1.). Although the final elution of the streptavidin beads appeared to be very little amount of protein in a westernblot (arrows in Fig. 3.2.1), the levels were enough for mass-spectrometry-analysis, since only a very little amount of eluate was loaded on the western-blot and since the LTQ Orbitraps runs with very high sensitivity. Surprisingly, mTLR7-cTAP appeared at a very small size in the western-blot, as well as mTLR3-cTAP. Therefore the TAP-pulldown was repeated twice, to exclude degradation during the experimental process, with same results. Since it was reported, that the cleavage of TLR7 is necessary to activate the receptors, the eluates have been sent to mass-spectrometry, albeit the smaller size.

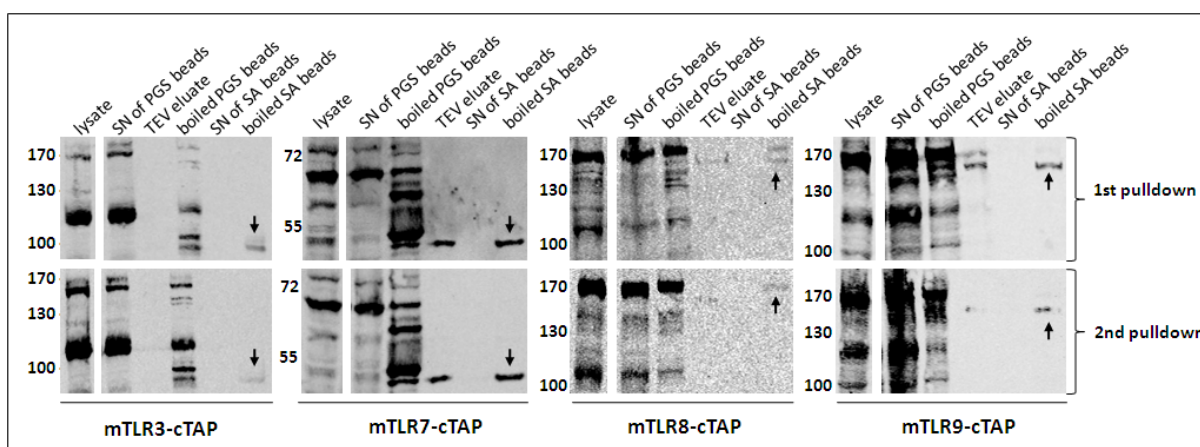
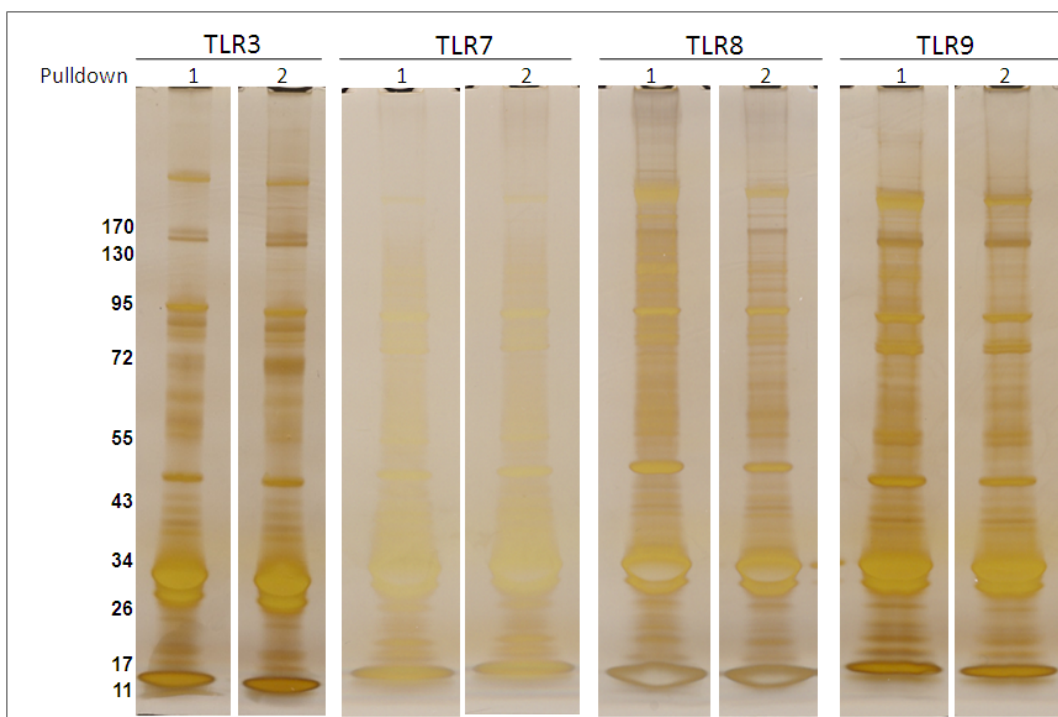


Figure 3.2.1.: Western-blot of TAP-pulldown samples to monitor the efficiency of the different purification steps. Western-blot incubated with  $\alpha$ -myc mAb.

### 3.2.2. Silver-gel of TAP Eluates

With the final eluates a silver-gel was performed by our mass-spectrometry team. On the gel single bands were cut out and analyzed via mass-spectrometry. The majority of bands could be only visualized on the silver-gel since this method is sensitive enough to show already little amounts of protein (Fig. 3.2.2.).



**Figure 3.2.2.: Silver gel of tandem-affinity purification eluates, kindly provided by the Mass-spectrometry team at CeMM (Melanie Planyavsky and André Müller).**

### 3.2.3. Mass Spectrometry and Statistical Analysis

Peptide counts reflect how many different peptides of a trypsinated protein have been found and were therefore taken as a read out in our mass spectrometry analysis. For unambiguous protein-identification at least two unique peptides were required to decrease the false positive rate of detected peptides. As negative control the core proteome of parental RAW264.7 macrophages was analyzed contrastable to the TLR-TAP-pulldown samples.

The resulting data can be divided into protein counts, which display each protein detected at least twice, and protein group counts, where different isoforms were combined to one group. Predominantly identical tryptic peptides were detected by mass-spectrometry for different isoforms. Thus specific isoforms were unlikely to be determined, wherefore those proteins were integrated in one protein group. Nevertheless some isoforms could be clearly identified by a unique tryptic peptide pattern; those proteins were classified as specific protein count. Further the rating of the bait protein was used as a quality feature for the pulldowns. In Table 3.2.3. the peptide counts for the two pulldowns of every single endosomal toll-like receptor are listed.

	mTLR3		mTLR7		mTLR8		mTLR9	
	PD-1	PD-2	PD-1	PD-2	PD-1	PD-2	PD-1	PD-2
bait protein count	29	32	19	21	13	14	25	26
protein count	366	366	746	746	1089	1056	1200	732
protein group count	50	50	140	135	216	213	222	125
specific protein count	35	32	93	84	134	125	124	82

**Table 3.2.3.: Peptide counts of pull-down duplets performed for endosomal toll-like receptors.**

Several interactors for endosomal TLRs have been published, such as Unc93B1 and GP96. From the published interactors of endosomal TLRs only GP96 was present in all pulldowns, despite mTLR3 pulldown-2, which kind of served as positive control for the pulldown conditions (Tab. 3.2.4.) (Akashi-Takamura and Miyake, 2008). Other constant endosomal toll-like receptor interactors, such as Unc93b1 have not been found in the pulldowns.

<b>Pull-down</b>	<b>IPI00830494</b>
	<b>Hsp90b1 Mouse</b>
mTLR3-1	2
mTLR3-2	-
mTLR7-1	3
mTLR7-2	5
mTLR8-1	6
mTLR8-2	7
mTLR9-1	6
mTLR9-2	6

**Table 3.2.4.: Appearance of GP96 in endosomal TLR pulldowns, listed with peptide counts.**

Between 1200 and 366 proteins have been detected in each of the eight different pulldowns (Tab. 3.2.3.). To eliminate non-significant proteins and to select intrinsic interactors, the data was further analyzed by our Bioinformatics Department (head: Jacques Colinge) at CeMM.

Two major criteria have been set to analyze the data and to select only significant proteins. The first is peptide enrichment over core proteome. Only proteins, which were enriched at least two peptide counts, according to the core proteome protein counts, have been selected. For this analysis the core proteome was used as a negative control that represents house-keeping genes generally expressed in RAW264.7 macrophages, or proteins preferentially detected by mass spectrometry. The second criterion was based on the appearance of proteins in any pulldown ever done at CeMM, which is termed as occurrence in ProtFollow, software designed at CeMM, to compare sets of different mass-spectrometry

data. Further all proteins have been screened by eye to ensure highest quality of data selection.

IPI Nr,	Protein	core proteom		TLR-3		TLR-7		TLR-8		TLR-9	
		P536-1	P536-2	P684	P686	P703	P705	P707	P709	P688	P690
IPI00320618	Tlr3	-	-	29,0	32,0	-	-	-	-	-	-
IPI00122181	Tlr7	6,0	7,0	-	-	19,0	21,0	-	-	-	-
IPI00831009	Tlr8	-	-	-	-	-	-	13,0	14,0	-	-
IPI00318748	Tlr9	-	-	-	-	-	-	-	-	25,0	26,0
IPI00126860	Taok1,Kiaa1361	6,0	4,0	3,0	-	-	-	-	-	-	-
IPI00229721	Poldip3	-	-	10,0	4,0	-	-	-	-	-	-
IPI00228150	Immt,HMP,P87,P89,P87/89,	4,0	4,0	-	12,0	4,0	3,0	19,0	3,0	7,0	-
IPI00230138	Lyn,Hck-2,AA407514	-	-	-	5,0	11,0	7,0	16,0	8,0	8,0	3,0
IPI00308990	Cd14	5,0	5,0	-	6,0	7,0	10,0	12,0	8,0	11,0	11,0
IPI00387204	Myo1g,myosin 1G,	-	-	-	6,0	23,0	16,0	15,0	9,0	19,0	13,0
IPI00468396	Rasa3	-	-	2,0	2,0	11,0	9,0	14,0	5,0	6,0	2,0
IPI00816935	Rasa3,C86362,GAPIII	-	-	2,0	2,0	11,0	9,0	15,0	5,0	7,0	2,0
IPI00114842	Raet1a	-	-	-	-	3,0	-	4,0	2,0	3,0	-
IPI00117534	Smpdl3b,Asml3b	-	-	-	2,0	7,0	4,0	10,0	3,0	2,0	2,0
IPI00135571		-	-	2,0	-	-	3,0	4,0	-	5,0	-
IPI00314075	Lrrfip2,AI850587,	-	-	-	-	3,0	3,0	8,0	5,0	6,0	5,0
IPI00469253	Rftn1,Kiaa0084	-	-	-	-	4,0	4,0	7,0	3,0	3,0	-
IPI00659860	Lrrfip2,AI850587	-	-	-	-	4,0	4,0	8,0	6,0	7,0	6,0
IPI00114844	Raet1b	-	-	-	-	3,0	2,0	3,0	2,0	2,0	-
IPI00229645	Specc1l,Cytsa,Kiaa0376	-	-	-	-	2,0	2,0	2,0	4,0	4,0	-
IPI00322097	Fyn,AI448320,AW552119,	-	-	-	-	2,0	-	6,0	-	-	-
IPI00407864	Kif23	-	-	-	-	4,0	-	4,0	-	-	-
IPI00129487	Hck,Bmk,Hck-1,AI849071	4,0	3,0	-	-	3,0	4,0	7,0	3,0	-	-
IPI00111856	Fcgr1,Fcg1	2,0	3,0	2,0	2,0	3,0	2,0	-	3,0	-	3,0
IPI00626402	Rcc1,Chc1	-	-	-	-	-	-	2,0	3,0	3,0	3,0
IPI00116859	Parp9,Bal,Bagl,MGC7868	-	2,0	-	-	-	-	5,0	3,0	6,0	3,0
IPI00123762	Rcc1,Chc1,AI326872	-	-	-	-	-	-	2,0	3,0	3,0	3,0
IPI00453863	Efr3a	-	-	-	-	-	-	4,0	-	-	-
IPI00750570	Gnas1,P1,P2,P3,GSP,Gsa	-	-	-	-	-	-	3,0	-	-	-
IPI00850551	Grtp1,C81211,Tbc1d6	-	-	-	-	-	-	2,0	-	-	-
IPI00110045	Rp2h,AI662636	-	-	-	-	1,0	-	5,0	2,0	-	-
IPI00126176	Racgap1,Mgcracgap	-	-	-	-	-	-	3,0	-	-	-
IPI00221608	Samm50	-	-	-	3,0	-	-	4,0	-	-	-
IPI00308065	Fgr	-	-	-	-	4,0	-	6,0	3,0	3,0	-
IPI00310205	Eefsec,Selb	-	-	-	-	-	-	2,0	-	4,0	-
IPI00408061	Lgals8,Lgals-8,AI326142,	-	-	-	-	-	-	5,0	-	2,0	-
IPI00420651	Ppp1r9b,MGC38940	-	-	-	-	4,0	2,0	-	-	3,0	-
IPI00466219	Hmmr,CD168,Rhamm	2,0	-	2,0	-	3,0	5,0	-	-	5,0	-

**Table 3.2.5.: List of potential candidates after statistical analysis, listed with peptide counts.**

After statistical analysis 34 candidates (Tab. 3.2.5.) have been selected as significant interacting proteins. Since a list of 34 proteins is unfeasibly large for interaction validation, a further selection was applied. Therefore literature search for the 34 possible candidates was

performed to ascertain any association to innate immunity and toll-like receptors. As tool the Bioinformatic Harvester III (beta) was used to search for structural information, localization, domains, interacting partners, literature and possible functions. Taking this information a further selection was performed to decrease the list of possible interactors to a maximum of a few proteins (Tab. 3.2.6.).

	core proteom		TLR-3		TLR-7		TLR-8		TLR-9	
Sptr GNs	P536-1	P536-2	P684	P686	P703	P705	P707	P709	P688	P690
Taok1	6,0	4,0	3,0	-	-	-	-	-	-	-
Poldip3	-	-	10,0	4,0	-	-	-	-	-	-
Cd14	5,0	5,0	-	6,0	7,0	10,0	12,0	8,0	11,0	11,0
Lyn	-	-	-	5,0	11,0	7,0	16,0	8,0	8,0	3,0
Smpdl3b	-	-	-	2,0	7,0	4,0	10,0	3,0	2,0	2,0
Rasa3	-	-	2,0	2,0	11,0	9,0	14,0	5,0	6,0	2,0
Rftn1	-	-	-	-	4,0	4,0	7,0	3,0	3,0	-

**Table 3.2.6.: List of final candidates after literature search, listed with peptide counts.**

Finally a list of seven candidates (Tab. 3.2.6) was selected for further validation. Interestingly, the proteins are either found in TLR3 pulldowns or in TLR7, -8 and -9 pulldowns. As described in the introduction TLR3 is the only endosomal toll-like receptor, which is downstream signaling via the adaptor protein TRIF, whereas the other three TLRs are interacting with MyD88. It seems that the selected candidates already show a pathway specificity, which further confirmed our selection as significant.

In addition to the non stimulated endosomal TLR pulldowns, two pulldowns for TLR3 have been performed where the cells have been stimulated 45min with 100ng/ml of polyI:C before harvesting. This pulldown was meant as a survey to see, if we get a different set of proteins pulled down, if we stimulate the cells. Since we have not found new proteins but only an enrichment of already present peptides in non stimulated TLR3 pulldowns, we finally decided not to perform stimulated pulldowns for the other receptors, as well because of limited mass-spectrometry time.

Taok1 was detected with very low peptide counts in non-stimulated TLR3 pulldowns and was present with much lower levels than in the core proteome of RAW264.7 cells. In stimulated TLR3 pulldowns TaoK1 was highly enriched, whereby we have been convinced to elect TaoK1 as promising co-receptor (Tab. 3.2.7.). Further Poldip3 was enriched in stimulated TLR3 pulldowns. Whereas Smpdl3b, Rasa3 and Rftn1 which have been present with very low peptide counts in the non stimulated TLR3 pulldowns, have not been enriched in stimulated TLR3 pulldowns, which confirms our estimation that the candidates show a

pathway specificity, since they are either detected in TLR3 pulldowns or in the TLR7, -8 and -9 dataset.

	core proteom		TLR-3		TLR-3 stim.	
Sptr GNs	P536-1	P536-2	P684	P686	P712	P714
TLR3	-	-	29,0	32,0	29,0	30,0
Taok1	6,0	4,0	3,0	-	4,0	13,0
Poldip3	-	-	10,0	4,0	14,0	16,0
Cd14	5,0	5,0	-	6,0	4,0	6,0
Lyn	-	-	-	5,0	-	2,0
Smpdl3b	-	-	-	2,0	-	-
Rasa3	-	-	2,0	2,0	-	-
Rftn1	-	-	-	-	-	-

**Table 3.2.7.:** Peptide counts for selected candidates in non-stimulated and stimulated TLR3 pulldowns. Stable RAW264.7 expressing mTLR3 have been stimulated with 200ng/ml polyI:C for 45 min.

In Table 3.2.8. the Prot-Follow data is listed to monitor how often our selected candidates ever appeared in any other pulldown. The more often one Protein shows up in any dataset the more abandoned it is supposed to be. The protein Lyn is also found in 18 other pulldowns. Smpdl3b appears only in eleven other pulldowns with low peptide counts. TaoK1 is only found in seven other datasets, but it is also very little present in the non stimulated TLR3 pulldown. Cd14 can be detected in 23 other experiments. Poldip3 appears in 22 other pulldowns. Rftn1 only appears in the endosomal TLR pulldowns and in one further dataset. Rasa3 is only present in two other pulldowns and is highly enriched in the TLR data.

Sample	IPI00117534	IPI00230138	IPI00126860	IPI00308990	IPI00229721	IPI00469253	IPI00468396
	Taok1	Poldip3	CD14	LYN	Smpdl3b	Rasa3	Raftlin
P178				3			
P217		6					
P227	3			2			
P243			4				
P244					4		
P245					3		
P246	2						
P247	2						
P260	2						
P261	2			2			
P286		15					
P334				2			
P336		3		2			
P385	3	4		12			
P386	3	6		11			
P387				7			
P398				3			

P488		4		4			
P526		6					
P527		3					
P536			6	6			
P614	5	10		8			
P615	3	11		9		2	
P617	2	2		3			
P618		3		4			
P619	2	3		4			
P636					3		
P637					7		
P639					4		
P642					2		
P643					5		
P644			3		2		
P671		2		10			
P674		2	6		15		
P675				10			
P678			2	2	13		
mTLR3-1			3		10		2
mTLR3-2	2	5		6	4		2
mTLR3-stim-1			4	4	14		
mTLR3-stim-2		2	13	6	16		
mTLR7-1	7	11		7		4	11
mTLR7-2	4	7		10		4	9
mTLR8-1	10	16		12		7	14
mTLR8-2	3	8		8		3	5
mTLR9-1	2	6		11		3	6
mTLR9-2	2	3		11			2
P716		3		5	2		
P717		3		4	3		
P720					4		3
P721					9		
P722					5		
P723					10		
P763					14		3
P764					9		
P936					2		
P937					3		
P1035		2					
P1036	3	2		3			
P1108					3		

**Table 3.2.8.: ProtFollow data for the seven selected candidates, listed with peptide counts.**

Many of the selected candidates appear in innate immunity related pulldowns. For example P243 is a pulldown, where polyI:C was used as bait. TaoK1 is specifically found in the TLR3 pulldown, in the polyI:C pulldown (P243), in the core proteome (P536) and in an ISD pulldown (P644). It is not surprising that the kinase Lyn is found in some dasatinib pulldowns

(P526/P527) since Lyn is a target of dasatinib. Interestingly, Cd14 and Lyn are also found in a pulldown, where the TLR adapter protein TIRAP was used as bait (P336). Moreover, Poldip3 is found in CpG pulldowns (P244/245), as well as in ISD pulldowns (P643/P644), which is not surprising, since the protein harbors an RNA binding motive. Rftn1 is only found in TLR pulldowns and in TBK-1 purification (P615) with low peptide counts.

In summary, up to 1200 proteins have been detected by mass-spectrometry in the different TLR pulldowns. This data suggests seven candidates, that fulfill our set criteria of significance and which are further highly interesting due to their predicted function in the literature.

### 3.3. The Interactor Candidates

For the selected seven candidates I performed an advanced literature search, using Bioinformatic Harvester III (beta) for protein properties and the NCBI database for literature search.

#### 3.3.1. Serine/Threonine-Protein Kinase TAO1 (TaoK1)

TaoK1 is mainly found in the TLR3 pulldown, especially in the stimulated mTLR3 pulldown with very high peptide counts (Tab.3.2.8.) and is indicated to play a role in innate immunity in the literature. Therefore it was selected as possible interacting protein for further validation.

#### Properties of TaoK1

Symbol:	TaoK1
Name:	TAO kinase 1
ID:	MGI:1914490
IPI:	IPI00126860
Synonyms:	2810468K05Rik, D130018F14Rik
Description:	Serine/Threonine kinase superfamily
Genetic MAP:	Chromosome 11
Base pairs:	3006 base pairs
Aminoacids:	1001 amino acids
Molecular weight:	116050.1 daltons
Domains:	Serine/Threonine protein kinases catalytic domain
Interactors:	self associates, interacts with MKK3
Localization:	Cytoplasm
Predicted function:	Activates p38 upon DNA-damage, activates MEK upon stress.



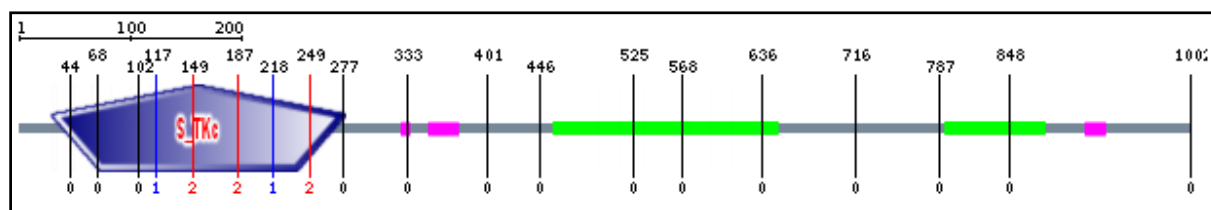


Figure 3.3.1.: Predicted structure of TaoK1 (figure taken from SMART-domain)

### 3.3.2. Polymerase Delta-Interacting Protein 3 (Poldip3)

We found Poldip3b in TLR3 pulldowns where it is present with high numbers of peptide counts and it is not found in the core proteome of parental RAW264.7 macrophages (Tab. 3.2.6.). The protein is highly present in the TLR3 pulldown, but it is also found in some other datasets (Tab.3.2.7.).

#### Properties of Poldip3

Symbol:	Poldip3
Name:	Polymerase (DNA-directed), delta interacting protein 3
ID:	MGI:1921076
IPI:	IPI00229721
Synonyms:	1110008P04Rik, PDIP46
Description:	Not known
Genetic MAP:	Chromosome 15
Base pairs:	1263 base pairs
Aminoacids:	420 amino acids
Molecular weight:	46132.4 daltons
Domains:	RRM domain, shows signal peptide and transmembrane domain prediction data
Interactors:	Pold2, Poldip2, Bag1, Hat1, Aasthppt, Irs1, Rps6kb1, Rps6kb2
Localization:	Nucleus
Predicted function:	Not known

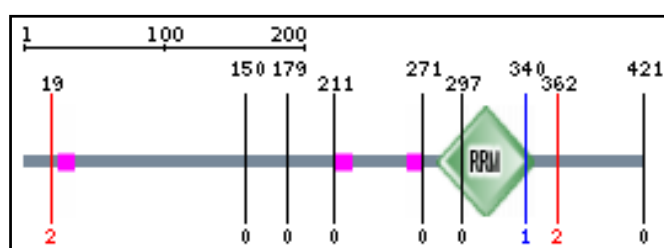


Figure 3.3.2.: Predicted structure of Poldip3 (figure taken from SMART-domain)

### 3.3.3. Ras P21 Protein Activator 3 (Rasa3)

We found Rasa3 highly enriched in TLR7, -8 and -9 pulldowns and present in low levels in the TLR3 data set (Tab.3.2.6). The protein is only significantly present in the TLR pulldowns (Tab.3.2.7.), which suggest that it is a very specific candidate.

#### Properties of Rasa3

Symbol:	Rasa3
Name:	RAS p21 protein activator 3
ID:	MGI:1197013
IPI:	IPI00816935
Synonyms:	GAPIII, GAPIII activator 3, Ras GTPase-activating protein III
Description:	Inhibitor regulator of the RAS cyclic-AMP pathway
Genetic MAP:	Chromosome 8
Base pairs:	2505 base pairs
Aminoacids:	834 amino acids
Molecular weight:	95987.3 daltons
Domains:	PH-domain like, C2 domain, GTPase activation domain
Interactors:	Hras1, Bsl2l11, Rasa2, Itpkb, Rap1a
Localization:	Not known
Predicted function:	Not known

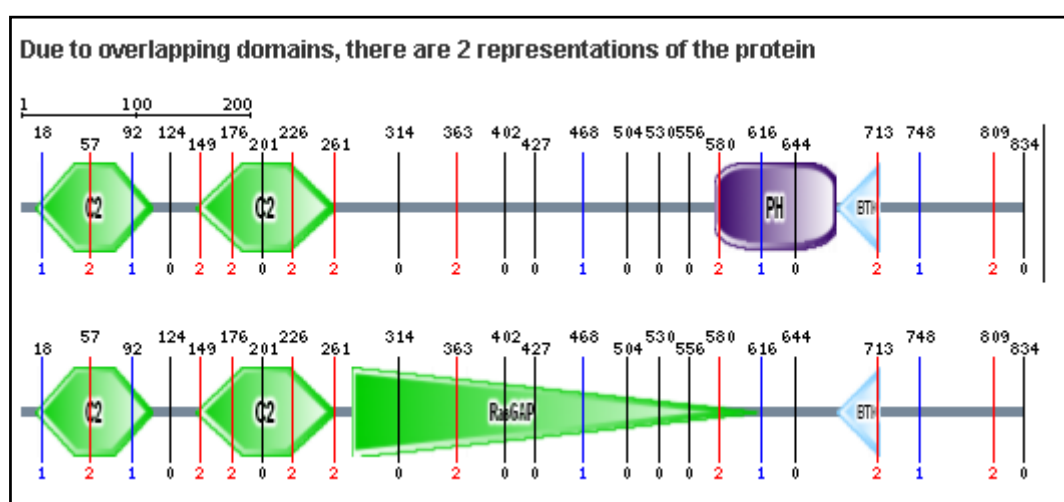


Figure 3.3.3.: Predicted structure of Rasa3 (figure taken from SMART-domains)

### 3.3.4. Raftlin Lipid Raft Linker 1 (Rftn1)

We found Rftn1 only in TLR7 and -8 pulldowns and - with very low peptide counts in the TLR9 dataset (Fig. 3.2.6.). The protein is only significantly present in the TLR pulldowns (Tab.3.2.7.), which suggests that Rftn1 may be a very specific candidate.

#### Properties of Rftn1

Symbol:	Rftn1
Name:	Raftlin lipid raft linker 1
ID:	MGI:1923688
IPI:	IPI00469253
Synonyms:	310015N21Rik
Superfamily:	Raftlin superfamily
Description:	The B cell-specific major raft protein, Raftlin, is necessary for the integrity of lipid raft and BCR signal transduction integrity of lipid rafts.
Genetic MAP:	Chromosome 17
Base pairs:	1665 base pairs
Aminoacids:	554 amino acids
Molecular weight:	61537.1 daltons
Domains:	No conserved domains
Interactors:	No known interactors
Localization:	cell membrane, lipid anchor
Predicted function:	May play a pivotal role in the formation and/or maintenance of lipid rafts. May regulate B-cell antigen receptor- mediated signaling.

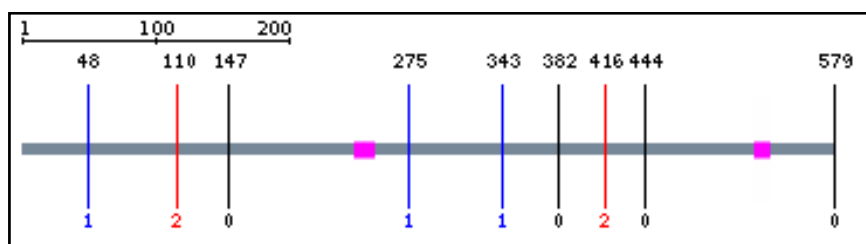


Figure 3.3.4.: Predicted structure of Rftn1 (figure taken from SMART-domain)

### 3.3.5. Yamaguchi Sarcoma Viral (v-yes-1) Oncogene Homolog (Lyn)

Lyn is present in all four Toll-like receptor pulldowns, but not in the core proteome of RAW264.7 macrophages (Tab. 3.2.6.). The protein is quite abundant compared to the other six candidates concerning the appearance in the CeMM pulldown database ProtFollow (Tab.3.2.7.).

#### Properties of Lyn

Symbol:	Lyn
Name:	Yamaguchi sarcoma viral (v-yes-1) oncogene homolog
ID:	MGI:96892
IPI:	IPI00230138
Synonyms:	Hck-2
Superfamily:	Tyrosine kinase superfamily
Description:	Tyrosine kinase
Genetic MAP:	Chromosome 4
Base pairs:	1476 base pairs
Aminoacids:	491 amino acids
Molecular weight:	56309.5 daltons
Domains:	SH2, SH3, tyrosine kinase domain
Interactors:	Evl, Hcls1, Cd19, Cd79a, Cd79b, Fcgr2, Cd22, Inpp5d, Gab2, Fcer1g
Localization:	Cytoplasm
Predicted function:	Interacts with phosphorylated LIME1 and with CD79A upon BCR activation. Interacts with Epstein-Barr virus LMP2A. Interacts with TGFB111. Interaction, via the SH2 and SH3, domains with MUC1 is stimulated by IL7 and, the subsequent phosphorylation increases the binding between MUC1 and CTNNB1/beta-catenin (By similarity). Interacts with PPP1R15A via the SH3 domain.

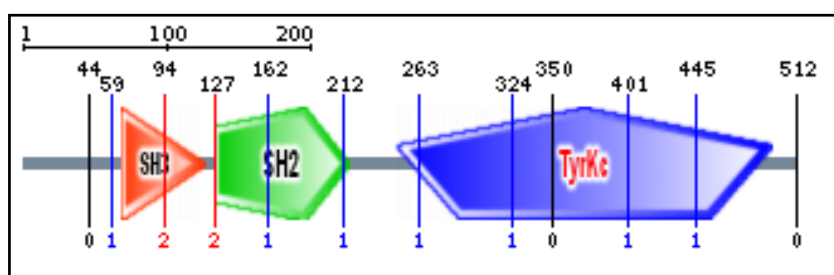


Figure 3.3.5.: Predicted structure of Lyn (figure taken from SMART-domain)

### 3.3.6. Monocyte Differentiation antigen Cd14 (Cd14)

Cd14 is a known interactor of TLR4 (Akashi-Takamura and Miyake, 2008) and TLR3 (Lee et al., 2006) and is also present in the pulldowns of TLR7, -8 and -9, with quite high peptide counts compared to the core proteome of RAW264.7 macrophages (Tab.3.2.6.).

#### Properties of Cd14

Symbol:	Cd14
Name:	Cd14 antigen
ID:	MGI:88318
IPI:	IPI00308990
Superfamily:	LRR_RI superfamily
Description:	Myeloid cell-specific leucine-rich glycoprotein
Genetic MAP:	Chromosome 18
Base pairs:	1101 base pairs
Aminoacids:	366 amino acids
Molecular weight:	39203.9 daltons
Domains:	11 leucine-rich-repeats
Interactors:	TLR1,TLR2, TLR3, TLR4, TLR5, MyD88, MD2, TNF, CD44, Ly96
Localization:	Plasma membrane, GPI and lipid anchor, endosome
Predicted function:	Cooperates with MD-2 and TLR4 to mediate the innate immune response to bacterial lipopolysaccharide (LPS). Acts via MyD88, TIRAP and TRAF6, leading to NF-kappa-B activation, cytokine secretion and the inflammatory response. Up-regulates cell surface molecules, including adhesion molecules (By similarity).

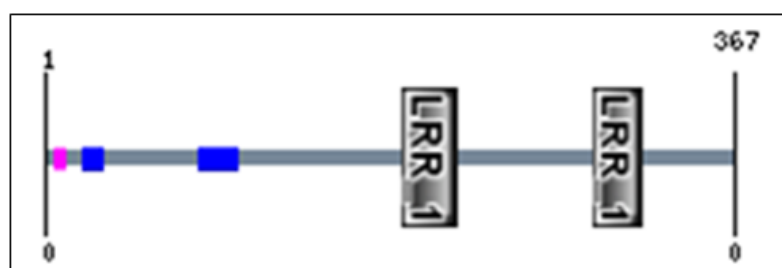


Figure 3.3.6.: Predicted structure of Cd14 (figure taken from SMART-domain)

### 3.3.7. Acid Sphingomyelinase-Like Phosphodiesterase 3B Precursor (Smpdl3b)

Smpdl3b was found significantly in TLR -9 pulldowns (Tab.3.2.6.). Although this protein was found in some other pulldowns according to the ProtFollow tool (Tab.3.2.7.), it seems to be the highest enriched in the TLR datasets.

#### Properties of Smpdl3b

Symbol:	Smpdl3b
Name:	Sphingomyelin phosphodiesterase, acid-like 3B
ID:	MGI:1916022
IPI:	IPI00117534
Synonyms:	1110054A24Rik, Asml3b
Superfamily:	PP2A superfamily
Description:	Protein phosphatase 2A homologues, PP2A superfamily, Metallodependent phosphatase, Type I membrane protein
Genetic MAP:	Chromosome 4
Base pairs:	1371 base pairs
Aminoacids:	456 amino acids
Molecular weight:	51599.6 daltons
Domains:	PP2A catalytic domain
Interactors:	No known interactors
Localization:	Lysosome, plasma membrane
Predicted function:	Not known

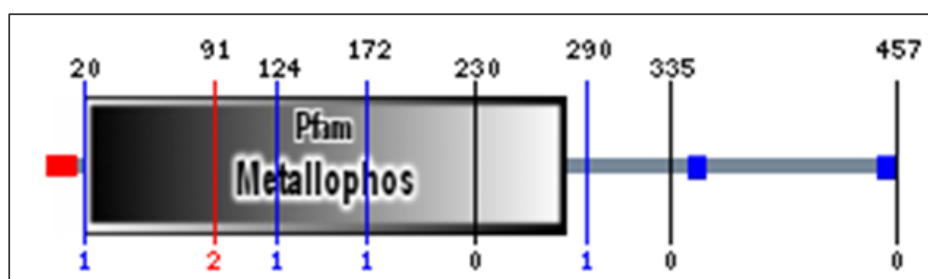


Figure 3.3.7.: Predicted structure of Smpdl3b (figure taken from SMART-domain)

### 3.4. Validation of the Candidates

As the first line of validation we performed co-immunoprecipitation in HEK293T cells. The reason why we switched to the human system for the validation, rather than performing endogenous co-immunoprecipitation in RAW264.7 macrophages, is simply determined by the availability of tools. So far no reliably working antibodies are available for the endogenous, endosomal Toll-like receptors as well as for our chosen candidates. Further RAW264.7 macrophages are hardly transiently transfectable, whereby we can't simply overexpress our fusion-proteins for co-immunoprecipitation. Co-immunoprecipitation was in the first line either performed using hTLR7, hTLR3 or hTLR9 according to the mass-spectrometry data. If the co-immunoprecipitation for the representative toll-like receptor was positive for a candidate, co-immunoprecipitation was performed for all four toll-like receptors.

Primarily we had to define the right conditions for co-immunoprecipitation. Therefore we tested different detergents and different pH settings and finally found the best conditions with NP-40 (1% for lysis and 0,2% for washing) as detergent and pH 6. To control our settings we used the positive control Unc93b1, which is constitutively interacting with endosomal toll-like receptors (Kim et al., 2008). For the HEK293T cell line the signaling ability for innate immunity pathways is not clearly determined. For Co-immunoprecipitation signaling competence is not required, since we estimate direct interactors to bind to each other, despite the signaling ability of the cell.

Additionally for the validation with immune-precipitation we performed immune-fluorescence staining in HeLa cells, where we tried to co-localize hTLR3 or hTLR9 with our chosen candidates. Moreover, immune-fluorescence gives insight on the localization of proteins. Although one has to admit that the localization of overexpressed proteins has to be taken with care, since overexpressed protein might localize unspecifically.

The immune-fluorescence data can't be taken as final proof of interaction, since we would have to confirm the co-localization with a confocal microscope and under more defined settings. I tried to use a representative cutout where the negative control (untransfected HeLa cells) is visible in the same picture.

### 3.4.1. Validation of TaoK1

TaoK1 was only present in TLR3 pulldowns with moderate peptide counts. The validation was performed together with hTLR3 in HEK293T cells (Fig. 3.4.1.). hTaoK1 was not co-precipitated with hTLR3 and vice versa, at least not under the used conditions. So far we have not been able to co-immunoprecipitate hTaoK1 with endosomal toll-like receptors. This might be due to wrong settings for this particular interactor, further it is also possible that both proteins are not direct interactors. Since the peptide counts for mTaoK1 in the mTLR3 pulldowns were rather low, we have not invested further efforts in validating hTaoK1 as interactor of hTLR3.

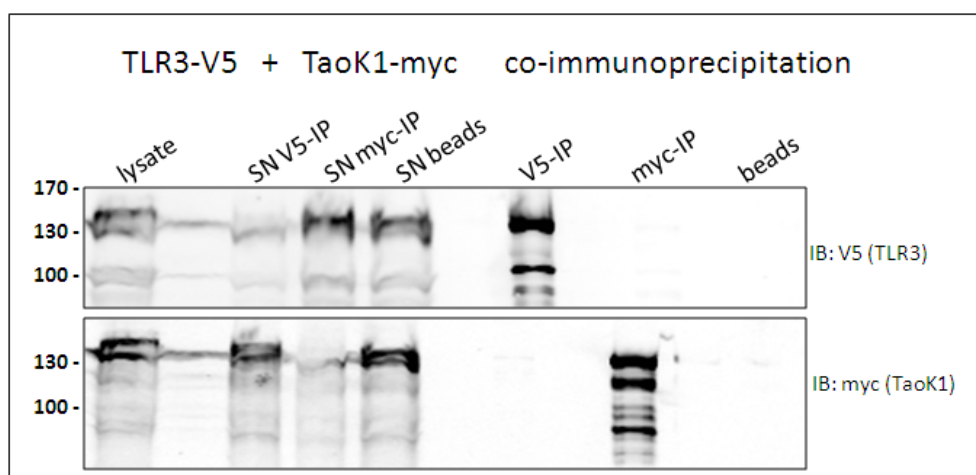


**Figure 3.4.1.:** Co-immunoprecipitation for hTLR3 and hTaoK1 in HEK293T cells. Double transient transfection of V5-tagged hTLR3 and myc-tagged hTaoK1 in HEK293T cells. Immune-precipitation was performed with an anti V5-antibody and myc-coupled beads as well as non coupled beads.

In the immune-fluorescence slides hTaoK1 is located at the plasma membrane, which might indicate that hTaoK1 interacts with cytoskeletal proteins, but it could be also miss-located due to overexpression (Fig. 3.4.2). It seems that the overexpression of hTaoK1 alters the structure of the cell quite significantly. Beside the noticeable shape of transfected cells no co-localization of hTLR3 and hTaoK1 was monitored, which confirms our initial co-immunoprecipitation data. However it might be that it is not possible to co-precipitate hTLR3 and hTaoK1 since the interaction might be not stable enough. Kinases are usually only transiently interacting with their targets and are not stably bound to the substrate. This assumption is fortified by the mass-spectrometry data, where TaoK1 is highly enriched upon TLR3 activation.



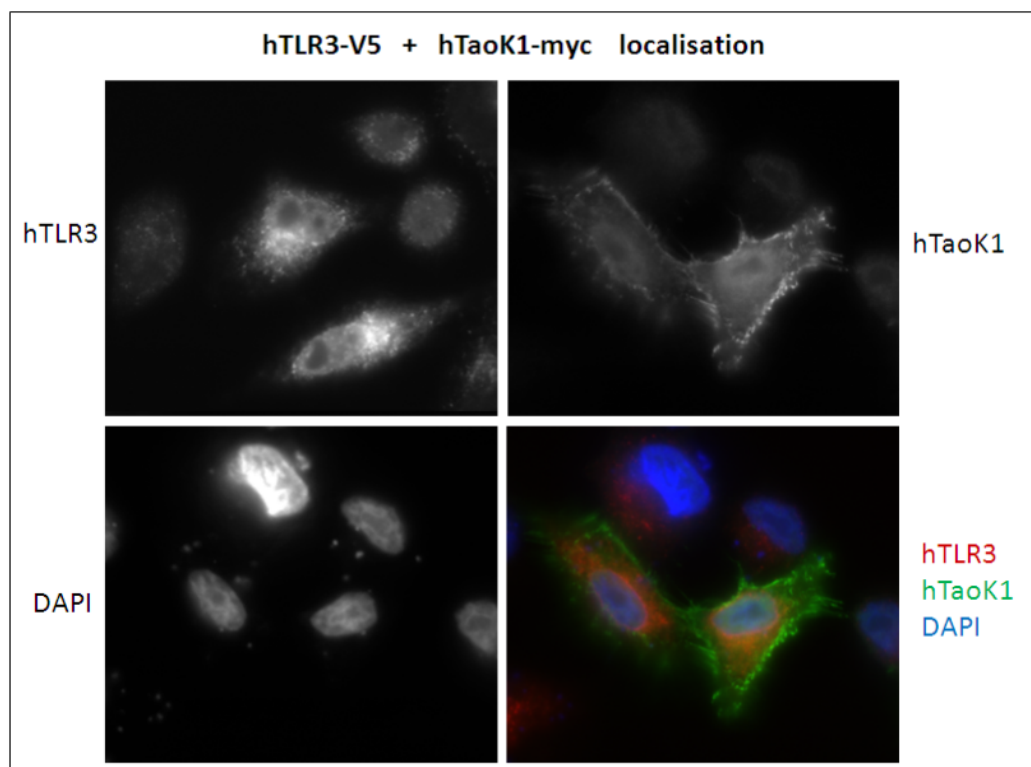


**Figure 3.4.2.:** Immune-fluorescence staining for hTaoK1 and hTLR3 in HeLa cells.

Transient double transfection of V5-tagged hTLR3 and myc-tagged hTaoK1 in HeLa cells for 24h prior fixation with formaldehyde. hTLR3-V5 is stained with an Alexa-Fuor594 secondary antibody (red) and hTaoK1-myc is stained with an Alexa-Fuor488 secondary antibody (green). Nucleic acids are dyed with DAPI in blue.

Since other candidates were far more promising no further investigations have been performed to validate hTaoK1 as positive interactor for endosomal toll-like receptors, since there might be no direct interaction between both proteins.

### 3.4.2. Validation of Poldip3

Poldip3 was only found in the TLR3 pulldowns, wherefore we performed co-immunoprecipitation together with hTLR3 in HEK293T cells. No significant interaction was found between hTLR3 and hPoldip3 using co-immunoprecipitation. A little bit of myc tagged hPoldip3 was found in the V5-immuno-precipitation together with V5-tagged hTLR3. But similar amounts of myc tagged hPoldip3, was also found on beads alone, without specific antibody (Fig. 3.4.3.). Thus the interaction of hPoldip3 and hTLR3 was not validated using co-immunoprecipitation.

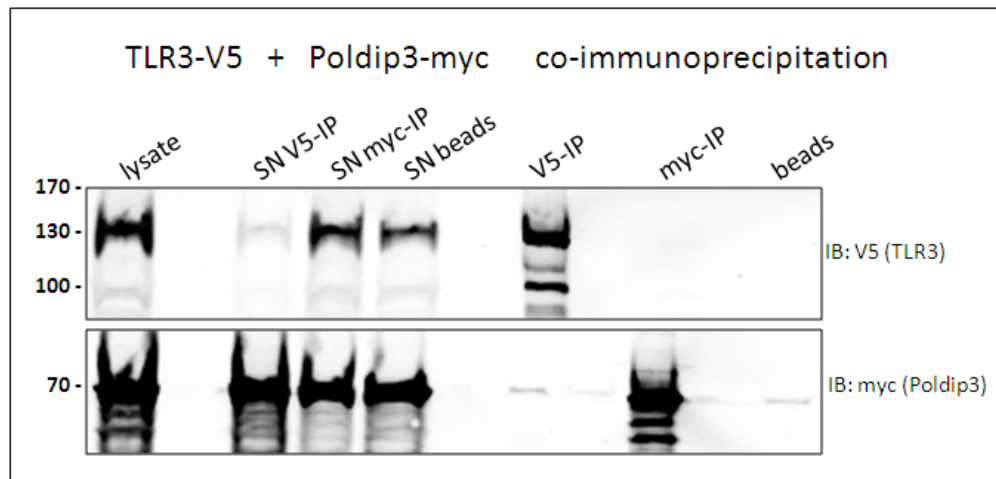


**Figure 3.4.3.: Co-immunoprecipitation for hTLR3 and hPoldip3 in HEK293T cells.** Double transient transfection of V5-tagged hTLR3 and myc-tagged hPoldip3 in HEK293T cells. Immune-precipitation was performed with an anti V5-antibody and myc-coupled beads as well as non coupled beads.

In the immune-fluorescence staining hPoldip3 is clearly localized in the nucleus (Fig. 3.4.4.), whereas hTLR3 is in subcellular compartments. What is not clarified in this setup is how hPoldip3 behaves in signaling competent stimulated cells. Since other candidates appear to be more interesting, concerning the co-immunoprecipitation and co-localization data, no further investigations have been performed to optimize the validation of Poldip3 so far. However we assume, that hPoldip3 and hTLR3 won't co-precipitate, since both proteins are located in different compartments. Poldip3 has to be tested in an autoimmune disease model to verify interaction with endosomal TLRs.

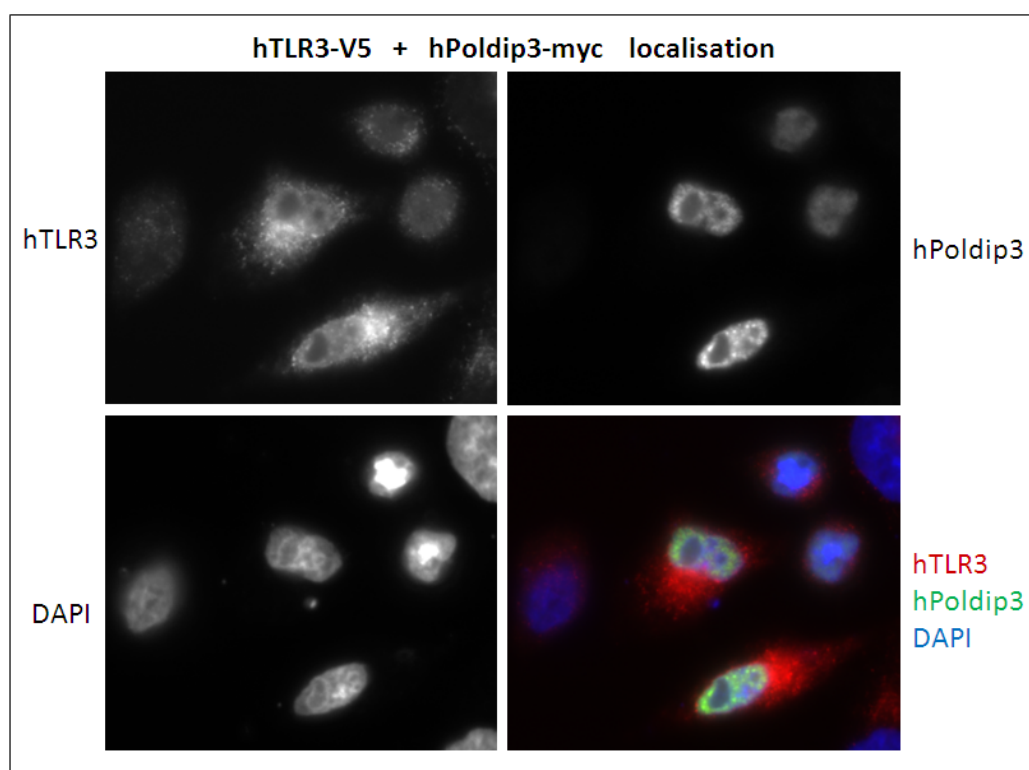


Figure 3.4.4.: Immune-fluorescence staining for hPoldip3 and hTLR3 in HeLa cells.

Transient double transfection of V5-tagged hTLR3 and myc-tagged hPoldip3 in HeLa cells for 24h prior fixation with formaldehyde. hTLR3-V5 is stained with an Alexa-Fuor594 secondary antibody (red) and hPoldip3-myc is stained with an Alexa-Fuor488 secondary antibody (green). Nucleic acids are dyed with DAPI in blue.

### 3.4.3. Validation of Rasa3

Rasa3 was with low peptide counts detected in mTLR3 pulldowns and was highly enriched in TLR7, -8 and -9 pulldowns (Tab. 3.2.6.). Therefore we performed co-immunoprecipitation for hRasa3 and hTLR7 in HEK293T cells (Fig. 3.4.5.).

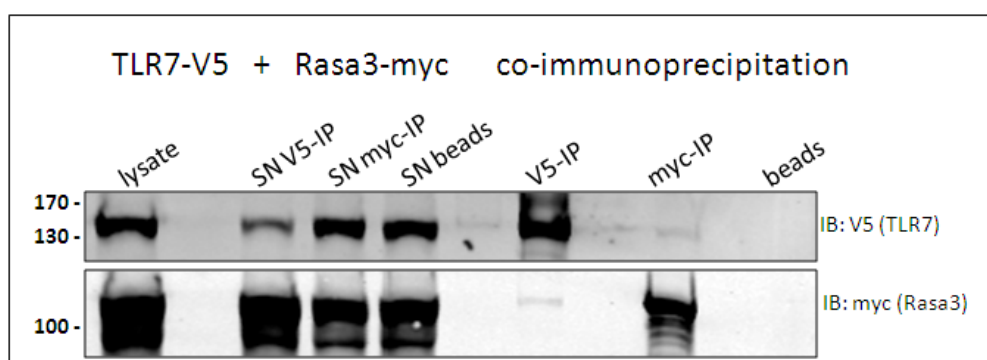


Figure 3.4.5.: Co-immunoprecipitation for hTLR7 and hRasa3 in HEK293T cells.

Double transient transfection of V5-tagged hTLR7 and myc-tagged hRasa3 in HEK293T cells. Immune-precipitation was performed with an anti V5-antibody and myc-coupled beads as well as non coupled beads.

Only a very weak band is visible in the co-immunoprecipitate of hRasa3 with endosomal toll-like receptors. This might be due to wrong settings for this particular interactor, further it is

also possible that both proteins are not direct interactors or that Hek293T cells do not provide the right environment for the interaction. Although the mass-spectrometry data looks very promising it could also be the case that hRasa3 is not interacting with endosomal toll-like receptors and is therefore not co-precipitated with TLR7.

The immune-fluorescence data indicates that hRasa3 is located at the plasma membrane (Fig. 3.4.6.). The staining might suggest that hRasa3 interacts with cytoskeletal proteins, which would confirm the literature data. It seems that the overexpression of hRasa3 alters the structure of the cell quite significantly, whereby it might not localize natively. Besides the noticeable shape of transfected cells no co-localization of hTLR9 and hRasa3 was monitored, which confirms our initial co-immunoprecipitation data.

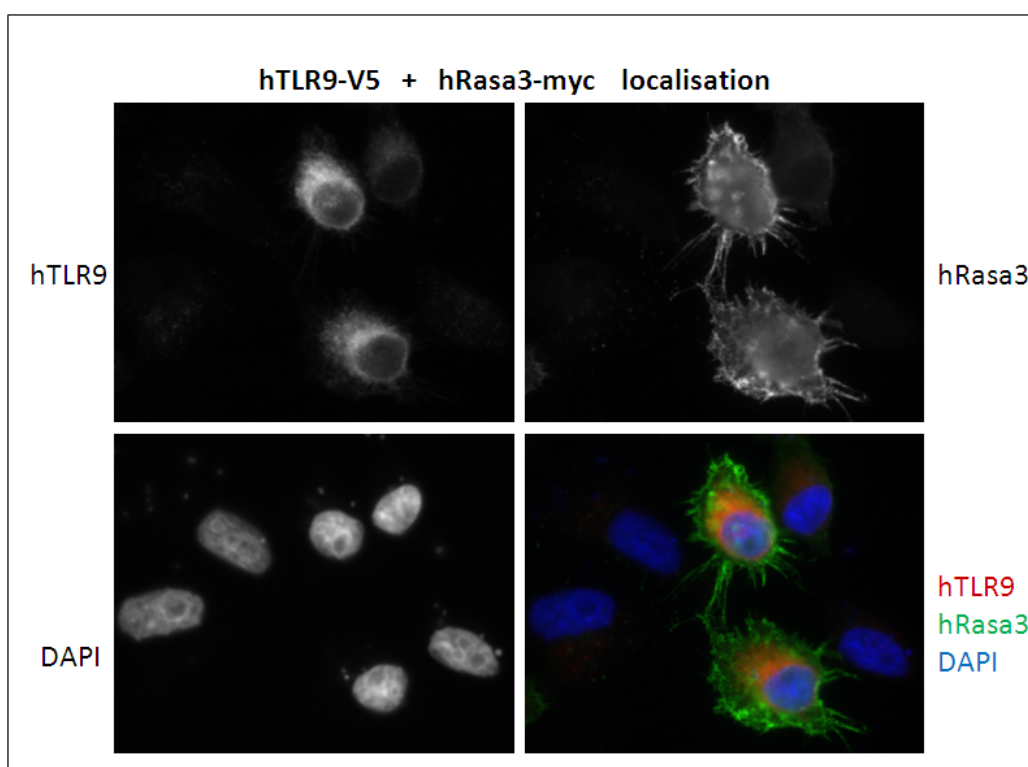


**Figure 3.4.6.: Immune-fluorescence staining for hRasa3 and hTLR9 in HeLa cells.**

Transient double transfection of V5-tagged hTLR9 and myc-tagged hRasa3 in HeLa cells for 24h prior fixation with formaldehyde. hTLR9-V5 is stained with an Alexa-Fluor594 secondary antibody (red) and hRasa3-myc is stained with an Alexa-Fluor488 secondary antibody (green). Nucleic acids are dyed with DAPI in blue.

Since other candidates are far more promising no further investigations have been performed to validate Rasa3 as positive interactor for endosomal toll-like receptors, since there might be no direct interaction between both proteins.

### 3.4.4. Validation of Rftn1

For hRftn1 only a very weak interaction with hTLR7 was detected with co-immunoprecipitation (Fig. 3.4.7.). In the mass-spectrometry data it was enriched in TLR7, -8 and -9 pulldowns. We have not been able to increase this weak interaction by simply trying different working conditions, which might indicate that it is not a true or direct interaction. On the other side, the HEK293 co-immunoprecipitation system has its limitations, therefore this candidates cannot be totally excluded as possible interactor.

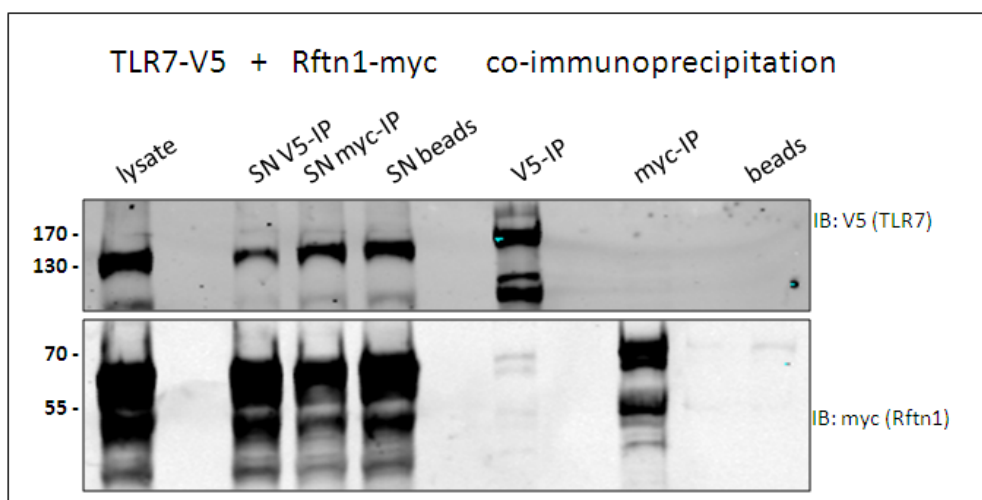


**Figure 3.4.7.:** Co-immunoprecipitation for hTLR7 and hRftn1 in HEK293T cells.

Double transient transfection of V5-tagged hTLR7 and myc-tagged hRftn1 in HEK293T cells. Immune-precipitation was performed with an anti V5-antibody and myc-coupled beads as well as non coupled beads.

The Immune-fluorescence data indicates that hRftn1 is located prominently at the plasma membrane (Fig. 3.4.8.). The overexpression of hRftn1 significantly modifies the shape of the cells, which would indicate, that it might associate with cytoskeleton proteins, but it is also possible, that it is wrongly located due to the overexpression. No distinct co-staining of hTLR9 and hRftn1 but only occasional overlap of fluorescent signals could be observed. These data might indicate that these proteins are not exclusive interactors and due to the lack of clear interaction data from Hek293T immunoprecipitation assays we decided to drop our focus on Rftn1.

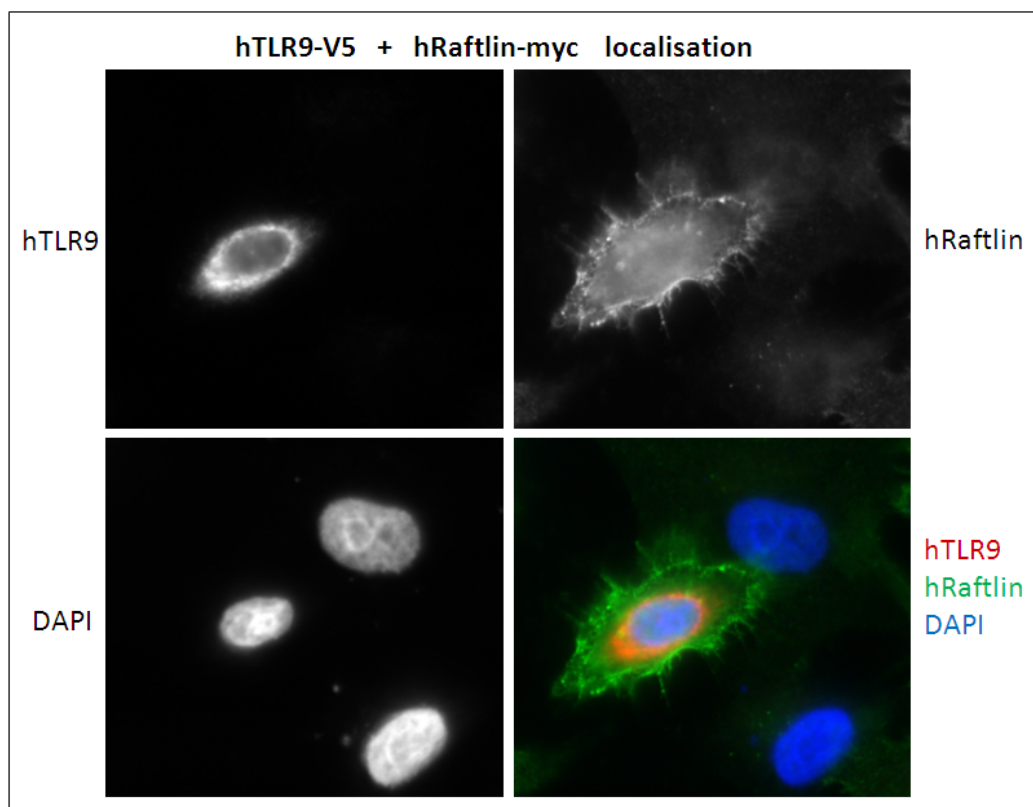


**Figure 3.4.8.:** Immune-fluorescence staining for hRftn1 and hTLR9 in HeLa cells.

Transient double transfection of V5-tagged hTLR9 and myc-tagged hRftn1 in HeLa cells for 24h prior fixation with formaldehyde. hTLR9-V5 is stained with an Alexa-Fuor594 secondary antibody (red) and hRaftlin-myc is stained with an Alexa-Fuor488 secondary antibody (green). Nucleic acids are dyed with DAPI in blue.

We have not investigated more efforts in validating hRftn1 as interactor of endosomal toll-like receptors, since we wanted to focus on the validation of more promising candidates.

### 3.4.5. Validation of Lyn

For hLyn only a very weak interaction with hTLR7 was detected with co-immunoprecipitation (Fig. 3.4.9.). In the mass-spectrometry data it was enriched in TLR7, -8 and -9 pulldowns with quite high peptide counts (Tab.3.2.6.). We have not been able to increase this weak interaction by simply trying different working conditions, which might indicate that it is not about true or direct interaction.

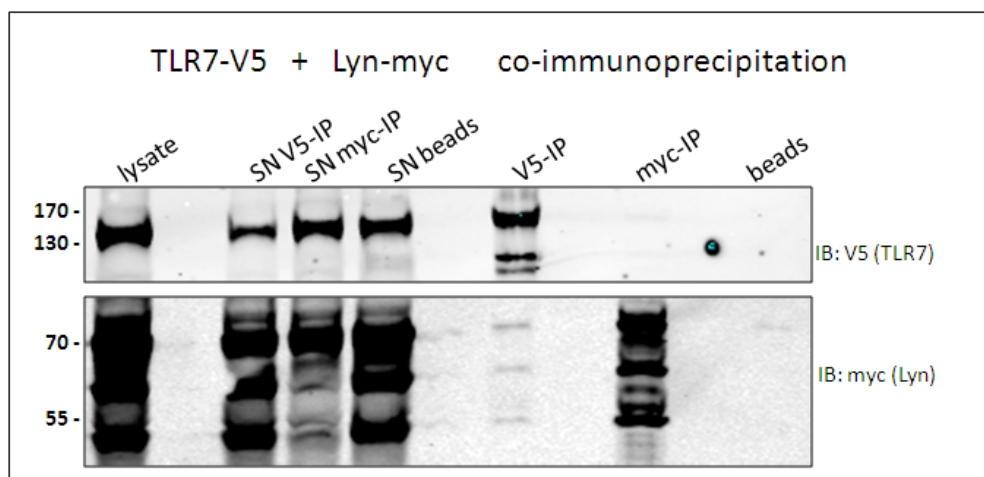


**Figure 3.4.9.: Co-immunoprecipitation for hTLR7 and hLyn in HEK293T cells.**

Double transient transfection of V5-tagged hTLR7 and myc-tagged hLyn in HEK293T cells. Immune-precipitation was performed with an anti V5-antibody and myc-coupled beads as well as non coupled beads.

The Immune-fluorescence data indicates that hLyn is located at the plasma membrane as well as in distinct compartments within the cell (Fig. 3.4.10.). This data correlates well with the literature, since Lyn is predicted to be localized in phagosomes (Sanjuan et al., 2006). The localization at the plasma membrane could be due to heavy overexpression. These compartments within the cell seem to co-localize with hTLR9, since co-localization is visible in structures closed to the nucleus which could be endoplasmic reticulum. This co-localization would need further confirmations, especially since the co-immunoprecipitation was not identifying hLyn as clear interactor.

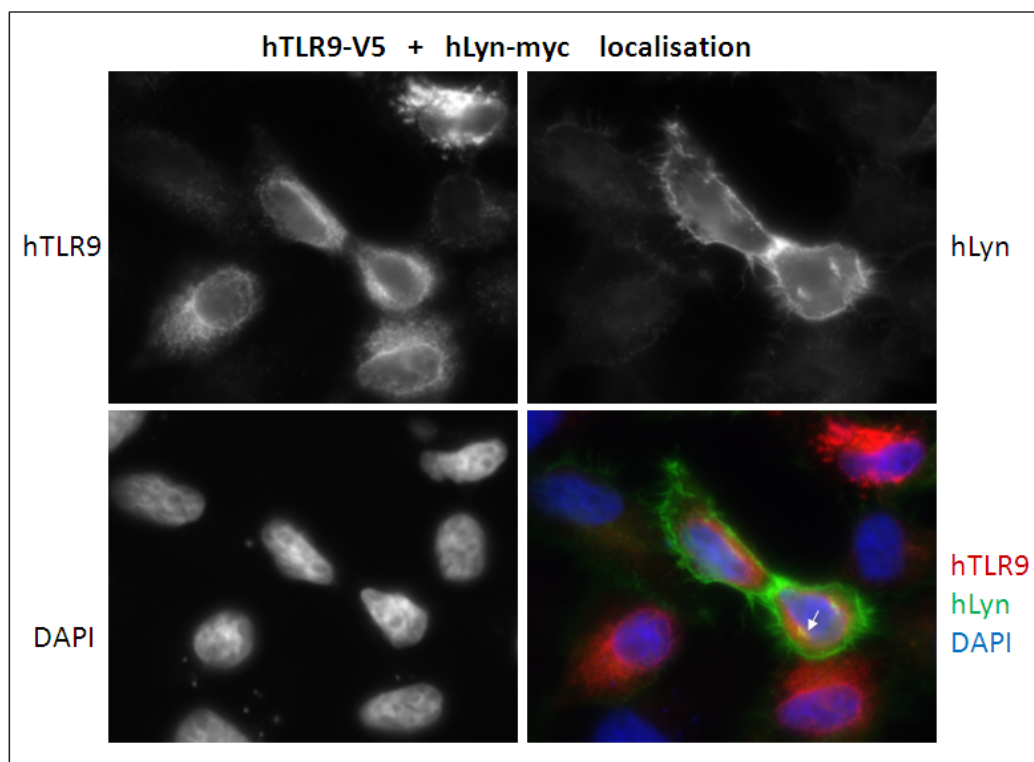


**Figure 3.4.10.: Immune-fluorescence staining for hLyn and hTLR9 in HeLa cells.**

Transient double transfection of V5-tagged hTLR9 and myc-tagged hLyn in HeLa cells for 24h prior fixation with formaldehyde. The arrow indicates area of co-localization. hTLR9-V5 is stained with an Alexa-Fuor594 secondary antibody (red) and hLyn-myc is stained with an Alexa-Fuor488 secondary antibody (green). Nucleic acids are dyed with DAPI in blue.

We have not investigated more efforts in validating Lyn as interactor of endosomal toll-like receptors, since we wanted to focus on the validation of more promising candidates. But Lyn is clearly a hot candidate considering the literature and will be further followed in a successional project.

### 3.4.6. Validation of Cd14

Precipitation of V5-tagged TLR9 readily co-precipitated myc-tagged CD14 and vice versa. hCd14-myc was co-purified with hTLR9-V5 in a V5-IP and vice versa (data not shown). Thus we further investigated on the interaction with hCd14 and all four endosomal toll-like receptors. For the second co-immunoprecipitation only a V5-IP was performed. Unfortunately in all four IPs the negative control for the hTLRs, ChiC-myc, a transmembrane protein, is not expressed. The fusion protein should have the same size than hCd14. As positive control for the toll-like receptors Unc93b1 was selected. As negative control for the precipitation of hCd14, hChiC-V5 was co-expressed. This negative control is much more important, since we don't know how hCd14 behaves and if it is highly abandoned.

In the co-immunoprecipitation of hTLR3-V5 and hCd14-myc, hCd14 is clearly co-precipitated with hTLR3, when we use the toll-like receptor as bait. This result confirms the data published by Lee et al., 2006 (Fig. 3.4.11.). As already shown Unc93b1 gets co-purified with



hTLR3 as well and Cd14 is not found in the ChiC-V5 IP. Not one of the proteins binds to beads alone, which serves as a further negative control.

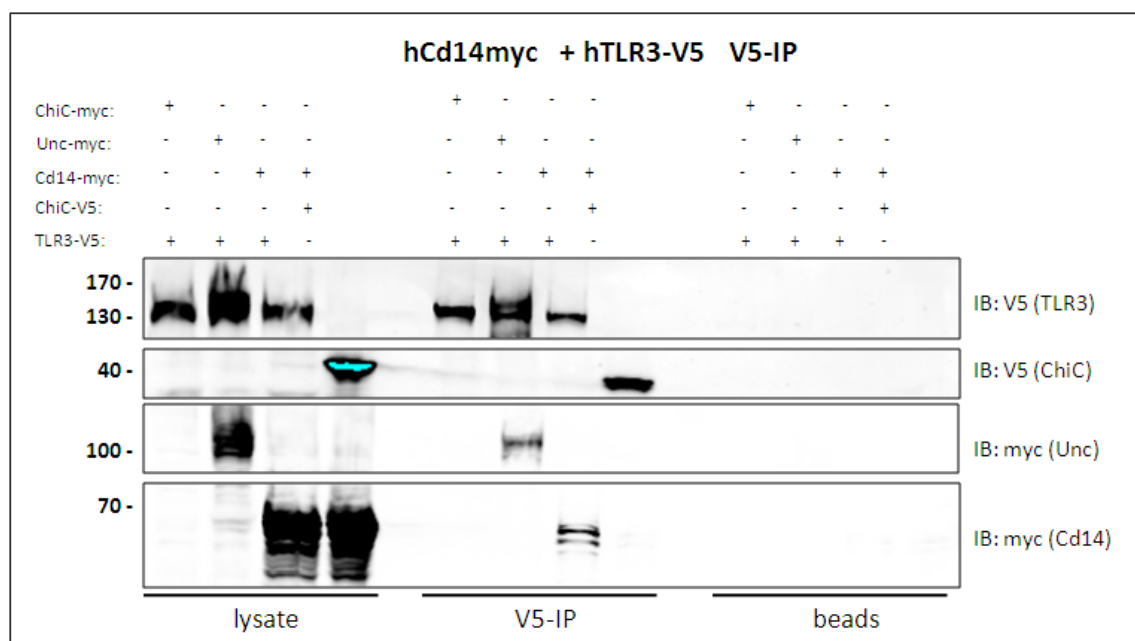


**Figure 3.4.11.: Co-immunoprecipitation for hTLR3 and hCd14 in HEK293T cells.**

Double transient transfection of V5-tagged hTLR3 and myc-tagged hCd14 in HEK293T cells. Immune-precipitation was performed with an anti V5-antibody and non coupled beads. The cyan color within a few bands is due to overexposure at the Odyssey Li-Cor.

Further we have been able to co-purify hCd14 together with hTLR7 (Fig. 3.4.12). So far no data is available that hCd14 is also interacting with hTLR7. Unfortunately there is an air-bubble within the hTLR7 band in the V5-precipitation. Nevertheless it is clearly visible, that hTLR7-V5 was pulled out by the V5-beads. The negative control for hTLR7, Chic-myc is not expressed again, but all other controls are as supposed.

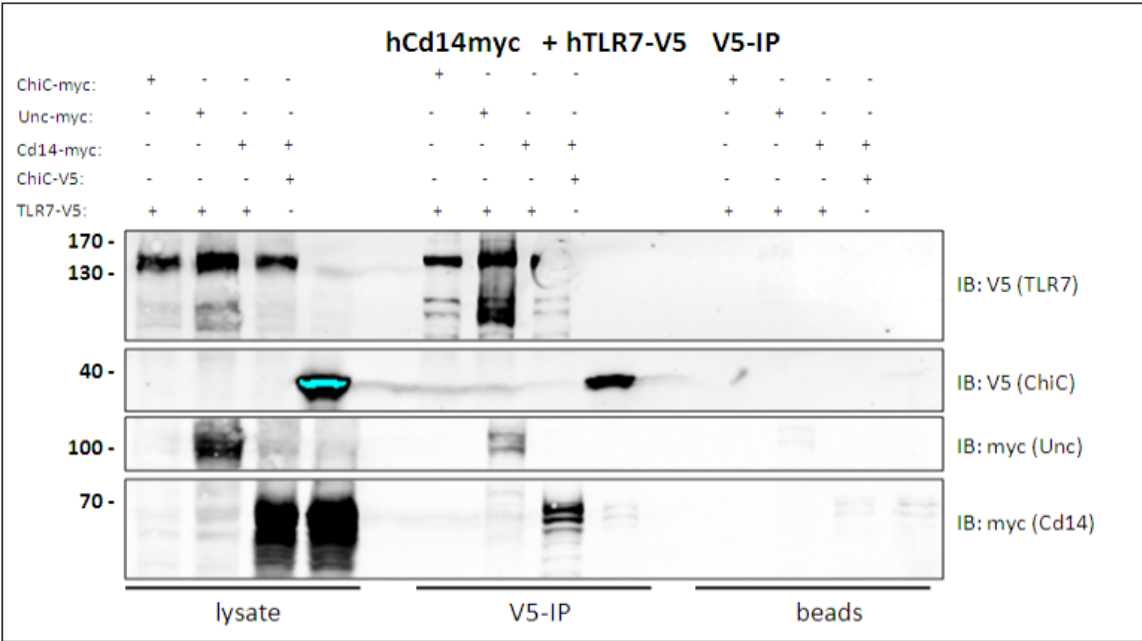


**Figure 3.4.12.: Co-immunoprecipitation for hTLR7 and hCd14 in HEK293T cells.**  
Double transient transfection of V5-tagged hTLR7 and myc-tagged hCd14 in HEK293T cells. Immune-precipitation was performed with an anti V5-antibody and non coupled beads.

hCd14 also co-precipitates with hTLR8, which was not shown so far (Fig. 3.4.13). The negative control for hTLR8, ChiC-myc is not expressed again, but all other controls are as supposed, Unc93b1 is co-precipitated with hTLR8 and ChiC-V5 is not co-precipitated with hCd14-myc. Very little amounts of Cd14 are present on beads alone, but compared to the co-precipitated hCd14 this weak band can be negligible.

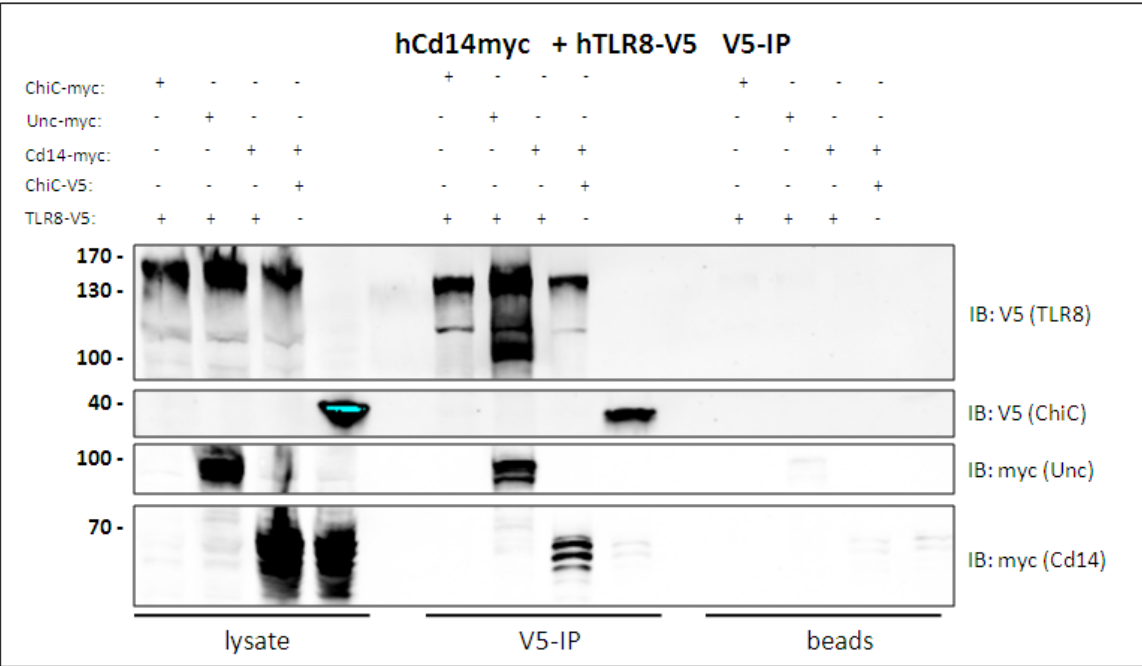


**Figure 3.4.13.: Co-immunoprecipitation for hTLR8 and hCd14 in HEK293T cells.**  
Double transient transfection of V5-tagged hTLR8 and myc-tagged hCd14 in HEK293T cells. Immune-precipitation was performed with an anti V5-antibody and non coupled beads.

Last but not least hCd14 is also co-precipitating with hTLR9 (Fig. 3.4.14). So far it was not shown before that hCd14 is co-precipitating also with hTLR9. The negative control for hTLR9, ChiC-myc is not expressed again, but all other controls are as supposed.

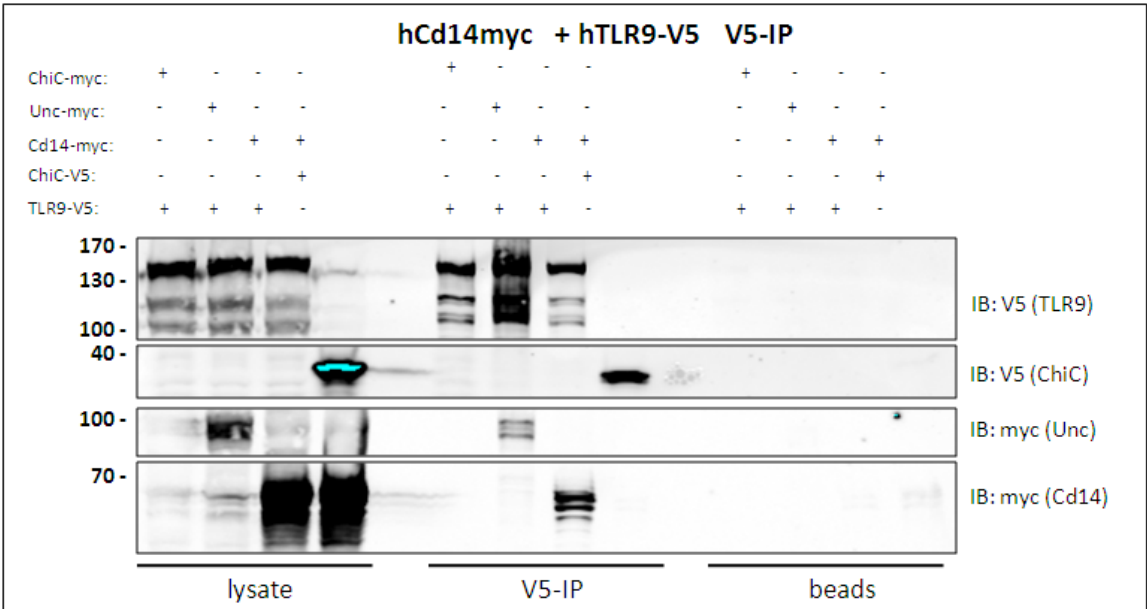


**Figure 3.4.14.: Co-immunoprecipitation for hTLR9 and hCd14 in HEK293T cells.**  
**Double transient transfection of V5-tagged hTLR9 and myc-tagged hCd14 in HEK293T cells.**  
**Immune-precipitation was performed with an anti V5-antibody and non coupled beads.**

Interestingly, all human endosomal Toll-like receptors are much better precipitated when Unc93b1 is present. This might indicate that Unc93b1 serves also as chaperon for endosomal toll-like receptors, beside its shuttling function. This finding needs to be further investigated in a successional project.

Further immune-fluorescence was performed of HeLa cells co-transfected with hTLR9 and hCd14, in order to repeat the findings from the co-immunoprecipitation (Fig. 3.4.15.).

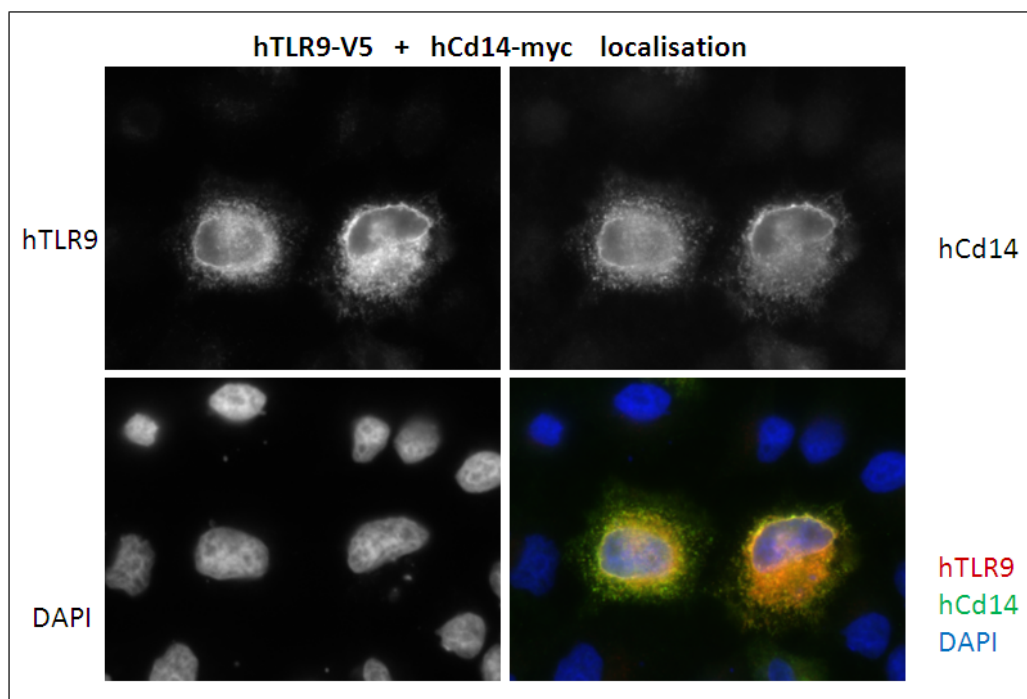


**Figure 3.4.15.: Immune-fluorescence staining for hCd14 and hTLR9 in HeLa cells.**

Transient double transfection of V5-tagged hTLR9 and myc-tagged hCd14 in HeLa cells for 24h prior fixation with formaldehyde. hTLR9-V5 is stained with an Alexa-Fluor594 secondary antibody (red) and hCd14-myc is stained with an Alexa-Fluor488 secondary antibody (green). Nucleic acids are dyed with DAPI in blue.

In the immune-fluorescence slides hTLR9 and hCd14 are co-localizing as well, indicated by the yellow staining. Clearly the immune-fluorescence data cannot be taken as final proof of interaction, since we would have to confirm the co-localization with a confocal microscope and more defined settings. However, taken together these data strongly indicate a functional link between the MyD88 dependent TLR7, -8 and -9 and CD14.

### 3.4.7. Validation of Smpdl3b

hSmpdl3b-myc was co-purified with hTLR9-V5 in a V5-IP and vice versa (data not shown). Thus we further investigated on the interaction with hSmpdl3b and all four endosomal toll-like receptors. For the second co-immunoprecipitation only a V5-IP was performed. In all four IPs the negative control for the hTLRs, ChiC-myc, a transmembrane protein, is not expressed. The fusion protein roughly should have the same size than hSmpdl3b. Since we have been the interaction with the toll-like receptors and any other protein is difficult to achieve, we considered the negative control for the toll-like receptors for less important, whereby the IPs have not been repeated. As positive control for the toll-like receptors Unc93b1 was selected. As negative control for the interactors hChiC-V5 was co-expressed. This negative control is much more important, since we don't know how abandoned hSmpdl3b is

Only a very weak hSmpdl3b band is visible in the hTLR3-IP (Fig. 3.4.16.). This finding very well confirms the mass-spectrometry data, where mSmpdl3b is only found in the second mTLR3 pulldown with 2 peptide counts (Tab. 3.2.6).

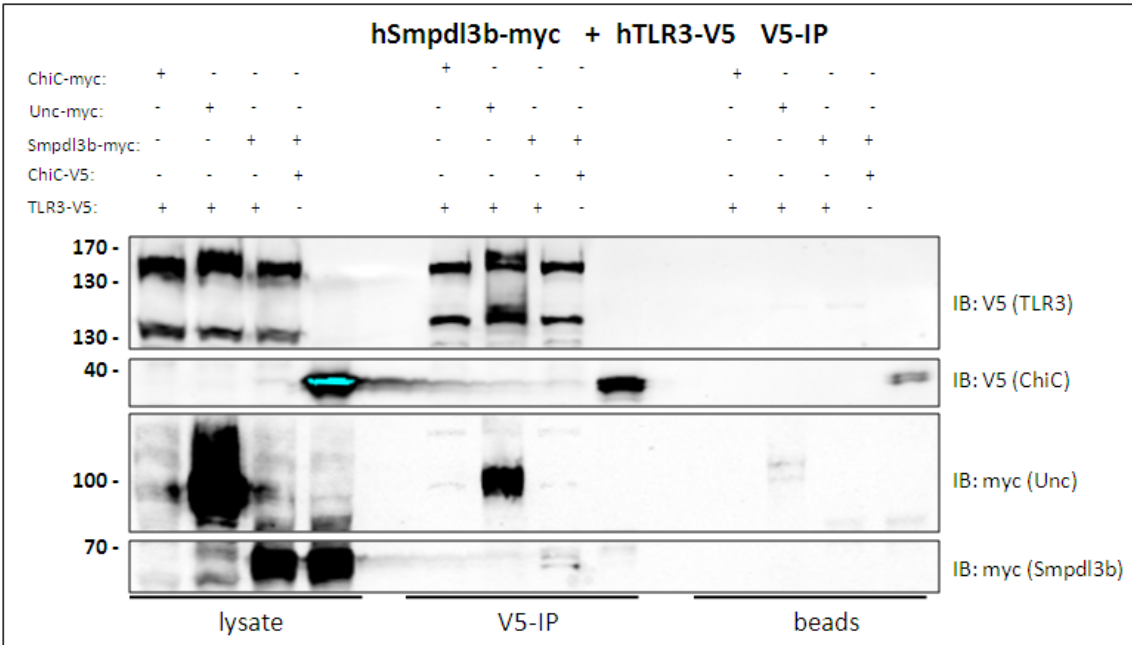


**Figure 3.4.16.: Co-immunoprecipitation for hTLR3 and hSmpdl3b in HEK293T cells.**  
Double transient transfection of V5-tagged hTLR3 and myc-tagged hSmpdl3b in HEK293T cells. Immune-precipitation was performed with an anti V5-antibody and non coupled beads. The cyan color within a few bands is due to overexposure at the Odyssey Li-Cor.

Further hSmpdl3b is only very little co-purified with hTLR7 (Fig. 3.4.17.), although mSmpdl3b was present with high peptide counts in the mTLR7 pulldowns (Tab. 3.2.6.)

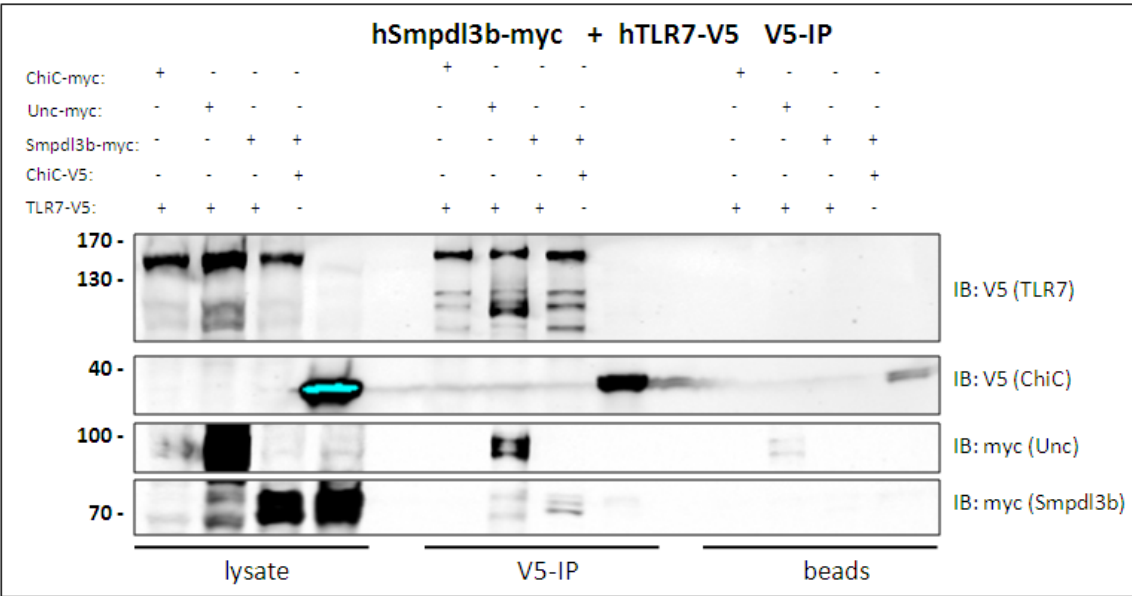


**Figure 3.4.17.: Co-immunoprecipitation for hTLR7 and hSmpdl3b in HEK293T cells.**  
Double transient transfection of V5-tagged hTLR7 and myc-tagged hSmpdl3b in HEK293T cells. Immune-precipitation was performed with an anti V5-antibody and non coupled beads.

A significant band for hSmpd13b is co-purified with hTLR8 (Fig. 3.4.18). hSmpd13b specifically appears in the hTLR8 IP and is not co-purified with ChiC-V5, nor is it bound on the plain beads. Thus we propose hSmpd13b as a clear interactor of hTLR8.

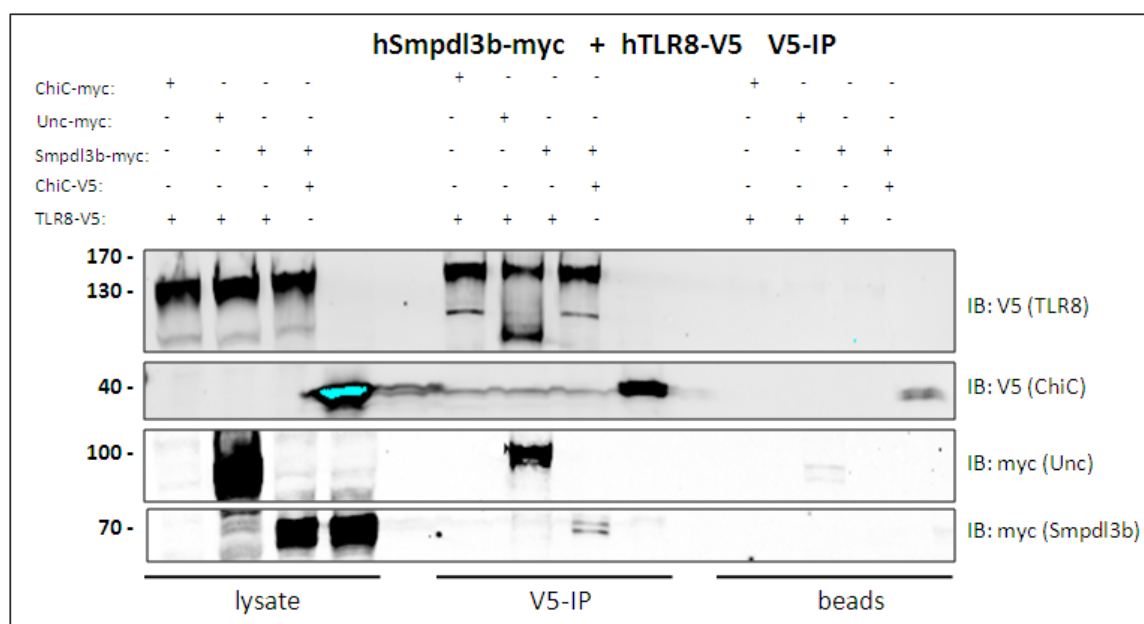


**Figure 3.4.18.: Co-immunoprecipitation for hTLR8 and hSmpd13b in HEK293T cells.**

Double transient transfection of V5-tagged hTLR8 and myc-tagged hSmpd13b in HEK293T cells. Immune-precipitation was performed with an anti V5-antibody and non coupled beads.

In the co-immunoprecipitation of hTLR9-V5 and hSmpd13b-myc, the interactor is clearly co-precipitated with hTLR9, when we use the toll-like receptor as bait (Fig. 3.4.19.). As already shown Unc93b1 gets co-purified with hTLR9 as well and Smpd13b is not found in the ChiC-V5 IP. The data is quite surprising considering the mTLR9 pulldown data (Tab. 3.2.6.) where mSmpd13b is only present with little peptide counts. Not one of the proteins binds to beads alone, which serves as a further negative control.

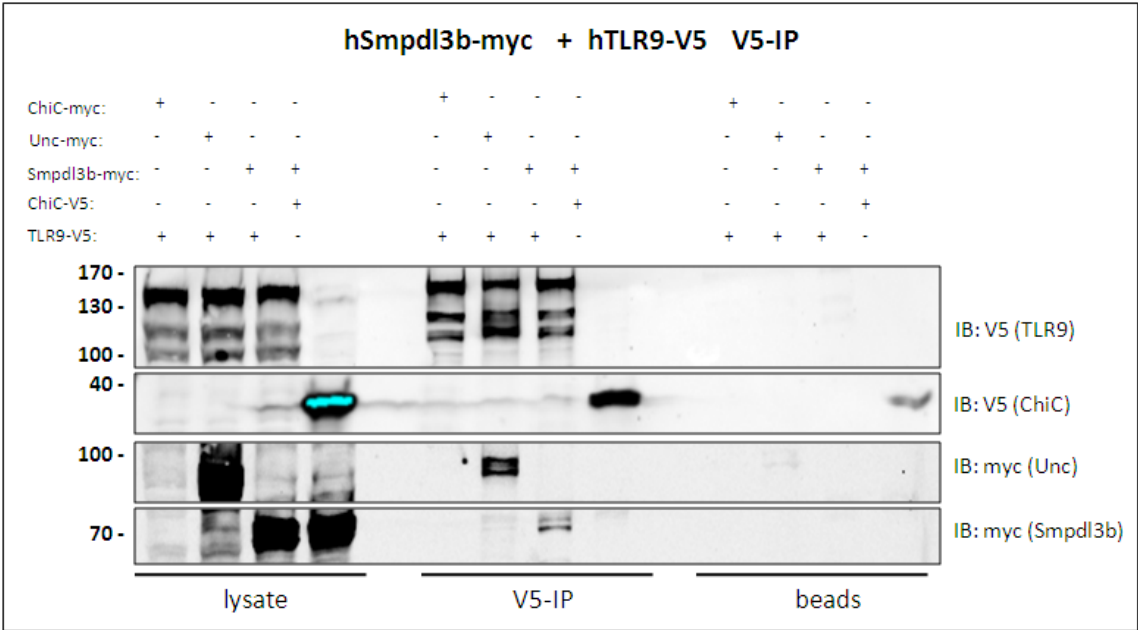


**Figure 3.4.19.: Co-immunoprecipitation for hTLR9 and hSmpdl3b in HEK293T cells.**  
Double transient transfection of V5-tagged hTLR9 and myc-tagged hSmpdl3b in HEK293T cells. Immune-precipitation was performed with an anti V5-antibody and non coupled beads.

Further we performed immune-fluorescence for hTLR9 and hSmpdl3b in HeLa cells to verify the co-immunoprecipitation results (Fig. 3.4.20.).

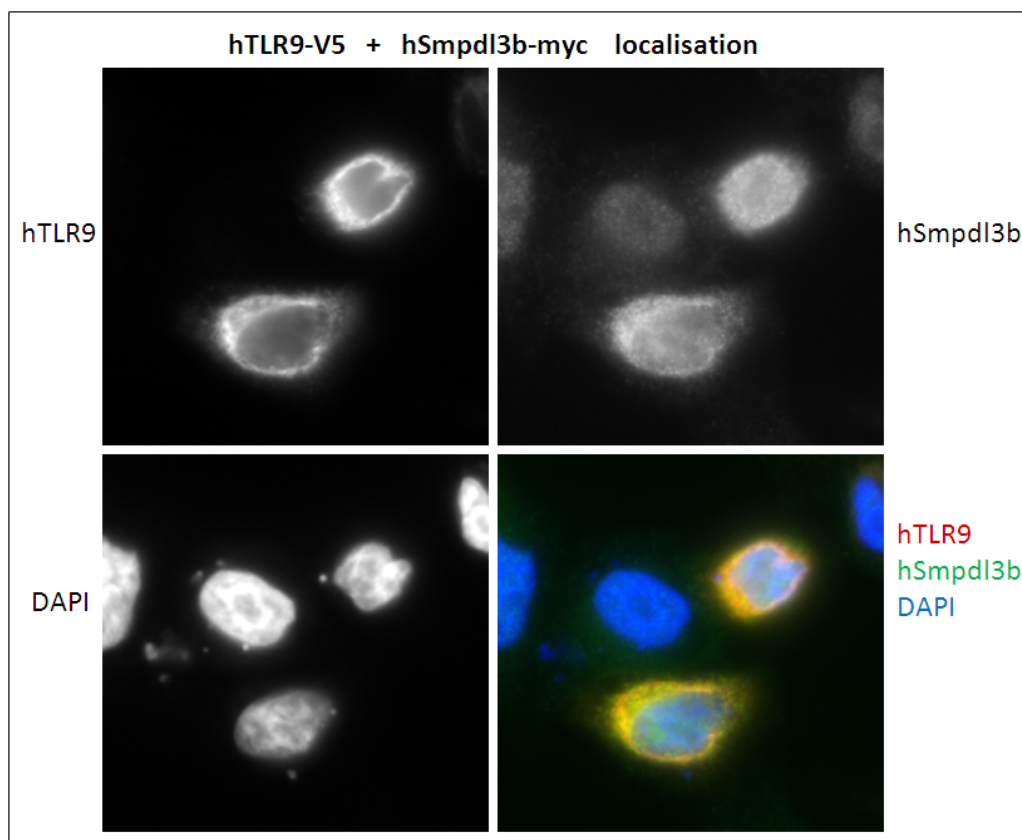


Figure 3.4.20.: Immune-fluorescence staining for hSmpd13b and hTLR9 in HeLa cells.

Transient double transfection of V5-tagged hTLR9 and myc-tagged hSmpd13b in HeLa cells for 24h prior fixation with formaldehyde. hTLR9-V5 is stained with an Alexa-Fluor594 secondary antibody (red) and hSmpd13b-myc is stained with an Alexa-Fluor488 secondary antibody (green). Nucleic acids are dyed with DAPI in blue.

In the immune-fluorescence staining hTLR9 and hSmpd13b clearly co-localize, indicated by the yellow color. The immune-fluorescence data can't be taken as final proof of interaction, since we would have to confirm the co-localization with a confocal microscope and further settings. Further the co-stained cells do not look very healthy, whereby the data has to be considered with caution.

### 3.5. Cd14 and Smpd13b Influence Endosomal TLR Signaling

Only very little efforts have been invested in the functional analysis of Cd14 and Smpd13b, since the functional research is not part of this project. By the reason that those interactors are very promising and indicate a highly interesting function in innate immunity signaling together with endosomal toll-like receptors, overexpression studies have been performed.

To see if we can reproduce the published finding, that hCd14 increases hTLR3 mediated signaling, we performed an NF- $\kappa$ B reporter gene assay for hCd14 overexpressed in HEK293 cells that stably express hTLR3 (Fig. 3.5.1.). The specific signaling ability of hTLR3-HEK293 cells was verified using siRNA and reporter gene assay (data not shown). As negative control



we used GFP overexpression and as positive control we used GFP overexpressed cells stimulated with polyI:C.

We either kept the amount of transfected hCd14 equal and titrated in increasing amounts of polyI:C or we titrated in increasing amounts of hCd14 and kept the polyI:C stimulation at an equal level. In all samples equal amounts of DNA have been used, since the amount of DNA was substituted with GFP.

High amounts of hCd14 and high amounts of polyI:C triple the induction of NF- $\kappa$ B, whereby we confirm the enhancement of TLR3 signaling with Cd14.

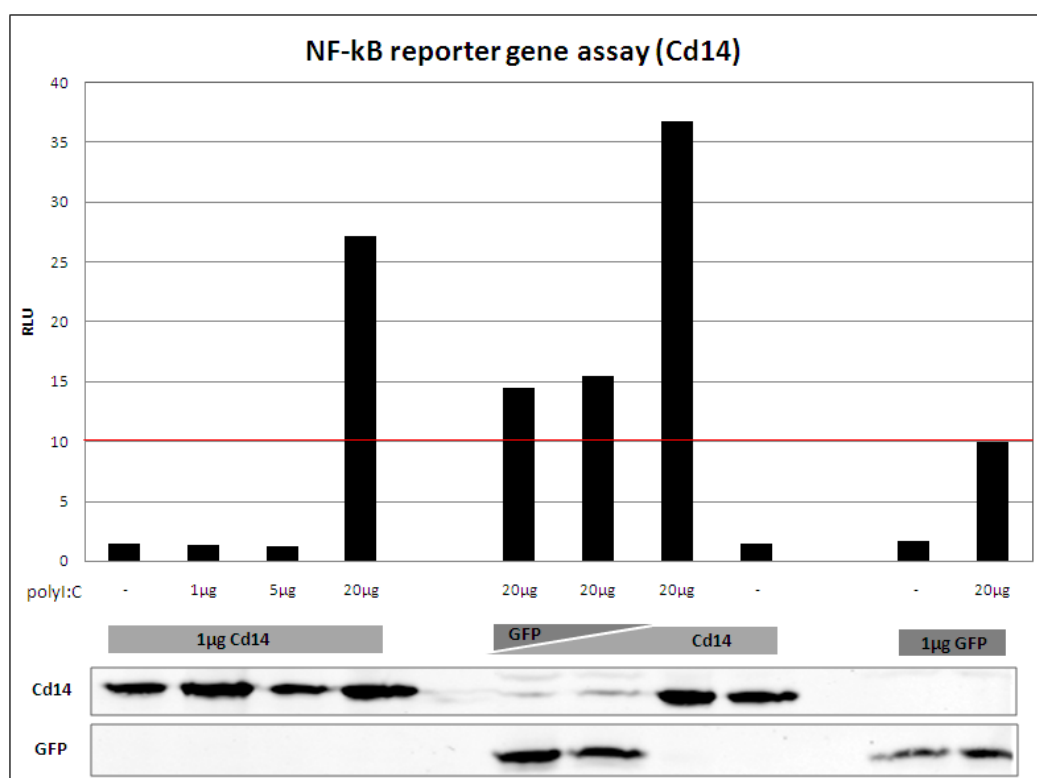


**Figure 3.5.1.: NF- $\kappa$ B reporter gene assay for overexpressed Cd14 in HEK293 cells stably expressing hTLR3.**  
Protein expression of Cd14, as well as the substitute GFP has been confirmed via western-blot.

Further we wanted to investigate on the effect of hCd14 and hSmpd13b on endosomal TLR signaling.

As readout reporter gene assay for NF- $\kappa$ B and IFN- $\beta$  was performed in HEK293T cells. The reporter constructs have been transfected together with the backbone vector for V5 tagged fusion proteins as negative control and MyD88 as stimulation for innate immunity signals since HEK293T cells do not express toll-like receptors. As positive control V5 was co-transfected with MyD88, and as negative control plain V5-vector was co-transfected with plain V5-vector. Always equal amount of DNA was added to every setting. If Cd14 is expressed and the cells are activated with MyD88 overexpression the NF- $\kappa$ B as well as the IFN- $\beta$  signal drops dramatically (Fig. 3.5.2.). Thus it seems that Cd14 has an inhibitory effect on endosomal toll-like receptors which are signaling only via MyD88, namely TLR7, -8 and -9.

If Smpdl3b is overexpressed together with MyD88 the signal is increased compared to the control, which indicates, that Smpdl3b activates the signaling pathways.

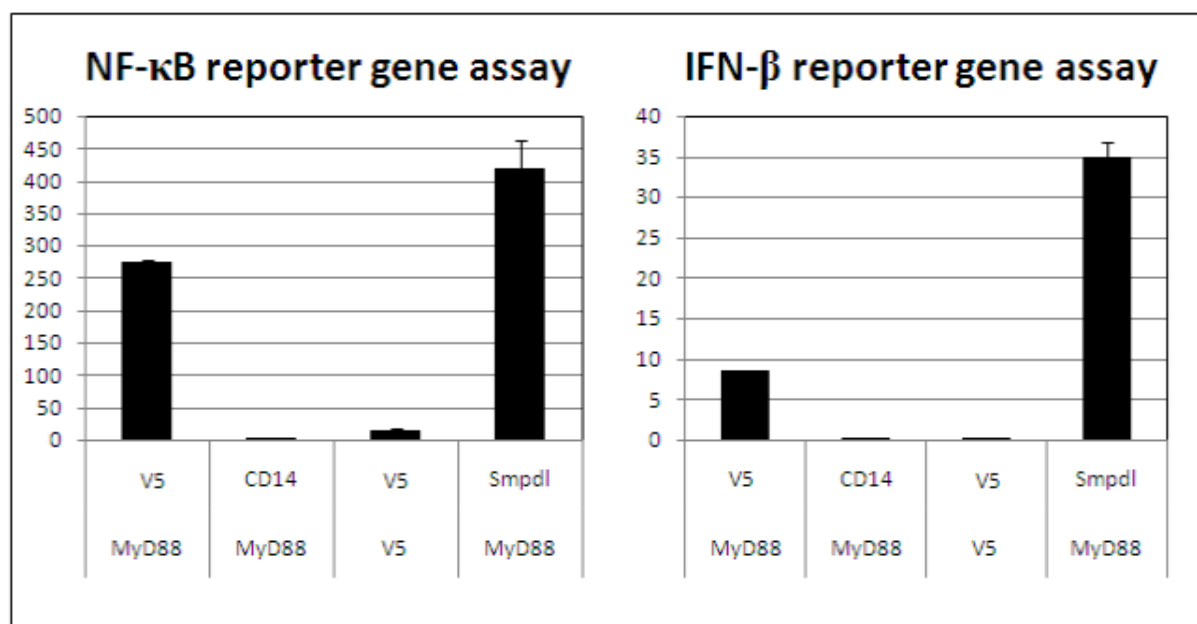
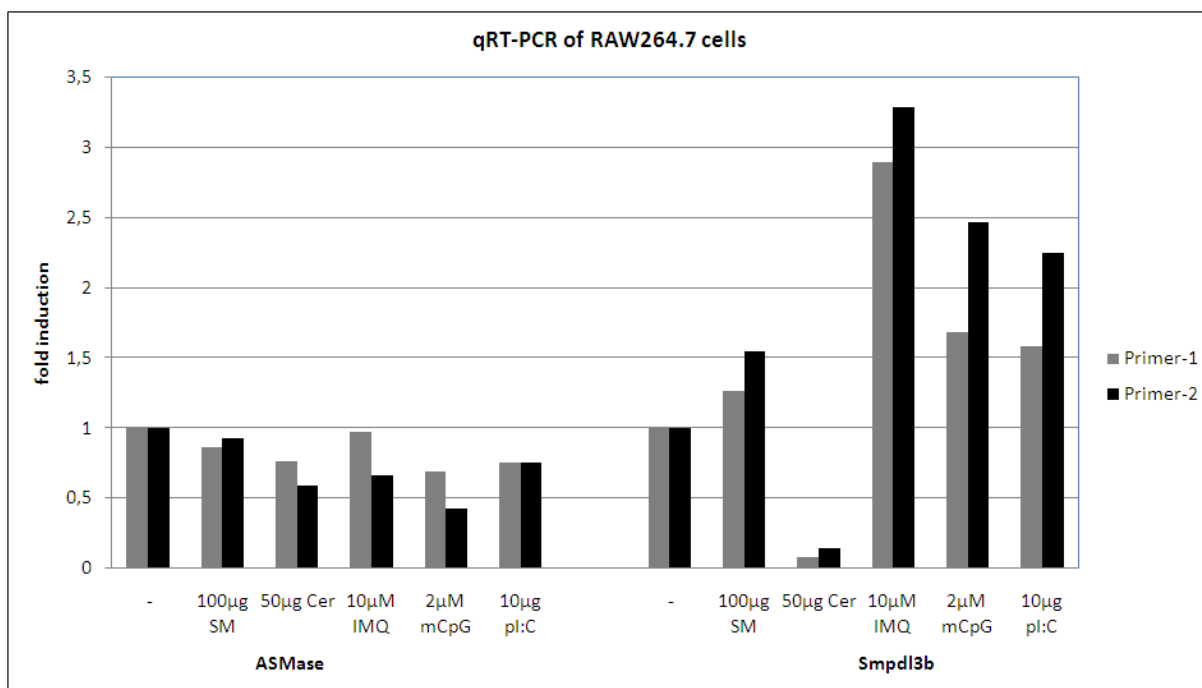


Figure 3.5.2.: NF-κB and IFN-β reporter gene assay in HEK293T cells, looking at the fold induction of NF-κB and IFN-β.

To verify if Smpdl3b and Toll-like receptors are also functionally linked to each other we monitored the levels of Smpdl3b mRNA of RAW264.7 upon different stimuli by quantitative real time PCR (Fig. 3.5.3.). Upon addition of the cleavage product ceramide the level of Smpdl3b mRNA drops significantly, which might indicate a negative feedback loop. After treatment with TLR ligands the levels of Smpdl3b mRNA are elevated, most significantly applying to the TLR7 ligand imiquimod. As control the mRNA levels of the closest related acid sphingomyelinase, ASMase, have been monitored, which remain unchanged throughout stimulation.

This data indicates that Smpdl3b is specifically involved in endosomal toll-like receptor signaling, whereas its distinct function still needs to be discovered.



**Figure 3.5.3.:** Quantitative real time PCR of RAW264.7 macrophage cDNA was performed using two different primer-pairs to amplify the mRNA of acid sphingomyelinase (ASMase) and for Smpd3b. Cells have been either untreated or treated with 100µg spingomyelin (SM), 50µg ceramide (Cer), 10µM imiquimod (IMQ), 2µM mCpG and 10µg polyI:C (pl:C). Two hours prior stimulation cells have been incubated with serum free medium and have been stimulated for 4h.

## Discussion

The aim of my project was to broaden our understanding of toll-like receptor mediated recognition of viral pathogens by the innate immune system, by identifying new players and co-factors of endosomal toll-like receptors.

Only little is known about endosomal toll-like receptors and their activation. It has been reported that endosomal TLRs are resting in the endoplasmic reticulum (ER) and are shuttled to the endosomes, mediated by Unc93b1, upon stimulation (Brinkmann et al., 2007). But how and where the initial recognition of PAMPs occur, is not known so far. Unfortunately we have not detected Unc93b1, which has been reported as constant interactor of endosomal TLRs, in any of our TAP pulldowns. But Unc93b1 is not present in any pull down ever done at CeMM, which suggests that the isolation of Unc93b1 is not trivial. Moreover, the expression of the protein for co-immunoprecipitation was causing difficulties, since lysate, including overexpressed Unc93b1, could not be boiled to denature the protein, in order not to lose the signal on the western-blot. Thus we assume that the used TAP conditions, where final eluates have been boiled, led to the loss of Unc93b1 detection.

So far it is not known how PAMP recognition and TLR activation occurs, considering all the information that are on-hand so far.

In general the ligand has to be recognized and bound at the surface of the cell and has to be internalized via phagocytosis. So far it is not known how this step is mediated. The PAMPs might be recognized by unspecific scavenger receptors that are present at the surface and are initiating phagocytosis. It could also be possible that innate immunity effector cells are constantly internalizing extracellular material, irrespectively of the present components. After endocytosis TLRs have to be shuttled from the endoplasmic reticulum, mediated by Unc93b1, to the endosomes, where they specifically bind to their ligands and induce downstream signaling. If TLRs are constantly shuttled between ER and endosome, or if they need a distinct signal for translocation, is unclear. If TLRs are not constantly shuttled between ER and endosome, a distinct factor is needed to alert the resting toll-like receptors and to initiate the shuttling to the endosome, where tight ligand binding is taking place. This hypothesis has to impart the first signal at the cell surface or from the endosome to the resting toll-like receptors in the ER. It has been shown, that endoplasmic toll-like receptors are cleaved to enforce the ligand binding. The cleavage data of Ewald, et al (2008) shows, that TLR9, as well as TLR7 are cleaved upon activation within their ectodomain. Further they show that a small portion of TLR9 remain uncleaved which is still able to bind to the ligand but is not able to induce signaling. Ewald, et al. (2008) claim, that this small fraction of uncleavable TLR9 is present in early endosomes. This data might indicate that TLRs, the uncleavable fraction, are constantly shuttled between ER and endosomes. After ligand binding cleavage of the ectodomain and increased shuttling could be mediated by distinct

cofactors, which enhances ligand binding and triggers downstream signaling and host defense.

The possibility, that endosomal toll-like receptors are present on the cell membrane, where they bind their specific ligand, internalize it and further the recruitment of toll-like receptors that are resting in the ER, seems not to apply. So far we do not have evidence that endosomal TLRs are present on the cell surface, since we found endosomal toll-like receptors solely in compartments within the cell and not at the surface in HeLa cells, looking at immune-fluorescence staining. The same is true for stable transfected RAW cells expressing V5 tagged murine TLRs (data not shown in the results), where the fusion proteins were only present within the cell. Hence we confirmed the finding of Ewald, et al. who have not found endosomal TLRs on the cell surface as well.

These theories are highly hypothetical; nevertheless it is very likely that distinct cofactors and co-receptors are needed for ligand binding and for the activation of downstream signaling.

#### **4.1. Tandem Affinity Purification**

Our aim was to elucidate the activation and signaling of endosomal toll-like receptors. Therefore we systematically search for endosomal Toll-like receptor complexes required for the innate immune response to viral infection. To implement this approach, we used RAW264.7 macrophages, since this cell line is signaling competent for innate immunity pathways, which assures, that all needed cofactors for proper TLR signaling are expressed. Furthermore, we have been restricted to cell lines, since we needed very high amounts of starting material for realizing this project.

We decided to implement our intention by tandem affinity purification, using the endosomal toll-like receptors as bait, since it represents the most straight forward way to identify the core complex of toll, like receptors.

Moreover, we decided to implement our approach in the non stimulated system because of two reasons: In the first place we searched for the endosomal TLR core-complex, which is assumed to be constitutively assembled, as it is the case for TLR4 and its cofactors Cd14 and Md2. Although we have to admit that the signaling and the assembly of the core-complex of cell membrane toll-like receptors and endosomal TLRs might differ. Secondly we have not discovered a change in detected proteins in the stimulated TLR3 test pulldowns compared to the non stimulated TLR3 pulldowns. Proteins, which have been already found in the non stimulated pulldowns have been enriched, put no new proteins appeared. Retrospectively it might have eased the analysis if we would have only performed stimulated pulldowns, since the difference between significant and non significant proteins might have been higher and therefore the analysis of the resulting data would have been more obvious.

Therefore a very important part of this project was the analysis of the resulting mass-spectrometry data to assure high significance for the selected candidates. Thus we assured

statistical significance by comparison to the core proteome of RAW264.7 macrophages, where we subtracted abundant proteins from the TLR datasets. A second important point is the appearance of distinct proteins in other non related pulldowns. The more often a distinct protein appears in other, non innate immunity related datasets, the more likely it is to be a non specific abandoned binder. Furthermore, the appearance in other pulldowns was helpful to select some proteins. For example TaoK1 appeared in the TLR3 dataset and in a polyI:C pulldown. This finding confirmed our selection since ToaK1 was also present in the TLR3 ligand pulldown. Moreover, we invested quite some time to ascertain the function and properties of statistical significant proteins by literature search.

Finally we selected seven candidates where we are confident about their association to endosomal toll-like receptors. Some of the selected proteins are statistically highly interesting, since they only appear in our TLR pulldowns, as it is the case for Rasa3 and Rftn1. Other proteins like TaoK1 or Smpdl3b are highly interesting because of their predicted function and properties.

## **4.2. Validation of Identified Candidates**

As validation for our seven candidates we decided to use co-immunoprecipitation, since it displays a direct and physiological way to show the interaction between two proteins. However the selected settings, such as the chosen cell-line, might not be ideal, since HEK293 cells might not be TLR signaling competent such as RAW264.7 macrophages. Unfortunately it is not possible to perform co-immunoprecipitation in RAW264.7 macrophages, which would have been the ideal cell line, since no reliably working antibodies for the endosomal TLRs, as well as for the candidates are available. Unfortunately the usage of a different validation strategy, such as the split-GFP system, would not have been ideal, since we are restricted to HEK293 cells for transient transfection. As already discussed above, HEK293 cells might not be TLR signaling competent. For the split GFP system it is necessary that the cell-line is TLR signaling competent to assure tight interaction.

We are still searching for better conditions for co-immunoprecipitation in HEK293 cells. Furthermore, we are currently producing antibodies for a few candidates, to validate the interaction with endogenous protein in RAW264.7 cells. The ideal verification would be in RAW264.7 macrophages under exactly the same conditions as the TAP pulldowns have been performed.

## **4.3. TAO kinase 1 (TaoK1)**

For TaoK1 (TAO1) nine publications are available on the NCBI database, so far. TaoK1 is related to the regulation of the p38-containing stress-responsive MAP kinase pathway, where it activates MEK3, MEK4 and MEK6 (Hutchison et al., 1998). TaoK1 activates p38 in response to various genotoxic stimuli and si-RNA mediated TaoK1 knock down decreases

p38 activation upon DNA damage (Raman et al., 2007). Further TaoK1 is shown to be an important regulator of mitotic progression, required for both chromosome congression and checkpoint induced anaphase delay. It is reported to interact with the checkpoint kinase BubR1 and to promote the enrichment of the checkpoint protein Mad2 at sites of defective attachment (Draviam et al., 2007). Beside the role in the stress-responsive MAP kinase pathway and in the spindle checkpoint, TaoK1 is further reported to play a role in microtubules dynamics (Johne et al., 2008). Interestingly, TaoK1 is localized in phagosomes of IFN- $\gamma$  treated macrophages (Trost et al., 2009).

The link, between TaoK1 and innate immunity is suggested by its interaction with the p38 pathway, which is also involved in innate immunity signaling. Toll-like receptors activate the major mitogen-activated protein (MAP) kinase subtypes and p38 MAP kinases, which are crucial for cell survival and controlling the expression of immune mediators (Symons et al., 2006). Since TaoK1 is upstream of p38 (Raman et al., 2007) and further specifically found in mTLR3 pulldowns, it indicates, that it might act as a co-factor of TLR3. Moreover, its finding in phagosomes of macrophages increased the assumption that TaoK1 is associated with endosomal TLRs.

Although we have not been able to show direct interaction between TLR3 and TaoK1 so far, we strongly believe that both proteins are associated, since it was highly enriched upon stimulation of TLR3 in the mass-spectrum data.

#### **4.4. Polymerase Delta-Interacting Protein 3 (Poldip3)**

Poldip3, also known as PDIP46 and SKAR, is reported to be a substrate of S6K1 and therefore plays a role in the mTOR and Pi3-kinase pathway, since S6K1 is a downstream target of mTOR and Pi3K in cell growth control. Poldip3 is phosphorylated by S6K1 in vitro on sites that are mitogen regulated and rapamycin sensitive in vivo (Richardson et al., 2004). Poldip3 and S6K1 increase translation efficiency of spliced mRNA. Poldip3 mediates the recruitment of activated S6K1 to newly processed mRNAs and serves as a catenation between mTOR checkpoint signaling and the pioneer round of translation (Ma et al., 2008).

So far only few information is available about the structure of Poldip3, except the presents of an RNA binding domain (RRM) (Ma et al., 2008). Moreover, Poldip3 was reported to play a role in the autoimmune disease vasculitides, where it was identified as auto-antigen (Avila et al., 2008). The protein HMGB1 is a nuclear DNA-binding protein, which is released from necrotic cells and is an essential component of DNA-containing immune complexes that stimulated cytokine production through a TLR9–MyD88 pathway involving the multivalent receptor RAGE (Tian et al., 2007). Increased concentrations of DNA-containing immune complexes in the serum are associated with systemic autoimmune diseases such as lupus (Denny et al., 2006).

Poldip3 and HMGB1 share similar properties; both are nuclear proteins with a nucleic-acid binding domain and are reported to play a role in autoimmune diseases (Avila et

al., 2008). Including this background and the fact that Poldip3 is significantly enriched in the mTLR3 pulldown, we hypothesize that Poldip3 forms a RNA-containing immune complex in the serum, which is further recognized by TLR3.

The candidate Poldip3 is related to innate immunity signaling via the kinase mTOR and Pi3-kinase. But we have not selected Poldip3 because of its signaling properties, but because of its RNA binding motive. Poldip3 is clearly located in the nucleus, as it is reported in the literature and as we confirmed in the immune-fluorescence staining. It could be that Poldip3 plays an important role, when it is released from necrotic cells, and when it is present in the extracellular space. Since it has an RNA binding motive it is likely to be part of immune complexes that are further activating different receptors, as it is the case for HMGB1. Thus this protein could have an important role in several autoimmune diseases, whereby it appears to be highly interesting.

#### 4.5. Ras P21 Protein Activator 3 (Rasa3)

Rasa3 was identified as Ras GTPase-activating proteins and was named as GAP111 (Baba et al., 1995). The Ras GAP activity of Rasa3 is inhibited by phospholipids and is specifically stimulated by Ins (1,3,4,5)P<sub>4</sub> (Cullen et al., 1995). Itpkb (B isoform of inositol 1,4,5-trisphosphate [Ins(1,4,5)P<sub>3</sub>] 3-kinase) and Ins(1,3,4,5)P<sub>4</sub> mediate a survival signal in B cells via a Rasa3–Erk signaling pathway (Marechal et al., 2007).

Beside its function in B-cell survival and development further features of Rasa3 are not determined so far. Nevertheless, the low-molecular-mass G-proteins Rac, Ras and Rap have been shown to be involved in innate immunity signaling via p38 (Palsson et al., 2000). Moreover, Fc-receptor mediated phagocytosis requires the activation of the Rho GTPases Cdc42 and Rac1. The calcium-promoted Ras inactivator (CAPRI), a Ras GTPase-activating protein, functions as an adaptor for Cdc42 and Rac1 during FcR-mediated phagocytosis (Zhang et al., 2005).

The evidence that low-molecular-mass G-proteins, as well as correlated GTPase-activating proteins, are involved in innate immunity signaling, as well as the mass-spectrometry data, convinced us to select Rasa as interacting candidate for endosomal toll-like receptors.

So far we have not been able to show interaction with endosomal toll-like receptors, which might indicate, that they are not directly binding to TLRs. Nevertheless we are encouraged that they might have an important role in TLR activation and signaling, not only because of our mass-spectrometry data, but also because of their properties. Rasa3 is related to B-cell signaling and survival. Small GTPases have already been linked to phagocytosis. Therefore we hypothesize that Rasa3 might play an important role in the phagocytosis of endosomal TLR ligands. It could be possible that Rasa3 is involved in transferring the signal from the cell surface to the endoplasmic reticulum, where the TLRs are located.



#### 4.6. Raftlin lipid raft linker 1 (Rftn1)

Little is known about Rftn1. The protein is linked to lipid raft formation and is important for B-cell receptor signaling (Saeki et al., 2003). Lipid rafts, play an important role in B-cell activation as platforms for B-cell receptor signal initiation (Cheng et al., 1999). In resting B cells, the B-cell receptor is excluded from rafts, which concentrate the Src-family kinase Lyn. Stable residency of the B-cell receptor in rafts results in association with Lyn, which phosphorylates the immunoreceptor tyrosine-based activation motifs (ITAMs) of the B-cell receptor, recruiting Syk and initiating signaling cascades (Weintraub et al., 2000). Raftlin is exclusively localized in lipid rafts and co-localizes with the BCR before and after BCR stimulation. B-cell receptor signal transduction is severely impaired in Raftlin deficient B-cells, thus this protein is considered to be important for forming and maintaining lipid rafts (Saeki et al., 2003).

So far it is not shown that toll-like receptors are clustered in lipid rafts, but it is quite likely as it is proven for other receptors. Rasa3 could play an important role in forming those lipid raft clusters within the membrane. It is already reported, that Rftn1 interacts with Lyn, which we have selected as interesting candidate as well, whereby both candidates are even more interesting.

#### 4.7. Yamaguchi Sarcoma Viral (v-yes-1) Oncogene Homolog (Lyn)

The Src kinase family member Lyn is well characterized, especially its function in Fcγ-receptor signaling. There is evidence that Lyn is linked to FC-receptor mediated phagocytosis. Three different FC-receptors (FcγRI, FcγRIIB, and FcγRIIIA) mediate phagocytosis of IgG-opsonized particles in macrophages (Anderson et al., 1990). FcγRI and FcγRIIIA contain IgG-binding sites and a dimer of the γ subunit that contains an immunoreceptor tyrosine-based activation motif (ITAM) (Cambier, 1995; Weiss and Littman, 1994). The phosphorylation of ITAM tyrosines is thought to be catalyzed by Src family tyrosine kinases (Allen and Aderem, 1996; Greenberg et al., 1993). In addition, Src kinases, such as Lyn, Hck and Fgr, were found to physically associate with Fc receptors, and their catalytic activity was shown to be increased by receptor aggregation (Eiseman and Bolen, 1992; Kihara and Siraganian, 1994). Crowley et al. found that FcγR-mediated phagocytosis is delayed but preserved in Lyn, Hck and Fgr knock out macrophages (Crowley et al., 1997).

Collectively these findings suggest that Src family kinases are differentially involved in FcγR-signaling and that selective kinases, including Lyn and Hck, are able to fully transduce FcγR-signaling (Suzuki et al., 2000).

Moreover, Lyn is linked to neutrophil phagocytosis where Lyn-coupled LacCer-enriched lipid rafts are required for CD11b/CD18-mediated phagocytosis (Nakayama et al.,

2008). Beside its involvement in phagocytosis, Lyn is necessary for a TLR9 independent signaling cascade (Sanjuan et al., 2006).

These data suggest that the tyrosine kinase Lyn is involved in distinct innate immunity pathways. Further it covers a broad spectrum of different functions and it is likely that a set of requirements is still not known. Although Lyn is present in several other pulldowns, according to the ProtFollow Database (Tab. 3.2.8.) it is highly enriched in TLR7, -8 and -9 pulldowns. Therefore we have selected Lyn as interesting candidate, since it might play a role in TLR activation as it is the case for the Fcγ-receptors.

It is already reported, that Lyn interacts with Rftn1, whereby both candidates are even more interesting. It might be that we have already isolated small complexes in our TLR pulldowns and that the candidates are not only interacting with the toll-like receptors but also with each other. It could be that Rftn1 creates the environment for toll-like receptors within the membrane and that Lyn is involved in the activation of TLRs as a co-factor. It is also possible that Lyn activates the shuttling of TLRs, together with other proteins, whereby it might also interact with Rftn1. Further it could be possible, that Rftn1 and Lyn are not interacting with the toll-like receptors in the endoplasmic reticulum but in the endosome, where they support downstream signaling. Moreover, it might be that both proteins are at the cell-surface, where they are involved in phagocytosis of endosomal TLR ligands which are further bound by the receptors.

#### **4.8. Monocyte Differentiation antigen Cd14 (Cd14)**

Already in 1999, Cd14 was linked to toll-like receptors and was reported to play a role in innate immunity signaling (Means et al., 1999). Thus Cd14 is a well characterized protein and is reported to be a regulatory molecule which directly interacts with TLR ligands and mediates the binding to toll-like receptors. Cd14 is a glycosylphosphatidylinositol (GPI)-anchored protein that is expressed on the cell surface, or it can be soluble present in the extracellular space (Labeta et al., 1993). Cd14 is involved in the LPS recognition by TLR4, where it binds to LPS and mediates the transfer to MD2 and the activation of TLR4 (Aderem and Ulevitch, 2000). Cd14 also amplifies many TLR2-specific responses, where it directly interacts with the toll-like receptor (Akashi-Takamura and Miyake, 2008). Further Cd14 is also physically interacting with polyI:C, where it enables polyI:C internalization by TLR3 (Lee et al., 2006).

Although Cd14 is a very well studied protein, the interaction with other endosomal toll-like receptors, beside TLR4, -2, and -3, was not shown so far. Since it is one of the most prominent and important co-factors of toll-like receptors we decided to validate the interaction with TLR7, -8 and -9.

In our approach we specifically identified Cd14 as cofactor for TLR3, -7, -8 and -9. The interaction of TLR3 and Cd14 is already known, but it was not shown so far that TLR7, -8 and -9 are interacting with Cd14, as we have demonstrated by co-immunoprecipitation. Further

our functional data suggests that Cd14 is rather inhibiting the downstream signaling of TLR7, -8 and -9 than having a cumulative effect, upon overexpression in HEK293T cells. Whereas the overexpression of Cd14 in TLR3 expressing HEK293 cells, elevated the production of NF- $\kappa$ B, detected by reporter gene assay. Therefore we clearly embrace Cd14 as interesting cofactor of TLR7, -8 and -9, although the protein is already associated with other toll-like receptors, which might decrease the innovation of our finding.

#### **4.9. Acid Sphingomyelinase-Like Phosphodiesterase 3B Precursor (Smpdl3b)**

Little is known about Smpdl3b, but other acid sphingomyelinases (ASMase) were studied in more detail. These proteins catalyze the catalytic cleavage of sphingomyelin to the second messenger ceramide and phosphorylcholine. As a readout the biophysical properties of the lipid bilayer is altered (Utermohlen et al., 2008). The second messenger ceramide can initiate the evolutionarily conserved sphingomyelin pathway. The production of ceramide by sphingomyelin triggers apoptosis in macrophages by facilitate assembly of death receptor complexes (Steinbrecher et al., 2004). Diverse receptor types and environmental stress utilize the sphingomyelin pathway as a downstream effector system. In some cellular systems, ceramide initiates differentiation or cell proliferation, while in other systems, ceramide signals apoptosis (Pena et al., 1997). Moreover, ASMases are activated by several pro-inflammatory cytokines (Hofmeister et al., 1997) and are required for phago-lysosomal fusion in macrophages infected with *Listeria monocytogenes* (Utermohlen et al., 2008). ASMases are localized to the lumen of endosomes, phagosomes and lysosomes as well as to the outer leaflet of the plasma membrane. Maturation of phagosomes into phagolysosomes is severely impaired in macrophages genetically deficient for ASMase (Schramm et al., 2008).

A possible role of the ASMase homologue Smpdl3b in innate immunity is elusive. Since homologues of Smpdl3b play a role in innate immunity and phago-lysosomal fusion, Smpdl3b appears to be an interesting interactor of endosomal TLRs. Further knowledge on Smpdl3b is scarce, which makes it attractive as potentially newly identified toll-like receptor cofactor candidate. It could be possible, that Smpdl3b, together with Rftn1, generates the right membrane environment for TLRs, by the modulation of lipids in response to TLRs.

Smpdl3b, which we have identified as interactor of TLR7, -8 and -9 by tandem affinity purification and verified with co-immunoprecipitation, might have a supportive role in the signaling of endosomal toll-like receptors by producing ceramide, which can act as second messenger. Further Smpdl3b might encourage the membrane integrity of endosomal toll-like receptors and therefore could act as chaperon for the toll-like-receptor core complex. The fact that other family members of acid sphingomyelinases (ASMase) are located in endosomes, phagosomes and lysosomes, encouraged us to further validate the function of Smpdl3b. Therefore we did “gain of function” experiments, where we found increased NF- $\kappa$ B production upon Smpdl3b overexpressen by reporter-gene assay. Further the finding, that mRNA levels of Smpdl3b are up-regulated in RAW264.7 macrophages upon stimulation with

imiquimod, CpG and polyI:C, convinced us that Smpdl3b is involved in endosomal toll-like receptor signaling.

For Smpdl3b as well as for the other candidates further validation and functional assays are planned for successional projects. A very important experiment would be loss of function, to see whether we can down or up regulate TLR signaling if one of the components is missing. Furthermore, the distinct function of the different co-factors needs to be determined by individual assays. For instance, the increased production of ceramide by Smpdl3b upon TLR activation could be used as individual assay. We are further planning in vivo experiments for Cd14 where knockout mice are available, to verify our preliminary results, where the signaling ability of cells, over-expressing TLR-7, -8 and -9, is decreased upon Cd14 over-expression.

Of course all these functional suggestions for the different candidates are highly hypothetical and might not apply in nature, but our data might suggest, that these seven proteins are associated to endosomal toll-like receptors, by detecting them in endosomal toll-like receptor pulldowns. Collective evidence strongly suggests that at least two proteins – CD14 and Smpdl3b – are functionally important interactors of endosomal TLRs. This is a striking finding and might prove the chosen strategy successful. How and by which mechanism they are interacting with TLRs, and their role in innate immunity signaling, still needs to be discovered in a follow up project. Five other candidates still await further validation.

The identification of new TLR interacting proteins is very rare, since in general working with transmembrane proteins appeared to be very difficult. So far only few co-factors and interactors of endosomal TLRs have been identified. Therefore we are very happy to show the newly identified association of a non related protein – Smpdl3b – to endosomal TLRs, and the newly identified association of a known interactor – Cd14 – to TLR7, -8 and -9.

## References

- Aderem, A., and Ulevitch, R.J. (2000). Toll-like receptors in the induction of the innate immune response. *Nature* **406**, 782-787.
- Akashi-Takamura, S., and Miyake, K. (2008). TLR accessory molecules. *Curr Opin Immunol* **20**, 420-425.
- Akira, S., Takeda, K., and Kaisho, T. (2001). Toll-like receptors: critical proteins linking innate and acquired immunity. *Nat Immunol* **2**, 675-680.
- Akira, S., Uematsu, S., and Takeuchi, O. (2006). Pathogen recognition and innate immunity. *Cell* **124**, 783-801.
- Alexopoulou, L., Holt, A.C., Medzhitov, R., and Flavell, R.A. (2001). Recognition of double-stranded RNA and activation of NF-kappaB by Toll-like receptor 3. *Nature* **413**, 732-738.
- Allen, L.A., and Aderem, A. (1996). Molecular definition of distinct cytoskeletal structures involved in complement- and Fc receptor-mediated phagocytosis in macrophages. *J Exp Med* **184**, 627-637.
- Anderson, C.L., Shen, L., Eicher, D.M., Wewers, M.D., and Gill, J.K. (1990). Phagocytosis mediated by three distinct Fc gamma receptor classes on human leukocytes. *J Exp Med* **171**, 1333-1345.
- Aravind, L., Dixit, V.M., and Koonin, E.V. (2001). Apoptotic molecular machinery: vastly increased complexity in vertebrates revealed by genome comparisons. *Science* **291**, 1279-1284.
- Avila, J., Acosta, E., Machargo, M.D., Arteaga, M.F., Gallego, E., Canete, H., Garcia-Perez, J.J., and Martin-Vasallo, P. (2008). Autoantigenic nuclear proteins of a clinically atypical renal vasculitis. *J Autoimmune Dis* **5**, 3.
- Baba, H., Fuss, B., Urano, J., Poulet, P., Watson, J.B., Tamanoi, F., and Macklin, W.B. (1995). GapIII, a new brain-enriched member of the GTPase-activating protein family. *J Neurosci Res* **41**, 846-858.
- Banchereau, J., and Steinman, R.M. (1998). Dendritic cells and the control of immunity. *Nature* **392**, 245-252.
- Barton, G.M., Kagan, J.C., and Medzhitov, R. (2006). Intracellular localization of Toll-like receptor 9 prevents recognition of self DNA but facilitates access to viral DNA. *Nat Immunol* **7**, 49-56.
- Bell, J.K., Askins, J., Hall, P.R., Davies, D.R., and Segal, D.M. (2006). The dsRNA binding site of human Toll-like receptor 3. *Proc Natl Acad Sci U S A* **103**, 8792-8797.
- Belvin, M.P., and Anderson, K.V. (1996). A conserved signaling pathway: the *Drosophila* toll-dorsal pathway. *Annu Rev Cell Dev Biol* **12**, 393-416.
- Bowie, A.G. (2007). Translational mini-review series on Toll-like receptors: recent advances in understanding the role of Toll-like receptors in anti-viral immunity. *Clin Exp Immunol* **147**, 217-226.
- Bowie, A.G., and Haga, I.R. (2005). The role of Toll-like receptors in the host response to viruses. *Mol Immunol* **42**, 859-867.
- Brinkmann, M.M., Spooner, E., Hoebe, K., Beutler, B., Ploegh, H.L., and Kim, Y.M. (2007). The interaction between the ER membrane protein UNC93B and TLR3, 7, and 9 is crucial for TLR signaling. *J Cell Biol* **177**, 265-275.

- Buchanan, S.G., and Gay, N.J. (1996). Structural and functional diversity in the leucine-rich repeat family of proteins. *Prog Biophys Mol Biol* 65, 1-44.
- Burckstummer, T., Bennett, K.L., Preradovic, A., Schutze, G., Hantschel, O., Superti-Furga, G., and Bauch, A. (2006). An efficient tandem affinity purification procedure for interaction proteomics in mammalian cells. *Nat Methods* 3, 1013-1019.
- Byrd-Leifer, C.A., Block, E.F., Takeda, K., Akira, S., and Ding, A. (2001). The role of MyD88 and TLR4 in the LPS-mimetic activity of Taxol. *Eur J Immunol* 31, 2448-2457.
- Cambier, J.C. (1995). New nomenclature for the Reth motif (or ARH1/TAM/ARAM/YXXL). *Immunol Today* 16, 110.
- Cheng, P.C., Dykstra, M.L., Mitchell, R.N., and Pierce, S.K. (1999). A role for lipid rafts in B cell antigen receptor signaling and antigen targeting. *J Exp Med* 190, 1549-1560.
- Choe, J., Kelker, M.S., and Wilson, I.A. (2005). Crystal structure of human toll-like receptor 3 (TLR3) ectodomain. *Science* 309, 581-585.
- Chu, W.M., Ostertag, D., Li, Z.W., Chang, L., Chen, Y., Hu, Y., Williams, B., Perrault, J., and Karin, M. (1999). JNK2 and IKKbeta are required for activating the innate response to viral infection. *Immunity* 11, 721-731.
- Crowley, M.T., Costello, P.S., Fitzer-Attas, C.J., Turner, M., Meng, F., Lowell, C., Tybulewicz, V.L., and DeFranco, A.L. (1997). A critical role for Syk in signal transduction and phagocytosis mediated by Fcgamma receptors on macrophages. *J Exp Med* 186, 1027-1039.
- Cullen, P.J., Hsuan, J.J., Truong, O., Letcher, A.J., Jackson, T.R., Dawson, A.P., and Irvine, R.F. (1995). Identification of a specific Ins(1,3,4,5)P4-binding protein as a member of the GAP1 family. *Nature* 376, 527-530.
- DeLotto, Y., and DeLotto, R. (1998). Proteolytic processing of the *Drosophila* Spatzle protein by easter generates a dimeric NGF-like molecule with ventralising activity. *Mech Dev* 72, 141-148.
- Denny, M.F., Chandaroy, P., Killen, P.D., Caricchio, R., Lewis, E.E., Richardson, B.C., Lee, K.D., Gavalchin, J., and Kaplan, M.J. (2006). Accelerated macrophage apoptosis induces autoantibody formation and organ damage in systemic lupus erythematosus. *J Immunol* 176, 2095-2104.
- Diebold, S.S., Massacrier, C., Akira, S., Paturel, C., Morel, Y., and Reis e Sousa, C. (2006). Nucleic acid agonists for Toll-like receptor 7 are defined by the presence of uridine ribonucleotides. *Eur J Immunol* 36, 3256-3267.
- Draviam, V.M., Stegmeier, F., Nalepa, G., Sowa, M.E., Chen, J., Liang, A., Hannon, G.J., Sorger, P.K., Harper, J.W., and Elledge, S.J. (2007). A functional genomic screen identifies a role for TAO1 kinase in spindle-checkpoint signalling. *Nat Cell Biol* 9, 556-564.
- Edelmann, K.H., Richardson-Burns, S., Alexopoulou, L., Tyler, K.L., Flavell, R.A., and Oldstone, M.B. (2004). Does Toll-like receptor 3 play a biological role in virus infections? *Virology* 322, 231-238.
- Eiseman, E., and Bolen, J.B. (1992). Engagement of the high-affinity IgE receptor activates src protein-related tyrosine kinases. *Nature* 355, 78-80.
- Ewald, S.E., Lee, B.L., Lau, L., Wickliffe, K.E., Shi, G.P., Chapman, H.A., and Barton, G.M. (2008). The ectodomain of Toll-like receptor 9 is cleaved to generate a functional receptor. *Nature* 456, 658-662.

- Field, A.K., Tytell, A.A., Lampson, G.P., and Hilleman, M.R. (1967). Inducers of interferon and host resistance. II. Multistranded synthetic polynucleotide complexes. *Proc Natl Acad Sci U S A* 58, 1004-1010.
- Fitzgerald, K.A., Rowe, D.C., Barnes, B.J., Caffrey, D.R., Visintin, A., Latz, E., Monks, B., Pitha, P.M., and Golenbock, D.T. (2003). LPS-TLR4 signaling to IRF-3/7 and NF-kappaB involves the toll adapters TRAM and TRIF. *J Exp Med* 198, 1043-1055.
- Gay, N.J., and Gangloff, M. (2008). Structure of toll-like receptors. *Handb Exp Pharmacol*, 181-200.
- Greenberg, S., Chang, P., and Silverstein, S.C. (1993). Tyrosine phosphorylation is required for Fc receptor-mediated phagocytosis in mouse macrophages. *J Exp Med* 177, 529-534.
- Hacker, H., Mischak, H., Miethke, T., Liptay, S., Schmid, R., Sparwasser, T., Heeg, K., Lipford, G.B., and Wagner, H. (1998). CpG-DNA-specific activation of antigen-presenting cells requires stress kinase activity and is preceded by non-specific endocytosis and endosomal maturation. *Embo J* 17, 6230-6240.
- Hashimoto, C., Hudson, K.L., and Anderson, K.V. (1988). The Toll gene of *Drosophila*, required for dorsal-ventral embryonic polarity, appears to encode a transmembrane protein. *Cell* 52, 269-279.
- Heil, F., Hemmi, H., Hochrein, H., Ampenberger, F., Kirschning, C., Akira, S., Lipford, G., Wagner, H., and Bauer, S. (2004). Species-specific recognition of single-stranded RNA via toll-like receptor 7 and 8. *Science* 303, 1526-1529.
- Hemmi, H., Kaisho, T., Takeuchi, O., Sato, S., Sanjo, H., Hoshino, K., Horiuchi, T., Tomizawa, H., Takeda, K., and Akira, S. (2002). Small anti-viral compounds activate immune cells via the TLR7 MyD88-dependent signaling pathway. *Nat Immunol* 3, 196-200.
- Hoebe, K., Du, X., Goode, J., Mann, N., and Beutler, B. (2003). *Lps2*: a new locus required for responses to lipopolysaccharide, revealed by germline mutagenesis and phenotypic screening. *J Endotoxin Res* 9, 250-255.
- Hofmeister, R., Wiegmann, K., Korherr, C., Bernardo, K., Kronke, M., and Falk, W. (1997). Activation of acid sphingomyelinase by interleukin-1 (IL-1) requires the IL-1 receptor accessory protein. *J Biol Chem* 272, 27730-27736.
- Honda, K., Takaoka, A., and Taniguchi, T. (2006). Type I interferon [corrected] gene induction by the interferon regulatory factor family of transcription factors. *Immunity* 25, 349-360.
- Honda, K., Yanai, H., Negishi, H., Asagiri, M., Sato, M., Mizutani, T., Shimada, N., Ohba, Y., Takaoka, A., Yoshida, N., *et al.* (2005). IRF-7 is the master regulator of type-I interferon-dependent immune responses. *Nature* 434, 772-777.
- Hu, X., Yagi, Y., Tanji, T., Zhou, S., and Ip, Y.T. (2004). Multimerization and interaction of Toll and Spatzle in *Drosophila*. *Proc Natl Acad Sci U S A* 101, 9369-9374.
- Hutchison, M., Berman, K.S., and Cobb, M.H. (1998). Isolation of TAO1, a protein kinase that activates MEKs in stress-activated protein kinase cascades. *J Biol Chem* 273, 28625-28632.
- Iwasaki, A., and Medzhitov, R. (2004). Toll-like receptor control of the adaptive immune responses. *Nat Immunol* 5, 987-995.

- Janeway, C.A., Jr. (1989). Approaching the asymptote? Evolution and revolution in immunology. *Cold Spring Harb Symp Quant Biol* 54 Pt 1, 1-13.
- Johne, C., Matenia, D., Li, X.Y., Timm, T., Balusamy, K., and Mandelkow, E.M. (2008). Spred1 and TESK1--two new interaction partners of the kinase MARKK/TAO1 that link the microtubule and actin cytoskeleton. *Mol Biol Cell* 19, 1391-1403.
- Jurk, M., Heil, F., Vollmer, J., Schetter, C., Krieg, A.M., Wagner, H., Lipford, G., and Bauer, S. (2002). Human TLR7 or TLR8 independently confer responsiveness to the antiviral compound R-848. *Nat Immunol* 3, 499.
- Kawai, T., and Akira, S. (2005). Toll-like receptor downstream signaling. *Arthritis Res Ther* 7, 12-19.
- Kawai, T., and Akira, S. (2006). Innate immune recognition of viral infection. *Nat Immunol* 7, 131-137.
- Keating, S.E., Maloney, G.M., Moran, E.M., and Bowie, A.G. (2007). IRAK-2 participates in multiple toll-like receptor signaling pathways to NFkappaB via activation of TRAF6 ubiquitination. *J Biol Chem* 282, 33435-33443.
- Khush, R.S., Leulier, F., and Lemaitre, B. (2001). Drosophila immunity: two paths to NF-kappaB. *Trends Immunol* 22, 260-264.
- Kihara, H., and Siraganian, R.P. (1994). Src homology 2 domains of Syk and Lyn bind to tyrosine-phosphorylated subunits of the high affinity IgE receptor. *J Biol Chem* 269, 22427-22432.
- Kim, Y.M., Brinkmann, M.M., Paquet, M.E., and Ploegh, H.L. (2008). UNC93B1 delivers nucleotide-sensing toll-like receptors to endolysosomes. *Nature* 452, 234-238.
- Klinman, D.M. (2004). Immunotherapeutic uses of CpG oligodeoxynucleotides. *Nat Rev Immunol* 4, 249-258.
- Krieg, A.M. (2002). CpG motifs in bacterial DNA and their immune effects. *Annu Rev Immunol* 20, 709-760.
- Krug, A., French, A.R., Barchet, W., Fischer, J.A., Dzionek, A., Pingel, J.T., Orihuela, M.M., Akira, S., Yokoyama, W.M., and Colonna, M. (2004a). TLR9-dependent recognition of MCMV by IPC and DC generates coordinated cytokine responses that activate antiviral NK cell function. *Immunity* 21, 107-119.
- Krug, A., Luker, G.D., Barchet, W., Leib, D.A., Akira, S., and Colonna, M. (2004b). Herpes simplex virus type 1 activates murine natural interferon-producing cells through toll-like receptor 9. *Blood* 103, 1433-1437.
- Labeta, M.O., Durieux, J.J., Fernandez, N., Herrmann, R., and Ferrara, P. (1993). Release from a human monocyte-like cell line of two different soluble forms of the lipopolysaccharide receptor, CD14. *Eur J Immunol* 23, 2144-2151.
- Latz, E., Schoenemeyer, A., Visintin, A., Fitzgerald, K.A., Monks, B.G., Knetter, C.F., Lien, E., Nilsen, N.J., Espevik, T., and Golenbock, D.T. (2004). TLR9 signals after translocating from the ER to CpG DNA in the lysosome. *Nat Immunol* 5, 190-198.
- Latz, E., Verma, A., Visintin, A., Gong, M., Sirois, C.M., Klein, D.C., Monks, B.G., McKnight, C.J., Lamphier, M.S., Duprex, W.P., *et al.* (2007). Ligand-induced conformational changes allosterically activate Toll-like receptor 9. *Nat Immunol* 8, 772-779.



- Lee, H.K., Dunzendorfer, S., Soldau, K., and Tobias, P.S. (2006). Double-stranded RNA-mediated TLR3 activation is enhanced by CD14. *Immunity* 24, 153-163.
- Lemaitre, B., Nicolas, E., Michaut, L., Reichhart, J.M., and Hoffmann, J.A. (1996). The dorsoventral regulatory gene cassette *spatzle/Toll/cactus* controls the potent antifungal response in *Drosophila* adults. *Cell* 86, 973-983.
- Lemaitre, B., Reichhart, J.M., and Hoffmann, J.A. (1997). *Drosophila* host defense: differential induction of antimicrobial peptide genes after infection by various classes of microorganisms. *Proc Natl Acad Sci U S A* 94, 14614-14619.
- Levashina, E.A., Langley, E., Green, C., Gubb, D., Ashburner, M., Hoffmann, J.A., and Reichhart, J.M. (1999). Constitutive activation of toll-mediated antifungal defense in serpin-deficient *Drosophila*. *Science* 285, 1917-1919.
- Liu, Y.J. (2005). IPC: professional type 1 interferon-producing cells and plasmacytoid dendritic cell precursors. *Annu Rev Immunol* 23, 275-306.
- Luna, C., Wang, X., Huang, Y., Zhang, J., and Zheng, L. (2002). Characterization of four Toll related genes during development and immune responses in *Anopheles gambiae*. *Insect Biochem Mol Biol* 32, 1171-1179.
- Lund, J., Sato, A., Akira, S., Medzhitov, R., and Iwasaki, A. (2003). Toll-like receptor 9-mediated recognition of Herpes simplex virus-2 by plasmacytoid dendritic cells. *J Exp Med* 198, 513-520.
- Ma, X.M., Yoon, S.O., Richardson, C.J., Julich, K., and Blenis, J. (2008). SKAR links pre-mRNA splicing to mTOR/S6K1-mediated enhanced translation efficiency of spliced mRNAs. *Cell* 133, 303-313.
- Marechal, Y., Pesesse, X., Jia, Y., Pouillon, V., Perez-Morga, D., Daniel, J., Izui, S., Cullen, P.J., Leo, O., Luo, H.R., *et al.* (2007). Inositol 1,3,4,5-tetrakisphosphate controls proapoptotic Bim gene expression and survival in B cells. *Proc Natl Acad Sci U S A* 104, 13978-13983.
- Marshall-Clarke, S., Downes, J.E., Haga, I.R., Bowie, A.G., Borrow, P., Pennock, J.L., Grencis, R.K., and Rothwell, P. (2007). Polyinosinic acid is a ligand for toll-like receptor 3. *J Biol Chem* 282, 24759-24766.
- Means, T.K., Lien, E., Yoshimura, A., Wang, S., Golenbock, D.T., and Fenton, M.J. (1999). The CD14 ligands lipoarabinomannan and lipopolysaccharide differ in their requirement for Toll-like receptors. *J Immunol* 163, 6748-6755.
- Medzhitov, R. (2001). Toll-like receptors and innate immunity. *Nat Rev Immunol* 1, 135-145.
- Medzhitov, R., and Janeway, C., Jr. (2000). Innate immunity. *N Engl J Med* 343, 338-344.
- Medzhitov, R., and Janeway, C.A., Jr. (1997). Innate immunity: impact on the adaptive immune response. *Curr Opin Immunol* 9, 4-9.
- Medzhitov, R., and Janeway, C.A., Jr. (1998). Self-defense: the fruit fly style. *Proc Natl Acad Sci U S A* 95, 429-430.
- Medzhitov, R., Preston-Hurlburt, P., and Janeway, C.A., Jr. (1997). A human homologue of the *Drosophila* Toll protein signals activation of adaptive immunity. *Nature* 388, 394-397.

- Miller, R.L., Gerster, J.F., Owens, M.L., Slade, H.B., and Tomai, M.A. (1999). Imiquimod applied topically: a novel immune response modifier and new class of drug. *Int J Immunopharmacol* 21, 1-14.
- Nagai, Y., Akashi, S., Nagafuku, M., Ogata, M., Iwakura, Y., Akira, S., Kitamura, T., Kosugi, A., Kimoto, M., and Miyake, K. (2002). Essential role of MD-2 in LPS responsiveness and TLR4 distribution. *Nat Immunol* 3, 667-672.
- Nakayama, H., Yoshizaki, F., Prinetti, A., Sonnino, S., Mauri, L., Takamori, K., Ogawa, H., and Iwabuchi, K. (2008). Lyn-coupled LacCer-enriched lipid rafts are required for CD11b/CD18-mediated neutrophil phagocytosis of nonopsonized microorganisms. *J Leukoc Biol* 83, 728-741.
- O'Neill, L.A., and Bowie, A.G. (2007). The family of five: TIR-domain-containing adaptors in Toll-like receptor signalling. *Nat Rev Immunol* 7, 353-364.
- Oganesyan, G., Saha, S.K., Guo, B., He, J.Q., Shahangian, A., Zarnegar, B., Perry, A., and Cheng, G. (2006). Critical role of TRAF3 in the Toll-like receptor-dependent and -independent antiviral response. *Nature* 439, 208-211.
- Palsson, E.M., Popoff, M., Thelestam, M., and O'Neill, L.A. (2000). Divergent roles for Ras and Rap in the activation of p38 mitogen-activated protein kinase by interleukin-1. *J Biol Chem* 275, 7818-7825.
- Park, B., Brinkmann, M.M., Spooner, E., Lee, C.C., Kim, Y.M., and Ploegh, H.L. (2008). Proteolytic cleavage in an endolysosomal compartment is required for activation of Toll-like receptor 9. *Nat Immunol* 9, 1407-1414.
- Pena, L.A., Fuks, Z., and Kolesnick, R. (1997). Stress-induced apoptosis and the sphingomyelin pathway. *Biochem Pharmacol* 53, 615-621.
- Poltorak, A., He, X., Smirnova, I., Liu, M.Y., Van Huffel, C., Du, X., Birdwell, D., Alejos, E., Silva, M., Galanos, C., *et al.* (1998). Defective LPS signaling in C3H/HeJ and C57BL/10ScCr mice: mutations in Tlr4 gene. *Science* 282, 2085-2088.
- Poltorak, A., Ricciardi-Castagnoli, P., Citterio, S., and Beutler, B. (2000). Physical contact between lipopolysaccharide and toll-like receptor 4 revealed by genetic complementation. *Proc Natl Acad Sci U S A* 97, 2163-2167.
- Raman, M., Earnest, S., Zhang, K., Zhao, Y., and Cobb, M.H. (2007). TAO kinases mediate activation of p38 in response to DNA damage. *Embo J* 26, 2005-2014.
- Reis e Sousa, C. (2004). Activation of dendritic cells: translating innate into adaptive immunity. *Curr Opin Immunol* 16, 21-25.
- Richardson, C.J., Broenstrup, M., Fingar, D.C., Julich, K., Ballif, B.A., Gygi, S., and Blenis, J. (2004). SKAR is a specific target of S6 kinase 1 in cell growth control. *Curr Biol* 14, 1540-1549.
- Rock, F.L., Hardiman, G., Timans, J.C., Kastelein, R.A., and Bazan, J.F. (1998). A family of human receptors structurally related to *Drosophila* Toll. *Proc Natl Acad Sci U S A* 95, 588-593.
- Saeki, K., Miura, Y., Aki, D., Kurosaki, T., and Yoshimura, A. (2003). The B cell-specific major raft protein, Raftlin, is necessary for the integrity of lipid raft and BCR signal transduction. *Embo J* 22, 3015-3026.
- Sanjuan, M.A., Rao, N., Lai, K.T., Gu, Y., Sun, S., Fuchs, A., Fung-Leung, W.P., Colonna, M., and Karlsson, L. (2006). CpG-induced tyrosine phosphorylation occurs via a TLR9-independent mechanism and is required for cytokine secretion. *J Cell Biol* 172, 1057-1068.

- Schmitz, F., Heit, A., Guggemoos, S., Krug, A., Mages, J., Schiemann, M., Adler, H., Drexler, I., Haas, T., Lang, R., *et al.* (2007). Interferon-regulatory-factor 1 controls Toll-like receptor 9-mediated IFN-beta production in myeloid dendritic cells. *Eur J Immunol* 37, 315-327.
- Schramm, M., Herz, J., Haas, A., Kronke, M., and Utermohlen, O. (2008). Acid sphingomyelinase is required for efficient phago-lysosomal fusion. *Cell Microbiol* 10, 1839-1853.
- Schroder, M., and Bowie, A.G. (2005). TLR3 in antiviral immunity: key player or bystander? *Trends Immunol* 26, 462-468.
- Schulz, O., Diebold, S.S., Chen, M., Naslund, T.I., Nolte, M.A., Alexopoulou, L., Azuma, Y.T., Flavell, R.A., Liljestrom, P., and Reis e Sousa, C. (2005). Toll-like receptor 3 promotes cross-priming to virus-infected cells. *Nature* 433, 887-892.
- Shimazu, R., Akashi, S., Ogata, H., Nagai, Y., Fukudome, K., Miyake, K., and Kimoto, M. (1999). MD-2, a molecule that confers lipopolysaccharide responsiveness on Toll-like receptor 4. *J Exp Med* 189, 1777-1782.
- Shin, S.W., Kokoza, V., Bian, G., Cheon, H.M., Kim, Y.J., and Raikhel, A.S. (2005). REL1, a homologue of *Drosophila* dorsal, regulates toll antifungal immune pathway in the female mosquito *Aedes aegypti*. *J Biol Chem* 280, 16499-16507.
- Slack, E.C., Robinson, M.J., Hernanz-Falcon, P., Brown, G.D., Williams, D.L., Schweighoffer, E., Tybulewicz, V.L., and Reis e Sousa, C. (2007). Syk-dependent ERK activation regulates IL-2 and IL-10 production by DC stimulated with zymosan. *Eur J Immunol* 37, 1600-1612.
- Steinbrecher, U.P., Gomez-Munoz, A., and Duronio, V. (2004). Acid sphingomyelinase in macrophage apoptosis. *Curr Opin Lipidol* 15, 531-537.
- Suzuki, N., Suzuki, S., Duncan, G.S., Millar, D.G., Wada, T., Mirtsos, C., Takada, H., Wakeham, A., Itie, A., Li, S., *et al.* (2002). Severe impairment of interleukin-1 and Toll-like receptor signalling in mice lacking IRAK-4. *Nature* 416, 750-756.
- Suzuki, T., Kono, H., Hirose, N., Okada, M., Yamamoto, T., Yamamoto, K., and Honda, Z. (2000). Differential involvement of Src family kinases in Fc gamma receptor-mediated phagocytosis. *J Immunol* 165, 473-482.
- Symons, A., Beinke, S., and Ley, S.C. (2006). MAP kinase kinase kinases and innate immunity. *Trends Immunol* 27, 40-48.
- Takaoka, A., Yanai, H., Kondo, S., Duncan, G., Negishi, H., Mizutani, T., Kano, S., Honda, K., Ohba, Y., Mak, T.W., *et al.* (2005). Integral role of IRF-5 in the gene induction programme activated by Toll-like receptors. *Nature* 434, 243-249.
- Takeda, K., and Akira, S. (2005). Toll-like receptors in innate immunity. *Int Immunol* 17, 1-14.
- Takeda, K., Kaisho, T., and Akira, S. (2003). Toll-like receptors. *Annu Rev Immunol* 21, 335-376.
- Tian, J., Avalos, A.M., Mao, S.Y., Chen, B., Senthil, K., Wu, H., Parroche, P., Drabic, S., Golenbock, D., Sirois, C., *et al.* (2007). Toll-like receptor 9-dependent activation by DNA-containing immune complexes is mediated by HMGB1 and RAGE. *Nat Immunol* 8, 487-496.

- Trost, M., English, L., Lemieux, S., Courcelles, M., Desjardins, M., and Thibault, P. (2009). The phagosomal proteome in interferon-gamma-activated macrophages. *Immunity* 30, 143-154.
- Uematsu, S., and Akira, S. (2007). Toll-like receptors and Type I interferons. *J Biol Chem* 282, 15319-15323.
- Utermohlen, O., Herz, J., Schramm, M., and Kronke, M. (2008). Fusogenicity of membranes: the impact of acid sphingomyelinase on innate immune responses. *Immunobiology* 213, 307-314.
- Weber, A.N., Moncrieffe, M.C., Gangloff, M., Imler, J.L., and Gay, N.J. (2005). Ligand-receptor and receptor-receptor interactions act in concert to activate signaling in the Drosophila toll pathway. *J Biol Chem* 280, 22793-22799.
- Weintraub, B.C., Jun, J.E., Bishop, A.C., Shokat, K.M., Thomas, M.L., and Goodnow, C.C. (2000). Entry of B cell receptor into signaling domains is inhibited in tolerant B cells. *J Exp Med* 191, 1443-1448.
- Weiss, A., and Littman, D.R. (1994). Signal transduction by lymphocyte antigen receptors. *Cell* 76, 263-274.
- Wright, S.D., Ramos, R.A., Tobias, P.S., Ulevitch, R.J., and Mathison, J.C. (1990). CD14, a receptor for complexes of lipopolysaccharide (LPS) and LPS binding protein. *Science* 249, 1431-1433.
- Zhang, J., Guo, J., Dzhagalov, I., and He, Y.W. (2005). An essential function for the calcium-promoted Ras inactivator in Fcγ receptor-mediated phagocytosis. *Nat Immunol* 6, 911-919.
- Zhu, J., Brownlie, R., Liu, Q., Babiuk, L.A., Potter, A., and Mutwiri, G.K. (2009). Characterization of bovine Toll-like receptor 8: Ligand specificity, signaling essential sites and dimerization. *Mol Immunol* 46, 978-990.
- Abbas, Abul and Lichtman, Andrew (2000). *Cellular and Molecular Immunology*. Elsevier Science (USA). ISBN 0-7216-0008-5.

**Irene M. Aspalter**  
Zehethof 32  
A-3261 Steinakirchen, Austria  
irene.aspalter@gmail.com



## ***CURRICULUM VITAE***

### **Personal Data**

Name:	Irene Maria Aspalter
Place and date of birth:	January 29, 1984, Randegg, Austria
Address:	Zehethof 32, A-3261 Steinakirchen, Austria
Phone:	0043-664-144-85-70
E-mail:	Irene.aspalter@gmail.com
Nationality:	Austrian

### **Education**

10/2003 till present:	Student, Diploma in "Molecular biology" at University of Vienna
08/2002 – 07/2003:	French studies and Au Pair in France (Paris)
06/2002:	Matura (Austrian baccalaureate) after high school
09/1998 – 06/2002:	High school in Scheibbs, Austria

### **Research Experience**

01/2008- present:	Diploma thesis at the <i>Center for Molecular Medicine (CeMM)</i> , Laboratory of Prof. Giulio Superti-Furga, Supervisor: Dr. Christoph Baumann Hunting for unknown interacting proteins of endosomal Toll-like receptors.
07/2007 – 11/2007:	Internship at <i>Dana Farber Cancer Institute (Harvard)</i> , Department: Cancer Biology, Laboratory of Prof. Thomas Roberts, Supervisor: Dr. Shidong Jia Role of PTEN and Pi3-K in prostatic tumor formation and NF1 in glioblastoma.
04/2007 – 06/2007:	Internship at the <i>Center for Brain Research (Medical University of Vienna)</i> , Laboratory of Prof. Hans Lassmann, Supervisor: Prof. Hans Lassmann Role of AN2 antibodies in EAE mouse model and multiple sclerosis.
01/2007 – 03/2007:	Internship at <i>Max F. Perutz Laboratories</i> , Institute of Molecular Genetics, Laboratory of Prof. Egon Ogris, Supervisor: Dr. Stefan Schüchner PP2A protein structure and function.
10/2006 – 12/2006:	Internship at <i>Boehringer Ingelheim</i> , Section: Cancer Research, Laboratory of Dr. Frank Hilberg, Supervisor: Dr. Frank Hilberg Tumorangiogenesis and Receptor-Tyrosin-Kinase-Inhibitors.
08/2006 – 10/2006:	Internship at <i>Novartis Institutes for BioMedical Research</i> , Department of Dr. Thomas Baumruker, Supervisor: Dr. Roland Reuschel Bioanalytical research in multiple sclerosis drug development.
12/2005 – 06/2006:	Internship at the <i>Medical University of Vienna</i> , Department for Infections and Chemotherapy, Internal Medicine I, Laboratory of Prof. Apostolos Georgopoulos, Supervisor: Dr. Martin Andreas The role of chlamydia in non small cell lung cancer.

## **Technical Skills**

### **Nucleic acids:**

- Conservative cloning and Gateway® cloning
- RNA and DNA isolation
- Quantitative real time PCR

### **Proteins:**

- Expression and purification of recombinant-proteins
- Gelelectrophoresis and western-blot
- Immuno-precipitation
- Tandem affinity purification
- Invitro translation
- ELISA

### **Cell culture:**

- Mammalian cell culture (cell lines, primary cells and stem cells)
- Viral transfecting systems
- Reporter-gene-assay
- FACS (FACScalibur)
- Thymidin assay

### **Immunohistochemistry:**

- Tissue preparation and paraffin embedded sectioning techniques
- Immunohistochemistry (Hämalaun-Eosin, Bielschowsky, Klüver Barrera-Pas)
- Immunofluorescence
- Microscopy including light- and confocal laser microscopy

### ***In vivo* (mice):**

- Prostate and neuronal stem cell isolation
- *In vivo* regeneration of murine prostate

### **Computer skills:**

- Word, Excel (Microsoft Office)
- Photoshop, Illustrator
- VectorNTI, Clontech

## **Scholarships:**

2007	Siegfried-Ludwig-Fonds scholarship
2006	TOP scholarship of the Lower Austrian government

## **Meetings and Conferences**

09/2008	TOLL Meeting 2008 Lisbon, Portugal (Poster presentation: Aspalter et al.: Hunting for unknown interacting proteins of endosomal Toll-like receptors)
05/2008	IMP conference, Vienna, Austria
11/2007	4th Annual Tony & Shelly Malkin Stem Cell Symposium: Cancer Stem Cells (Harvard Stem Cell Institute)

## **Other skills**

06/2001 till present:	Voluntary emergency paramedic at the Austrian Red Cross
03/2004:	Member of the local organization team, annual AIVS-Meeting in Lech (Austria)
Foreign languages:	English (fluently in written and spoken), French (fluently in spoken)